Nucleon structure in 3D: experimental status and perspectives

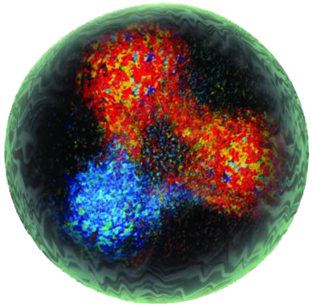

Daria Sokhan
University of Glasgow, UK

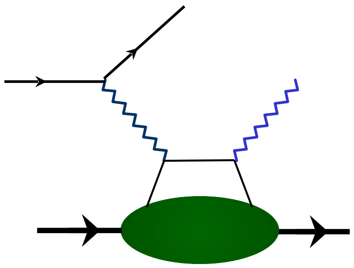

XVIII International Conference on Hadron Spectroscopy and Structure
Guilin, China — 19th August 2019

An abridged history of nucleon structure

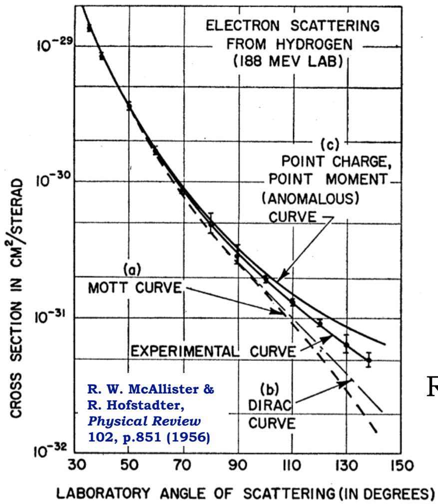

Robert Hofstadter
1915 - 1990
(Wikipedia)

1956: Elastic scattering at Stanford: the proton has internal structure! *Hofstadter: Nobel Prize 1961.*

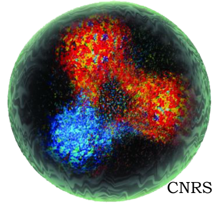

1960s: the Quark Model. Nucleons are composed of three valence quarks! *Gell-Mann (Nobel Prize 1969), Zweig.*

1968: Deep Inelastic scattering at SLAC: scaling observed. The proton consists of point-like charges: partons! *Friedman, Kendall, Taylor: Nobel Prize 1990*

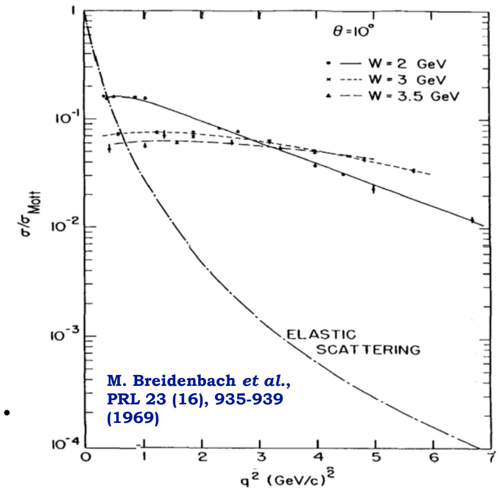

1972: Theory of QCD developed.

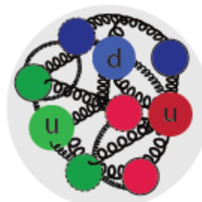

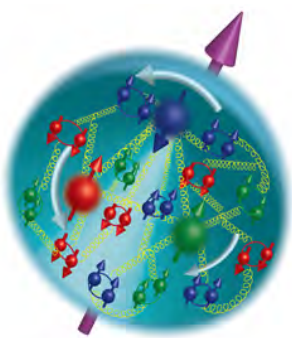

1970s-1990s: Deep Inelastic Scattering reveals a rich structure: quark-gluon sea, flavour distributions, puzzles of spin and mass… what you see depends on how closely you look!

21st Century: High-precision imaging of quarks and gluons. 3D tomography of the nucleon: spatial and momentum distributions inside it, mechanical properties of the nucleon, …

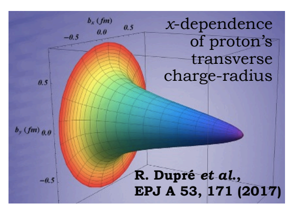

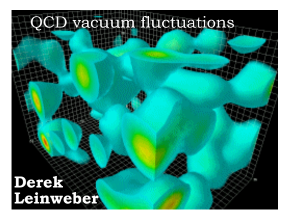

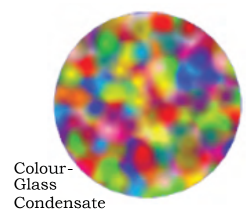

A constructivist view of the nucleon

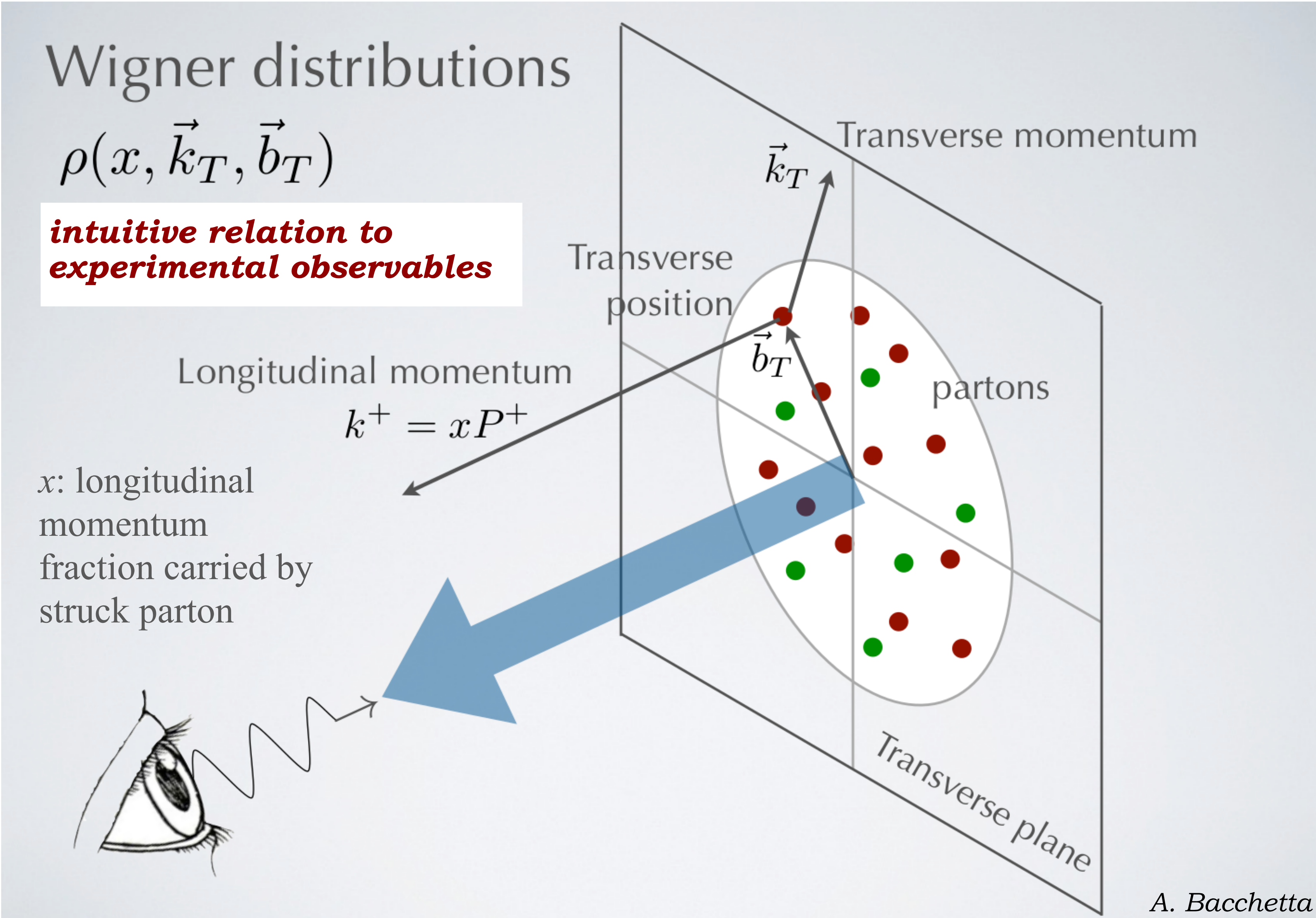

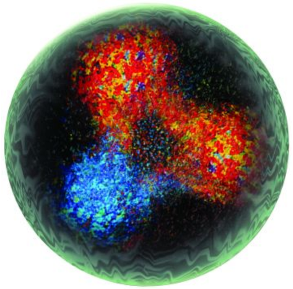

Wigner function: full phase space parton distribution of the nucleon

Generalised Transverse Momentum Distributions (GTMDs)

$\int d^2 k_T$

$\int d^2 b_T$

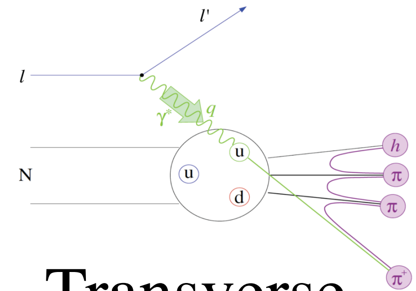

Transverse Momentum Distributions (TMDs)

Generalised Parton Distributions (GPDs)

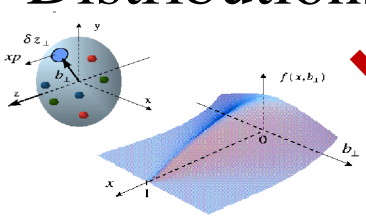

$\int dx$

$\int d^2 b_T$

$\int d^2 k_T$

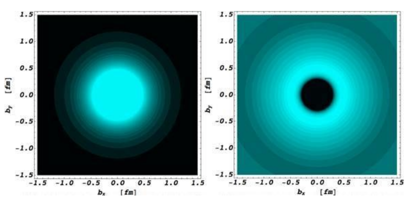

Form Factors

eg: G_E, G_M

Parton Distribution Functions (PDFs)

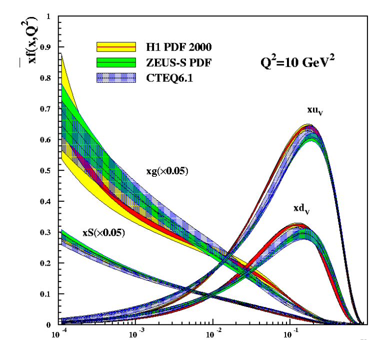

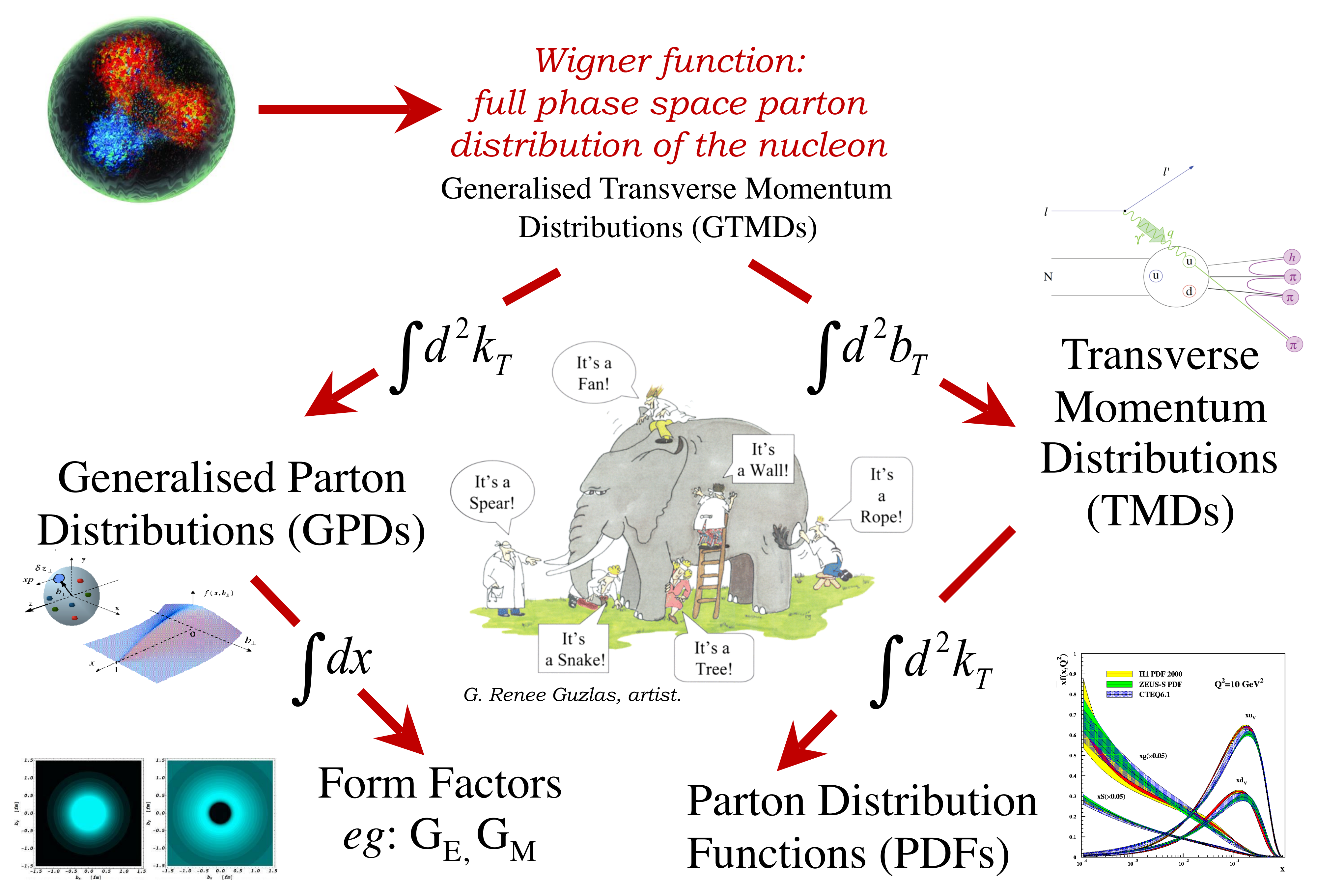

G. Renee Guzlas, artist.

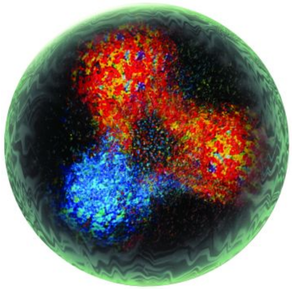

Wigner function:
full phase space parton
distribution of the nucleon

Generalised Transverse Momentum
Distributions (GTMDs)

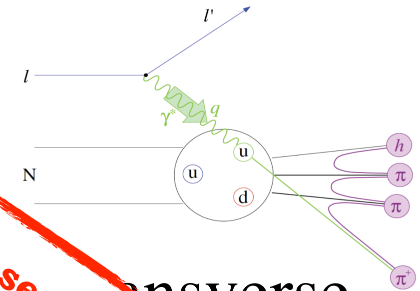

$\int d^2k_T$

$\int d^2b_T$

Generali ... (GPDs)

Parallel session 6 on Tuesday

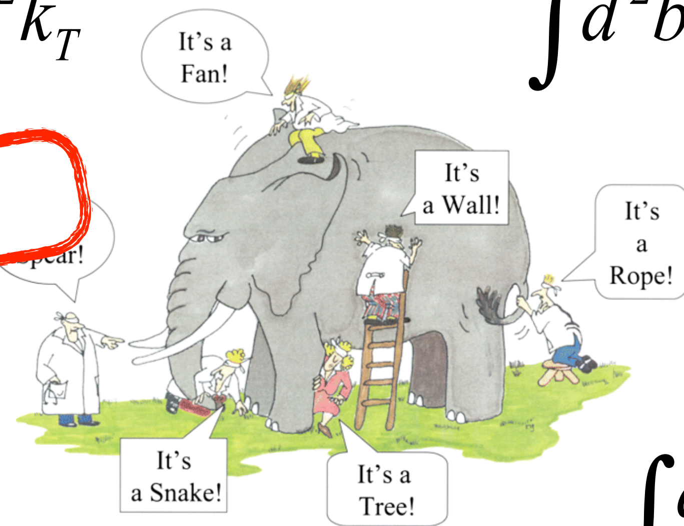

G. Renee Guzlas, artist.

... nsverse ... tum
Distr ... s
(TMDs)

Parallel session 6 on Tuesday

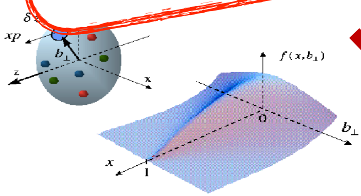

$\int dx$

$\int d^2k_T$

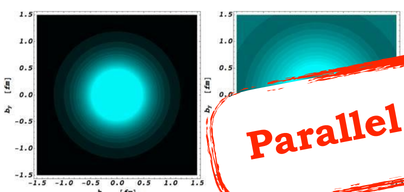

F ... G_E, G_M

Parallel session 6 on Saturday

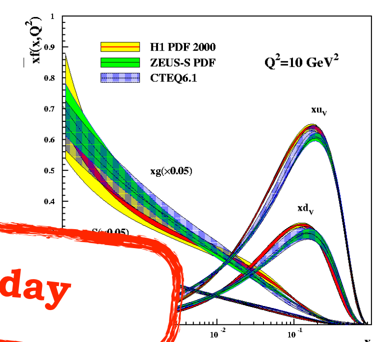

Functions (PDFs)

Parallel session 6 on Sunday

Generalised Parton Distributions

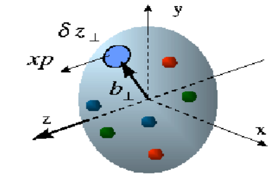

- proposed by Müller (1994), Radyushkin, Ji (1997).
- can be interpreted as relating, in the infinite momentum frame, transverse position of partons (impact parameter $b_\perp$) to longitudinal momentum fraction (x).

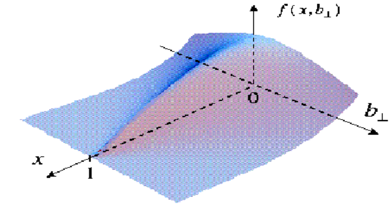

* **Tomography** of the nucleon: transverse spatial distributions of quarks and gluons in longitudinal momentum space.

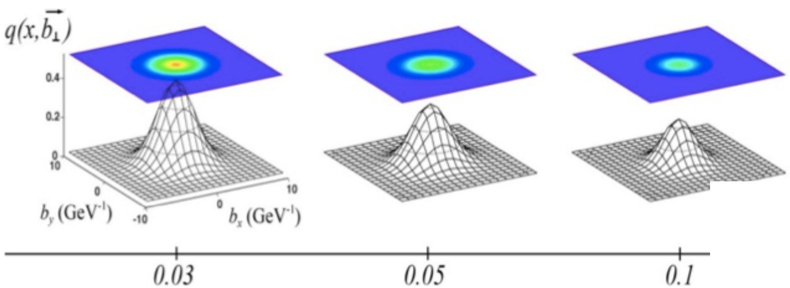

* Information on the orbital angular momentum contribution to nucleon spin: **the spin puzzle**.

$$J_N = \frac{1}{2} = \frac{1}{2}\Sigma_q + L_q + J_g$$

Ji's relation:

$$J^q = \frac{1}{2} - J^g$$

$$= \frac{1}{2}\int_{-1}^{1} x\,dx \left\{ H^q(x,\xi,0) + E^q(x,\xi,0) \right\}$$

* Indirect access to mechanical properties of the nucleon: possibilities of extracting **pressure distributions** within the nucleon.

* Combine with TMDs to access **spin-orbit correlations** of quarks and gluons, study non-perturbative interactions of partons.

Experimental processes for accessing GPDs

Accessible in *exclusive* processes, where all final state particles are determined:

- Deeply Virtual Compton Scattering (DVCS)
- Deeply Virtual Meson Production (DVMP) / Hard Exclusive Meson Production (HEMP)
- Time-like Compton Scattering (TCS)
- Double DVCS
- Production of a meson-photon pair, ...

Relies on *factorisation* of the process amplitude into a hard, perturbative part and the soft non-perturbative part containing GPD information.

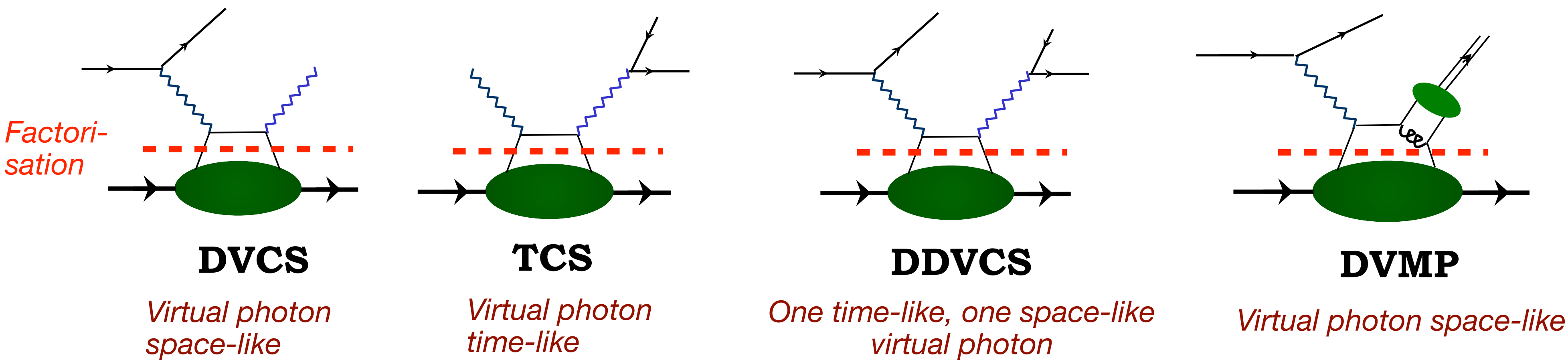

Deeply Virtual Compton Scattering

the "golden channel" for GPD extraction

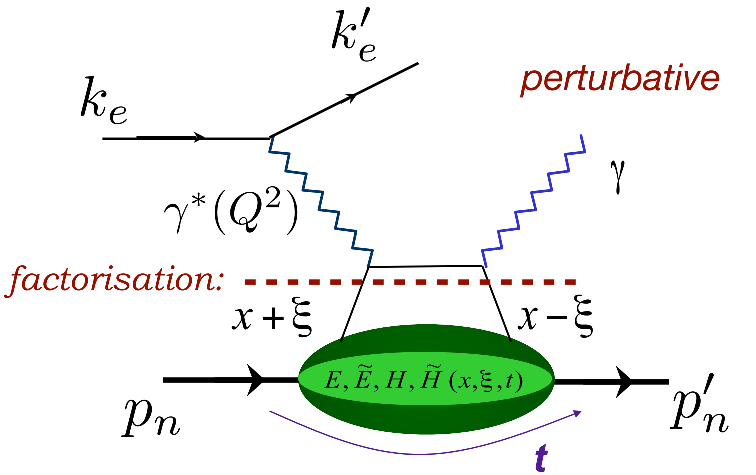

"Handbag" diagram

$$Q^2 = -(\mathbf{k} - \mathbf{k}')^2 \qquad t = (\mathbf{p'_n} - \mathbf{p_n})^2$$

Bjorken variable: $x_B = \dfrac{Q^2}{2\mathbf{p_n} \cdot \mathbf{q}}$

$x \pm \xi$ *longitudinal momentum fractions of the struck parton*

Skewness: $\xi \cong \dfrac{x_B}{2 - x_B}$

- At high exchanged Q^2 and low t access to four parton helicity-conserving, chiral-even GPDs:

$$E^q, \tilde{E}^q, H^q, \tilde{H}^q(x, \xi, t)$$

- Can be related to PDFs:

$$H(x,0,0) = q(x) \qquad \tilde{H}(x,0,0) = \Delta q(x)$$

and form factors:

$$\int_{-1}^{+1} H dx = F_1 \qquad \int_{-1}^{+1} \tilde{H}\, dx = G_A$$

$$\int_{-1}^{+1} E\, dx = F_2 \qquad \int_{-1}^{+1} \tilde{E}\, dx = G_P$$

(Dirac and Pauli) *(axial and pseudo-scalar)*

- Small changes in nucleon transverse momentum allows mapping of transverse structure at large distances.

Measuring DVCS

- Process measured in experiment:

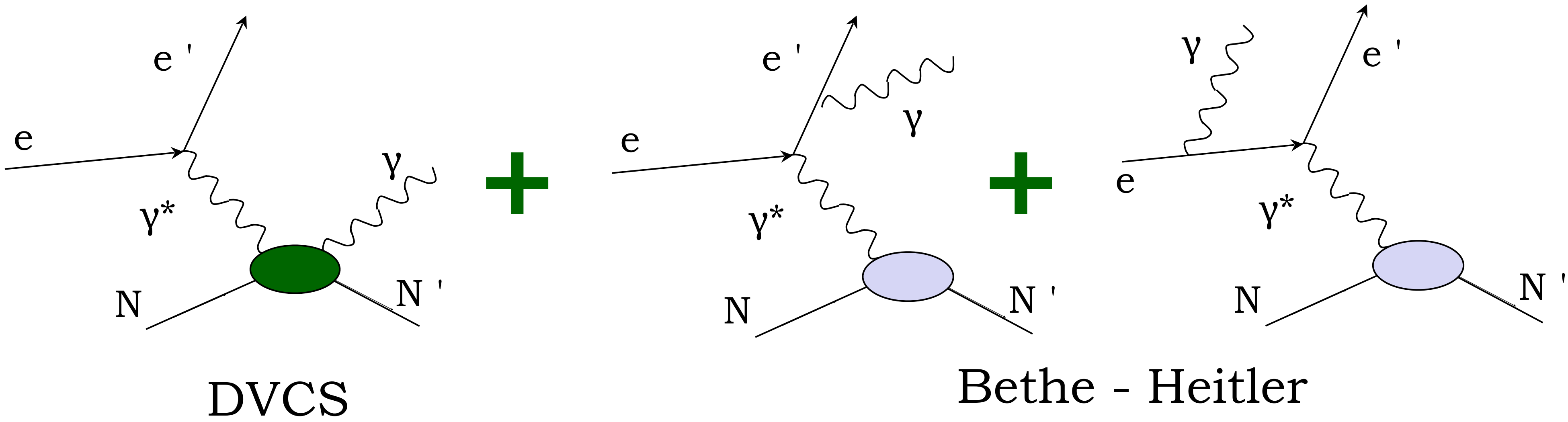

$$d\sigma \propto \left|T_{DVCS}\right|^2 + \left|T_{BH}\right|^2 + T_{BH}T^*_{DVCS} + T_{DVCS}T^*_{BH}$$

Amplitude parameterised in terms of Compton Form Factors

Amplitude calculable from elastic Form Factors and QED

Interference term

$$\left|T_{DVCS}\right|^2 << \left|T_{BH}\right|^2$$

Compton Form Factors in DVCS

Experimentally accessible in DVCS cross-sections and spin asymmetries, eg:

$$A_{LU} = \frac{d\vec{\sigma} - d\overleftarrow{\sigma}}{d\vec{\sigma} + d\overleftarrow{\sigma}} = \frac{\Delta\sigma_{LU}}{d\vec{\sigma} + d\overleftarrow{\sigma}}$$

cross-sections,
beam-charge and
double polarisation asymmetries

single-spin
asymmetries

At leading twist, leading order:

$$T^{DVCS} \sim \int_{-1}^{+1} \frac{GPDs\,(x,\xi,t)}{x \pm \xi + i\varepsilon}\,dx + \ldots \sim \quad P\int_{-1}^{+1} \frac{GPDs\,(x,\xi,t)}{x \pm \xi}\,dx \pm i\pi GPDs\,(\pm\xi,\xi,t) + \ldots$$

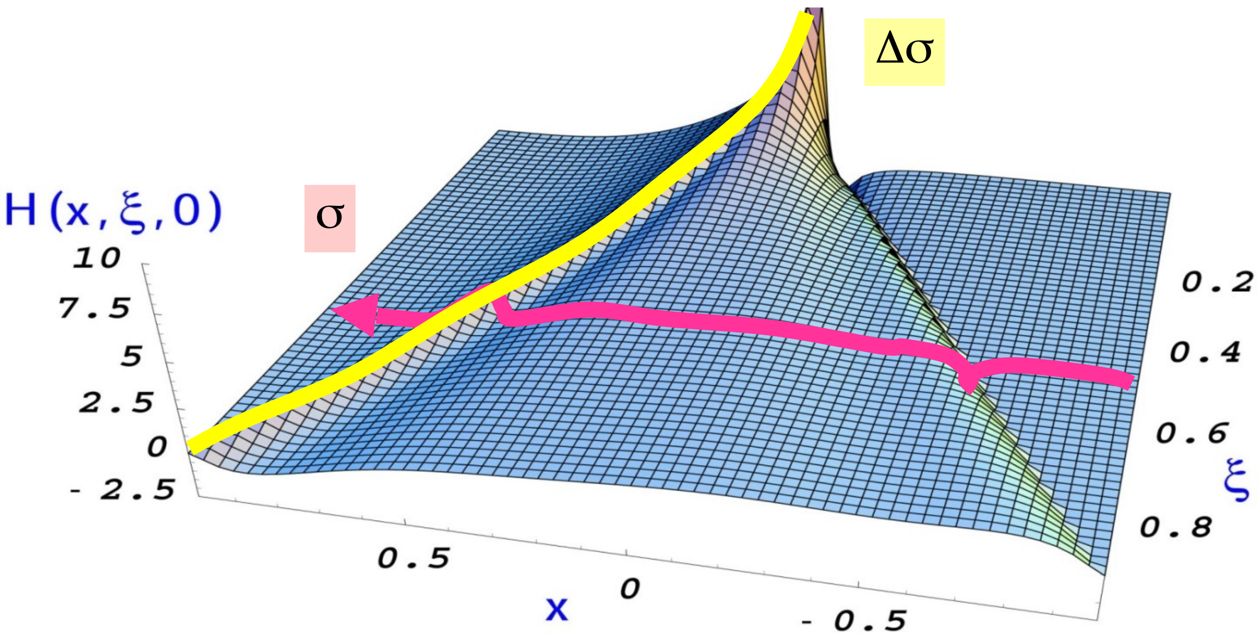

Only ξ and t are accessible experimentally!

To get information on x need extensive measurements in Q^2.

Need measurements off proton and neutron to get flavour separation of CFFs in DVCS.

Nucleon at different scales

Valence quarks

Jefferson Lab: fixed-target electron scattering

$0.1 < x_B < 0.7$

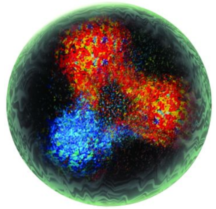

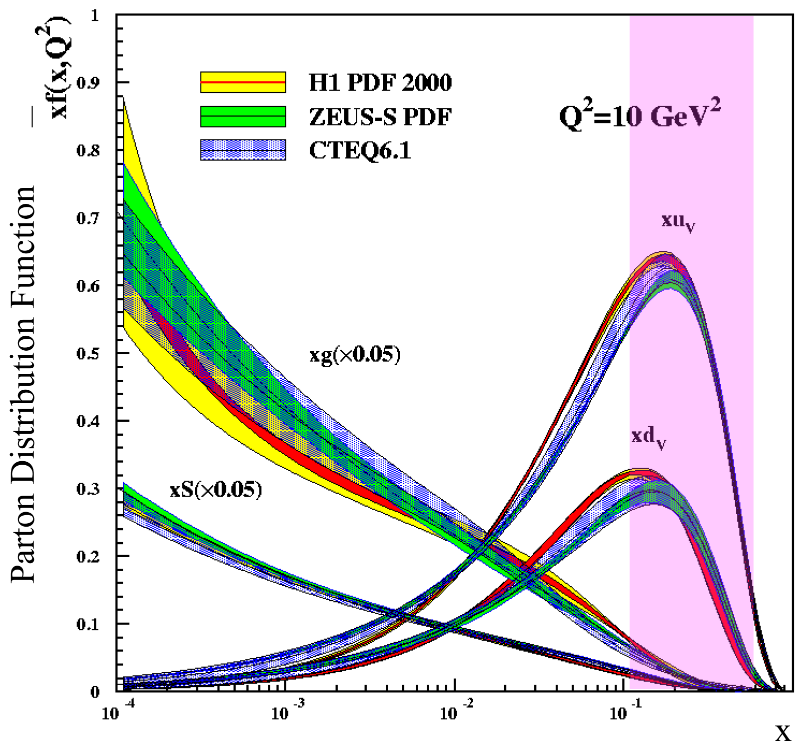

Nucleon at different scales

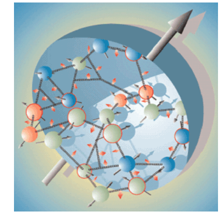

Valence quarks

Jefferson Lab: fixed-target electron scattering

$0.1 < x_B < 0.7$

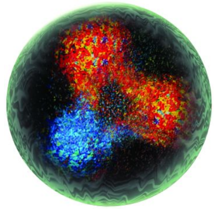

Sea quarks

HERMES: fixed gas-target electron/positron scattering

$0.02 < x_B < 0.3$

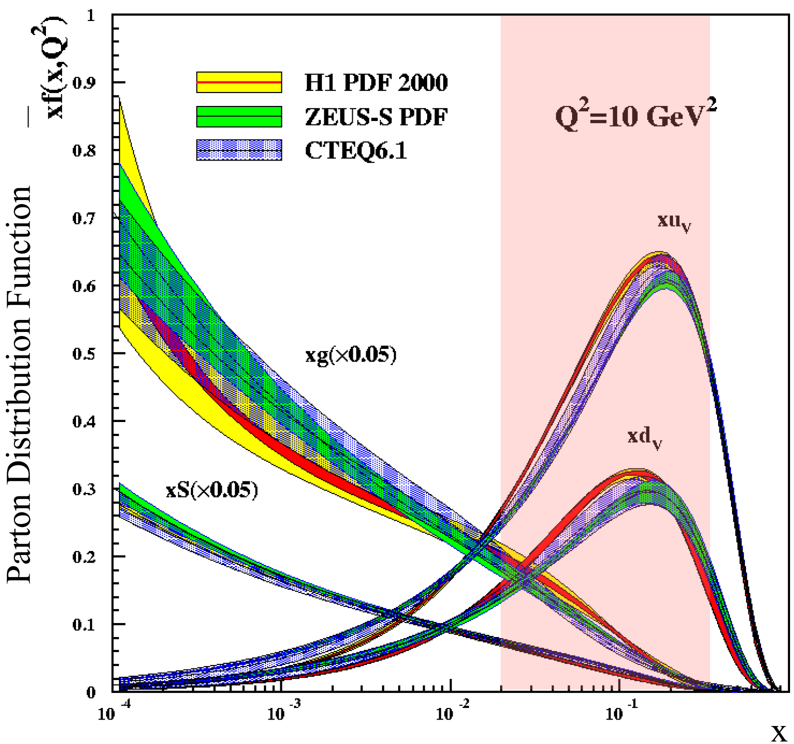

Nucleon at different scales

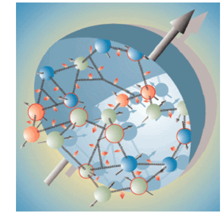

Valence quarks

Jefferson Lab: fixed-target electron scattering

$0.1 < x_B < 0.7$

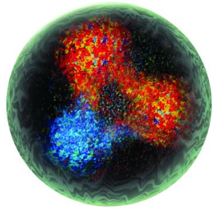

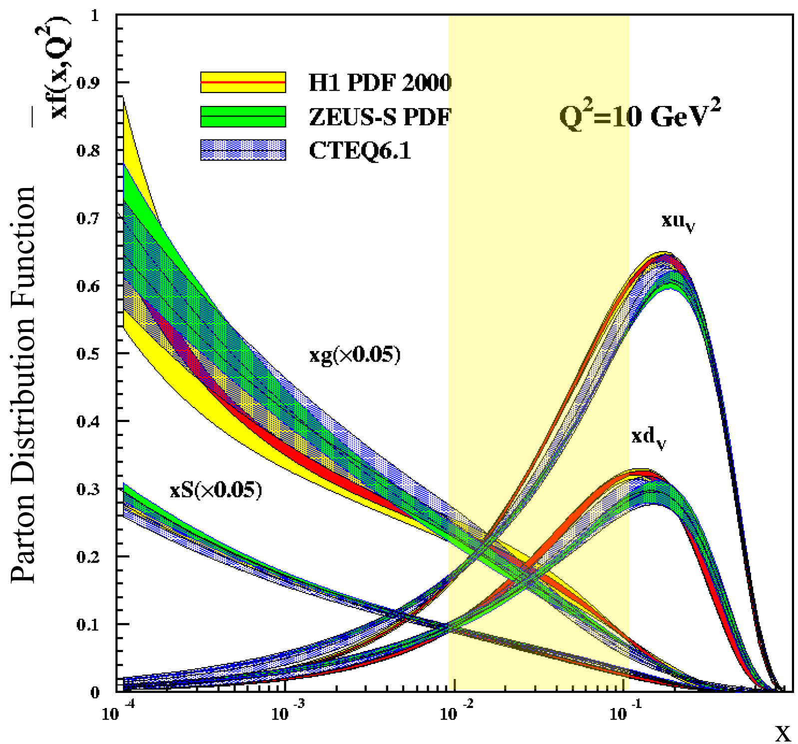

Sea quarks

HERMES: fixed gas-target electron/positron scattering

$0.02 < x_B < 0.3$

COMPASS: fixed-target muon scattering

$0.01 < x_B < 0.1$

Nucleon at different scales

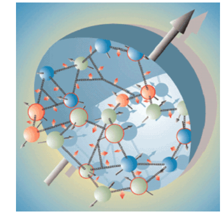

Valence quarks

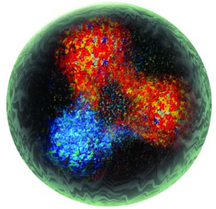

Jefferson Lab: fixed-target electron scattering

$0.1 < x_B < 0.7$

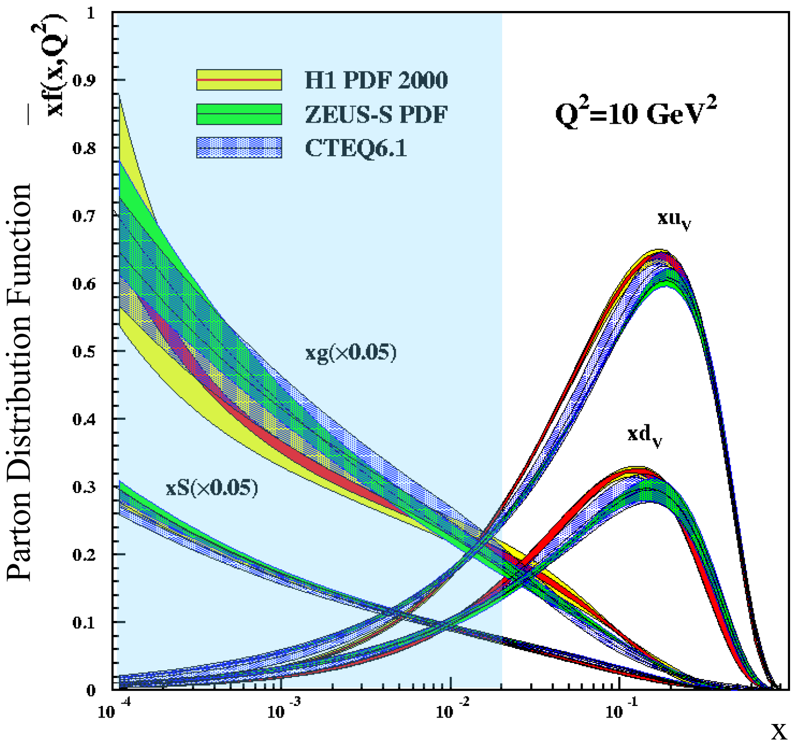

Sea quarks

HERMES: fixed gas-target electron/positron scattering

$0.02 < x_B < 0.3$

COMPASS: fixed-target muon scattering

$0.01 < x_B < 0.1$

The glue

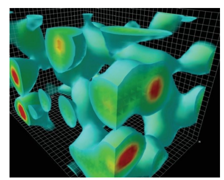

Derek Leinweber

ZEUS/H1: electron/positron-proton collider

$10^{-4} < x_B < 0.02$

Nucleon at different scales

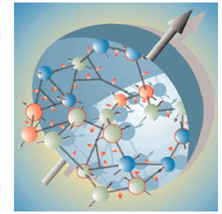

Valence quarks

Jefferson Lab: fixed-target electron scattering

$0.1 < x_B < 0.7$

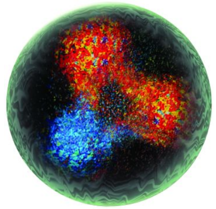

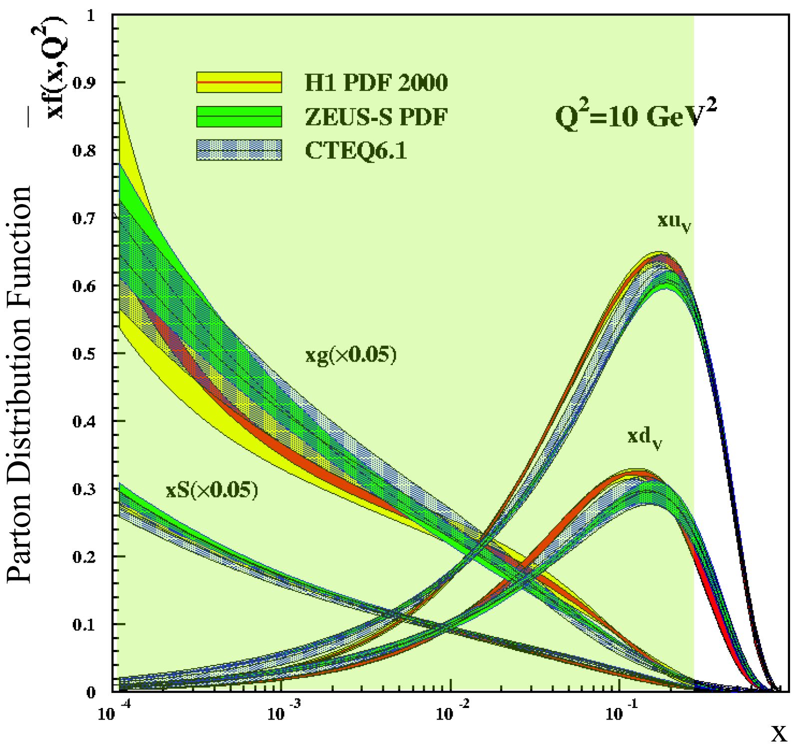

Sea quarks

HERMES: fixed gas-target electron/positron scattering

$0.02 < x_B < 0.3$

COMPASS: fixed-target muon scattering

$0.01 < x_B < 0.1$

The glue

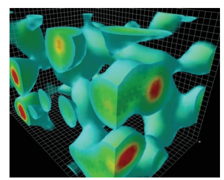

Derek Leinweber

ZEUS/H1: electron/positron-proton collider

$10^{-4} < x_B < 0.02$

Electron-ion collider: $10^{-4} < x_B < 10^{-1}$

Luminosity 100 - 1000 times that of HERA

Nucleon at different scales

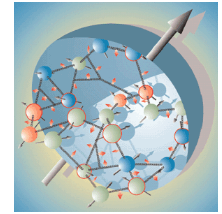

Valence quarks

Jefferson Lab: fixed-target electron scattering

$0.1 < x_B < 0.7$

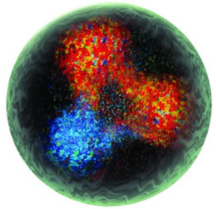

Sea quarks

HERMES: fixed gas-target electron/positron scattering

$0.02 < x_B < 0.3$

COMPASS: fixed-target muon scattering

$0.01 < x_B < 0.1$

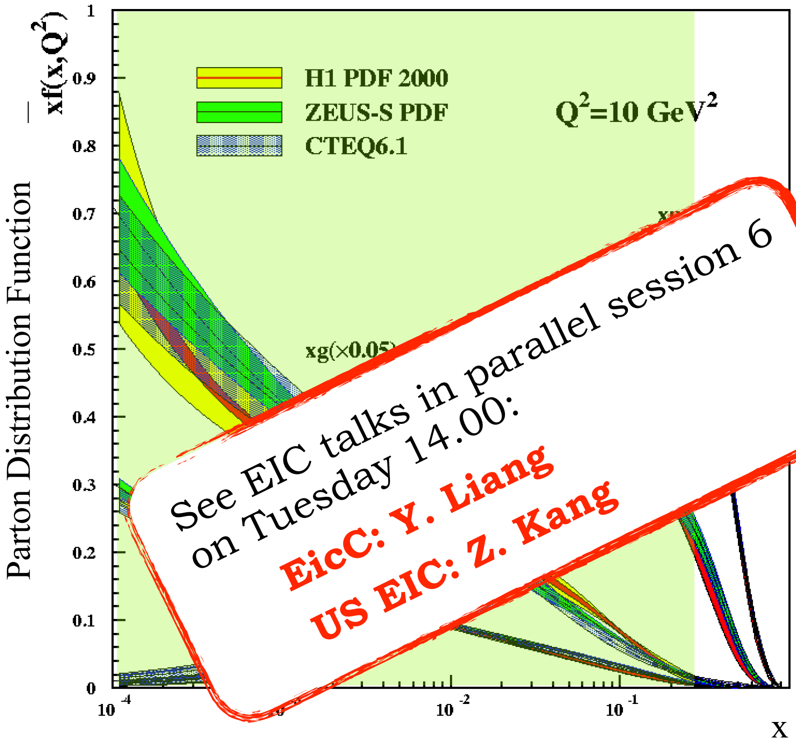

See EIC talks in parallel session 6 on Tuesday 14.00:

EicC: Y. Liang

US EIC: Z. Kang

The glue

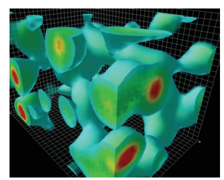

Derek Leinweber

ZEUS/H1: electron/positron-proton collider

$10^{-4} < x_B < 0.02$

Electron-ion collider: $10^{-4} < x_B < 10^{-1}$

Luminosity 100 - 1000 times that of HERA

Kinematic landscape

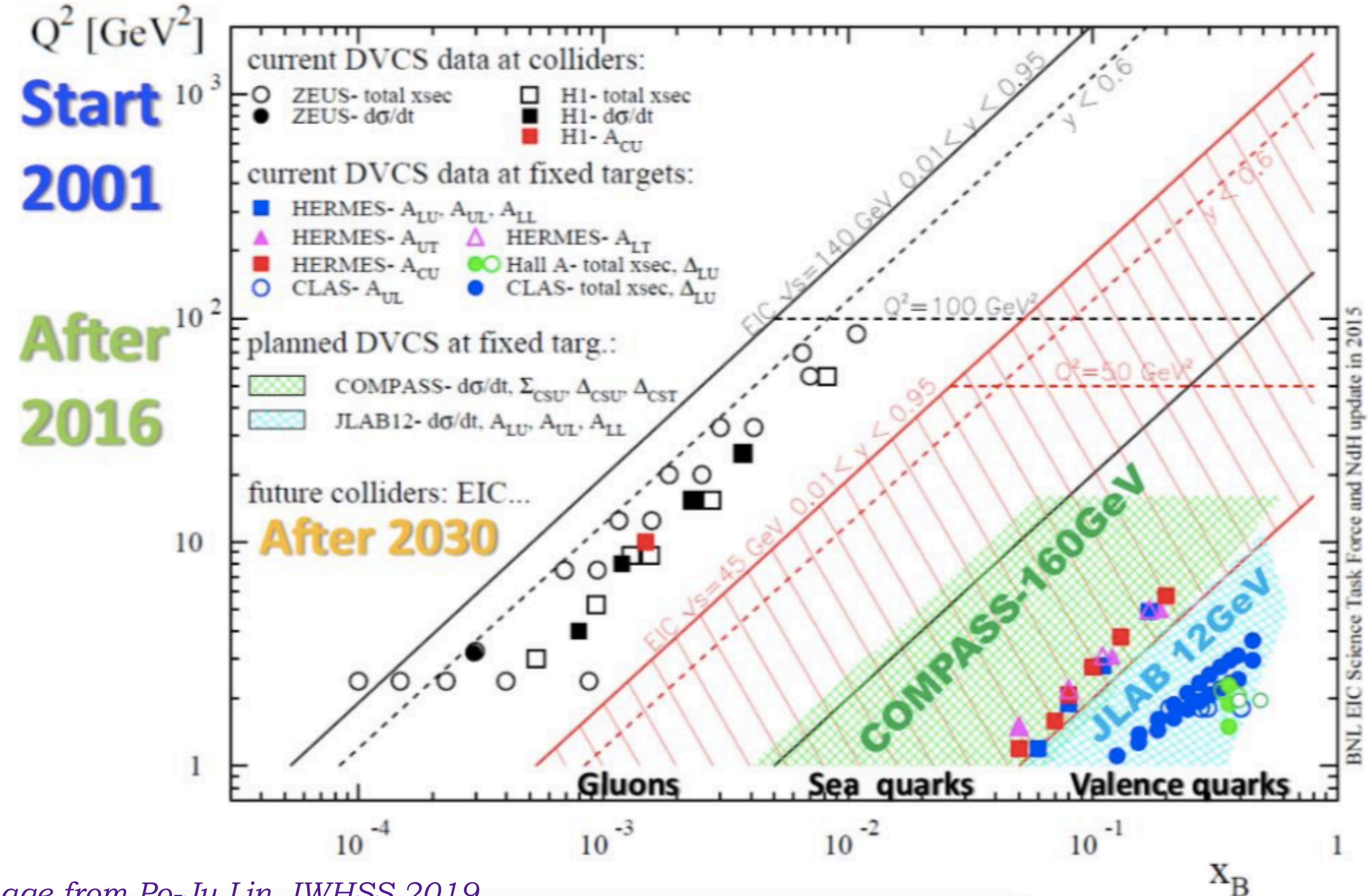

Image from Po-Ju Lin, IWHSS 2019

Jefferson Lab: 6 GeV era

CEBAF: Continuous Electron Beam Accelerator Facility.

- Energy up to ~6 GeV
- Energy resolution $\delta E/E_e \sim 10^{-5}$
- Longitudinal electron polarisation up to ~85%

Hall A:

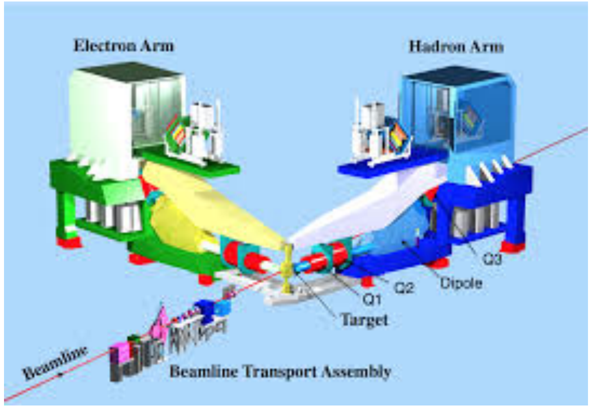

- High resolution($\delta p/p = 10^{-4}$) spectrometers, very high luminosity.

Hall B: CLAS

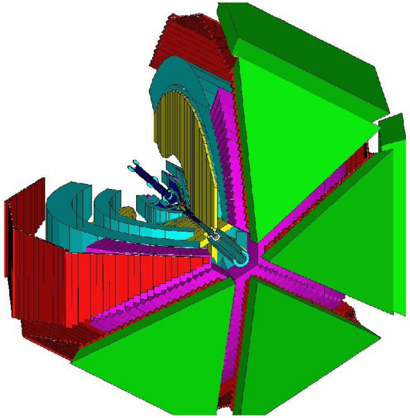

- Very large acceptance, detector array for multi-particle final states.

Hall C:

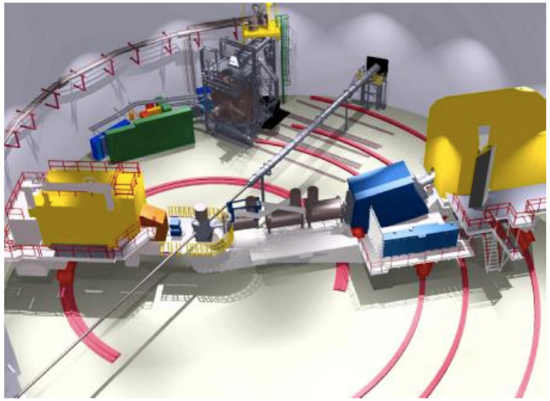

- Two movable spectrometer arms, well-defined acceptance, high luminosity

JLab @ 12 GeV

Hall A

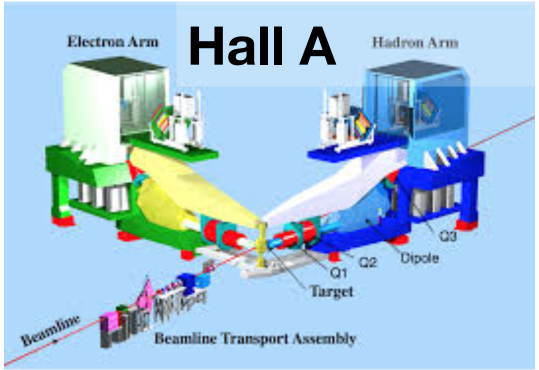

High resolution($\delta p/p = 10^{-4}$) spectrometers, very high luminosity, large installation experiments.

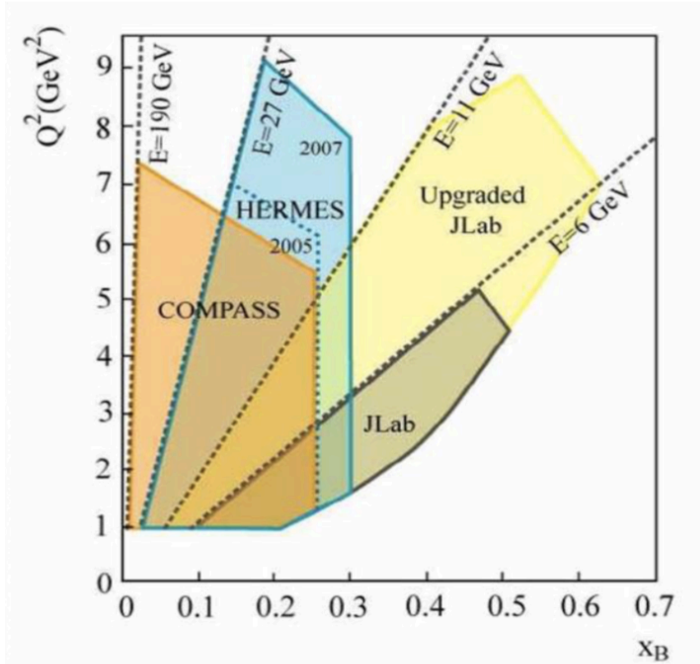

Hall C

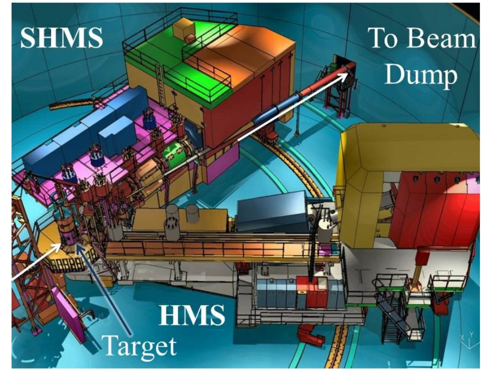

Two movable high momentum spectrometers, well-defined acceptance, very high luminosity.

Hall D

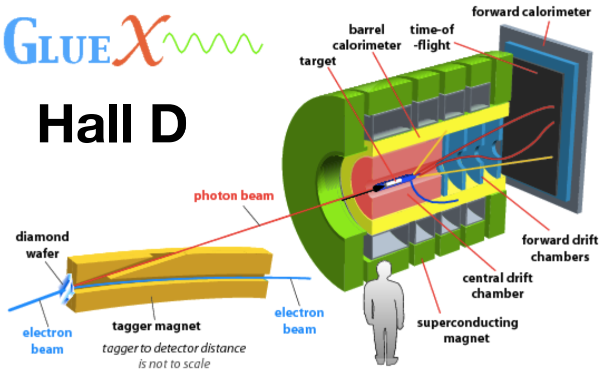

9 GeV tagged polarised photons, full acceptance

Hall B: CLAS12

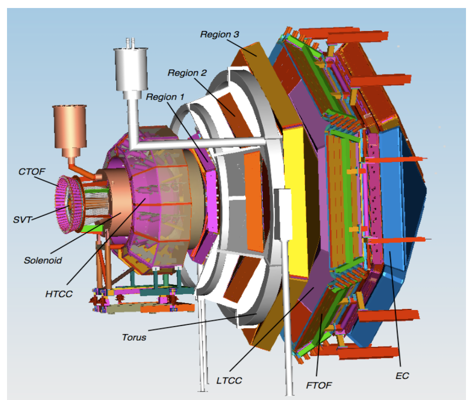

Very large acceptance, high luminosity.

JLab @ 12 GeV

Hall A

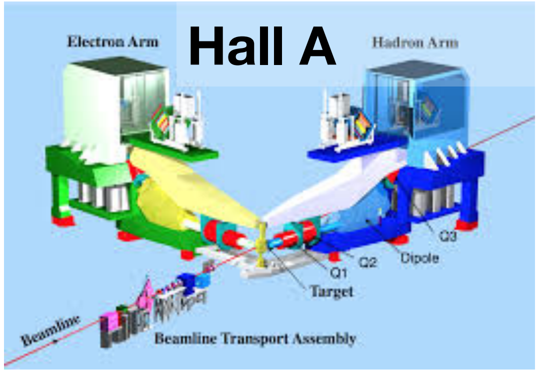

High resolution($\delta p/p = 10^{-4}$) spectrometers, very high luminosity, large installation experiments.

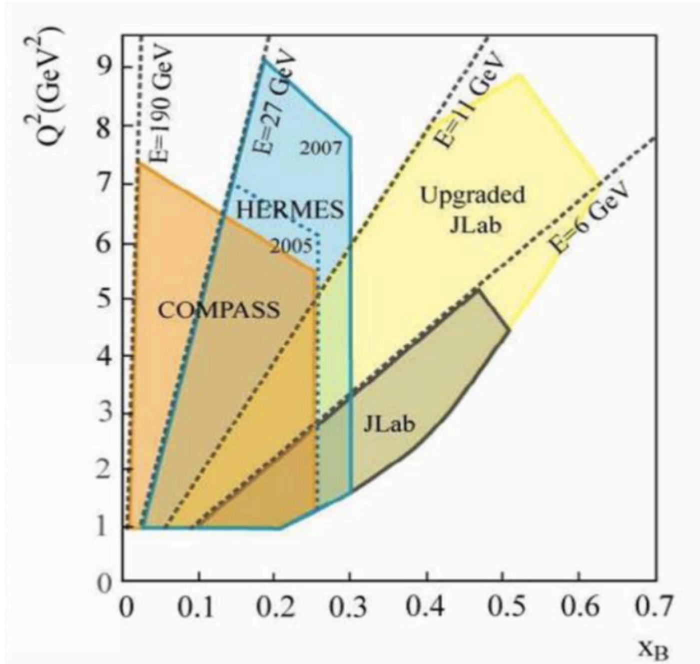

Hall C

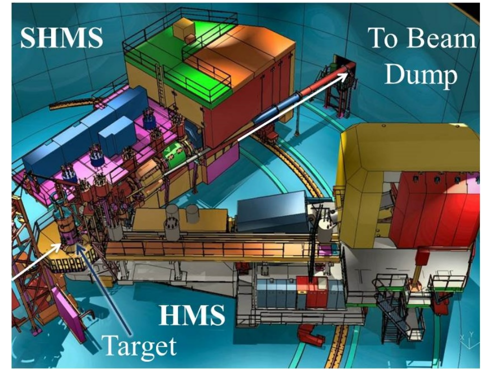

Two movable high momentum spectrometers, well-defined acceptance, very high luminosity.

Hall B: CLAS12

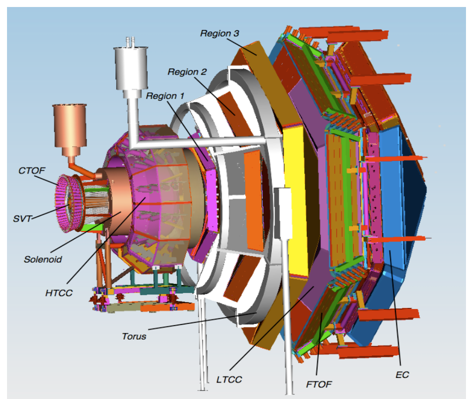

Very large acceptance, high luminosity.

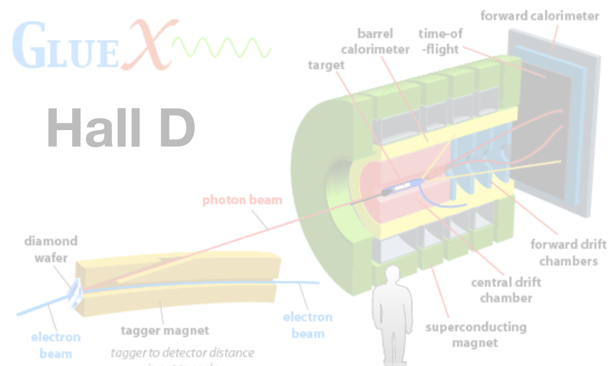

9 GeV tagged polarised photons, full acceptance

CLAS12

Design luminosity

$L \sim 10^{35}\ cm^{-2}\ s^{-1}$

High luminosity & large acceptance:
Concurrent measurement of exclusive, semi-inclusive, and inclusive processes

Acceptance for photons and electrons:
- $2.5^o < \theta < 125^o$

Acceptance for all charged particles:
- $5^o < \theta < 125^o$

Acceptance for neutrons:
- $5^o < \theta < 120^o$

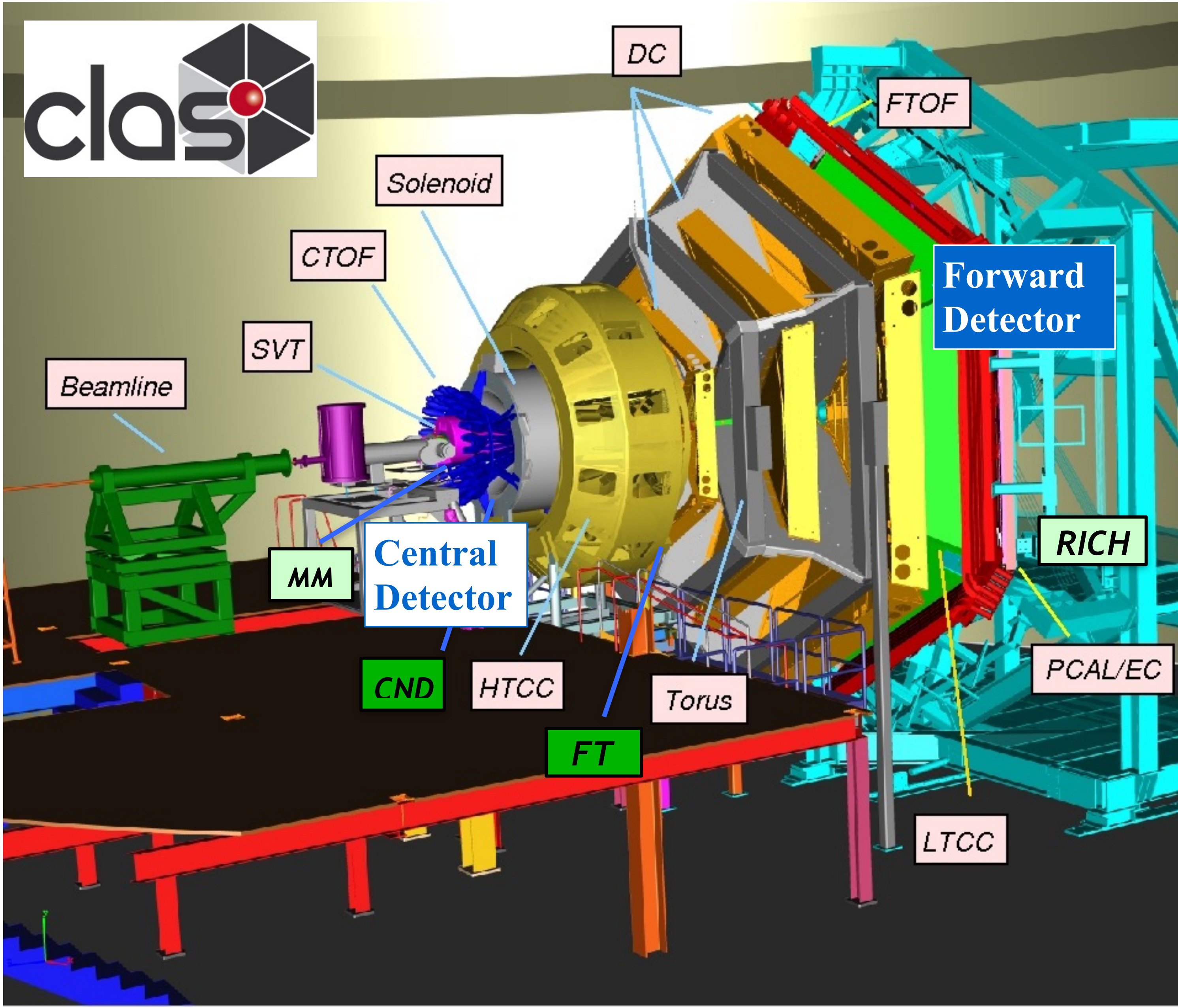

DVCS in Hall A

* 15 cm long liquid H_2 target
* Luminosity $=10^{37}$ cm^{-2}s^{-1}

$$ep \to e'\gamma(p')$$

Reconstructed through missing mass

Detected in High Resolution Spectrometer (SRS)

Detected in PbF_2 Calorimeter

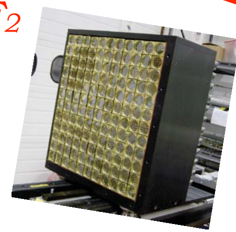

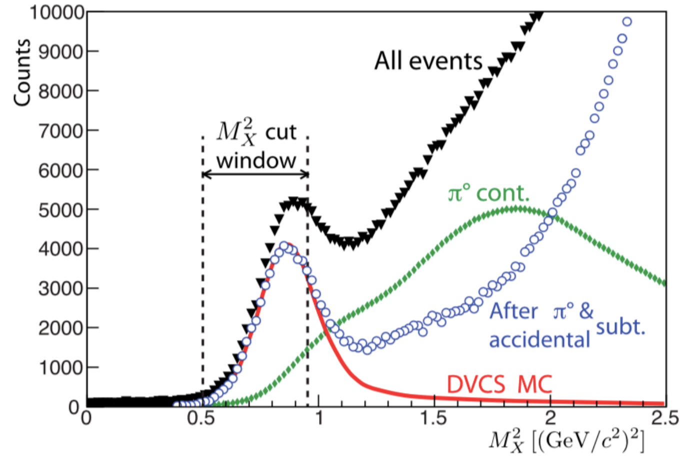

M. Defurne *et al*, ***PRC* 92** (2015) 055202.

* **E00-110 experiment** (2004): 5.75 GeV polarised electron beam

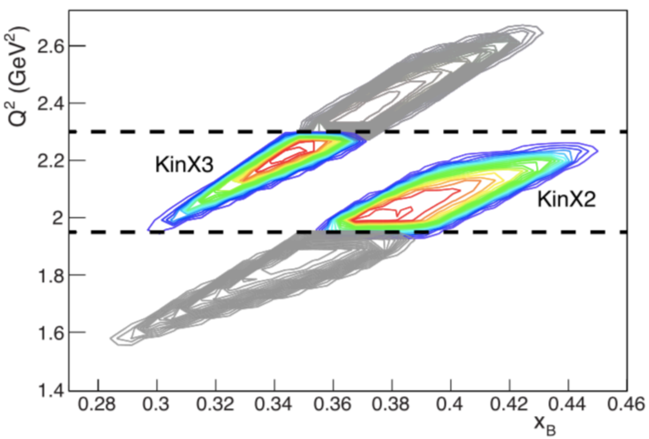

M. Defurne *et al*, ***PRC* 92** (2015) 055202.

* **E07-004 experiment** (2010): Energy scan for fixed x_B, Q^2:

Q^2 (GeV^2)	x_B	E^{beam} (GeV)	$-t$ (GeV^2)
1.50	0.36	3.355 5.55	0.18, 0.24, 0.30
1.75	0.36	4.455 5.55	0.18, 0.24, 0.30, 0.36
2.00	0.36	4.455 5.55	0.18, 0.24, 0.30, 0.36

High-precision cross-sections: Hall A

- High precision cross-section measurement in a small kinematic region: Generalised Rosenbluth separation of the $DVCS^2$ (scales as E_e^2) and the BH-DVCS interference (scales as E_e^3) terms. NLO and/or higher-twist improve model agreement.

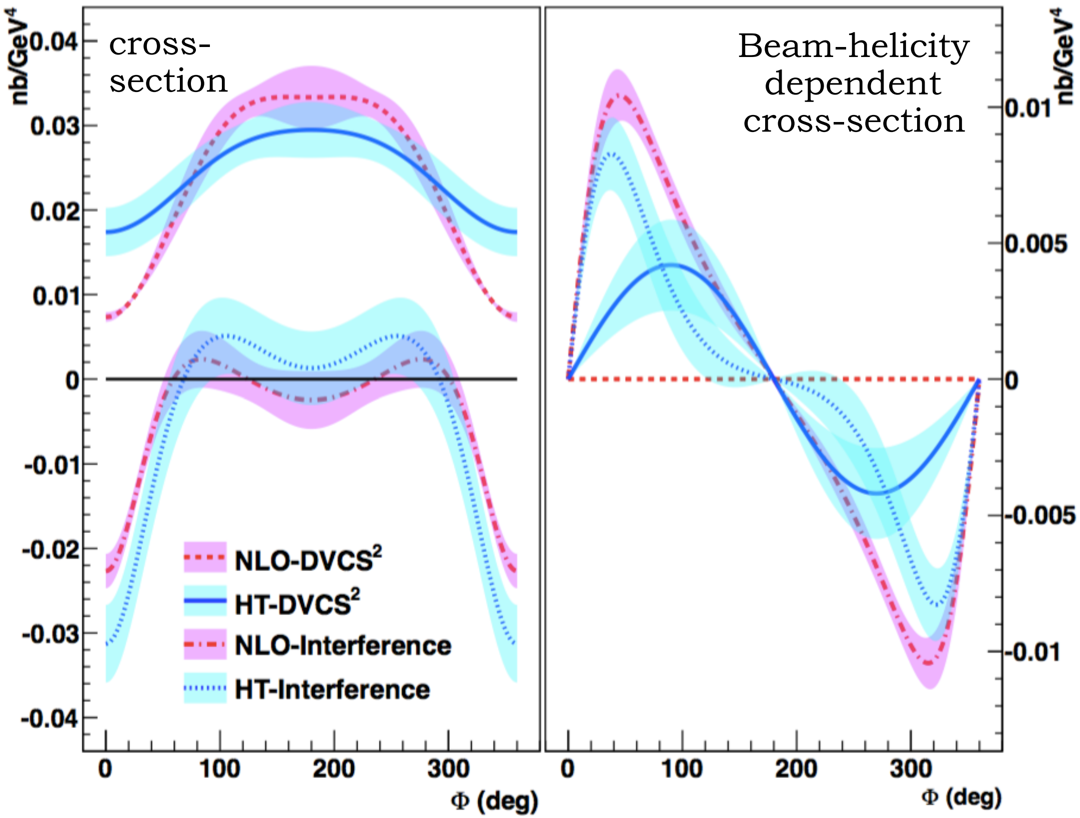

E_e: 4.5, 5.6 GeV.

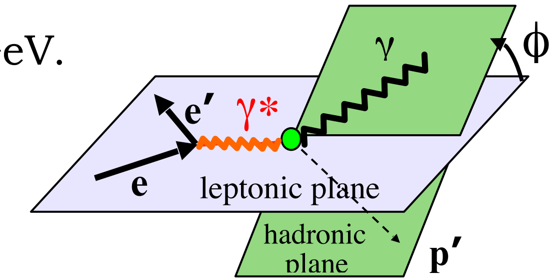

- Significant differences between pure DVCS and interference contributions.
- If NLO: sensitivity to gluons.
- Separation of HT and NLO effects requires scans across wider ranges of Q^2 and beam energy: JLab12.

Q^2: 1.5, 1.9, 2.3 GeV^2 at fixed x_B 0.36
$-t$: 0.18, 0.24, 0.30

M. Defurne *et al*, ***Nature Communications* 8** (2017) 1408.

Large kinematic coverage: CLAS

- Unpolarised DVCS cross-sections and helicity-dependent cross-section differences in a wide kinematic range:

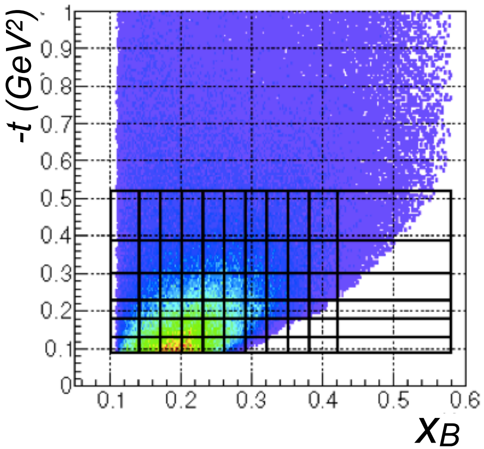

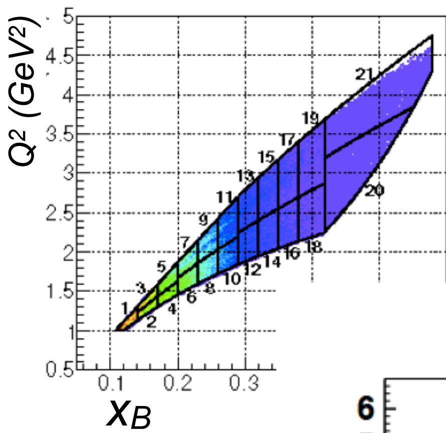

- CFFs extracted in a VGG fit.

$$F_{Im}(\xi, t) = F(\xi, \xi, t) \mp F(-\xi, \xi, t)$$

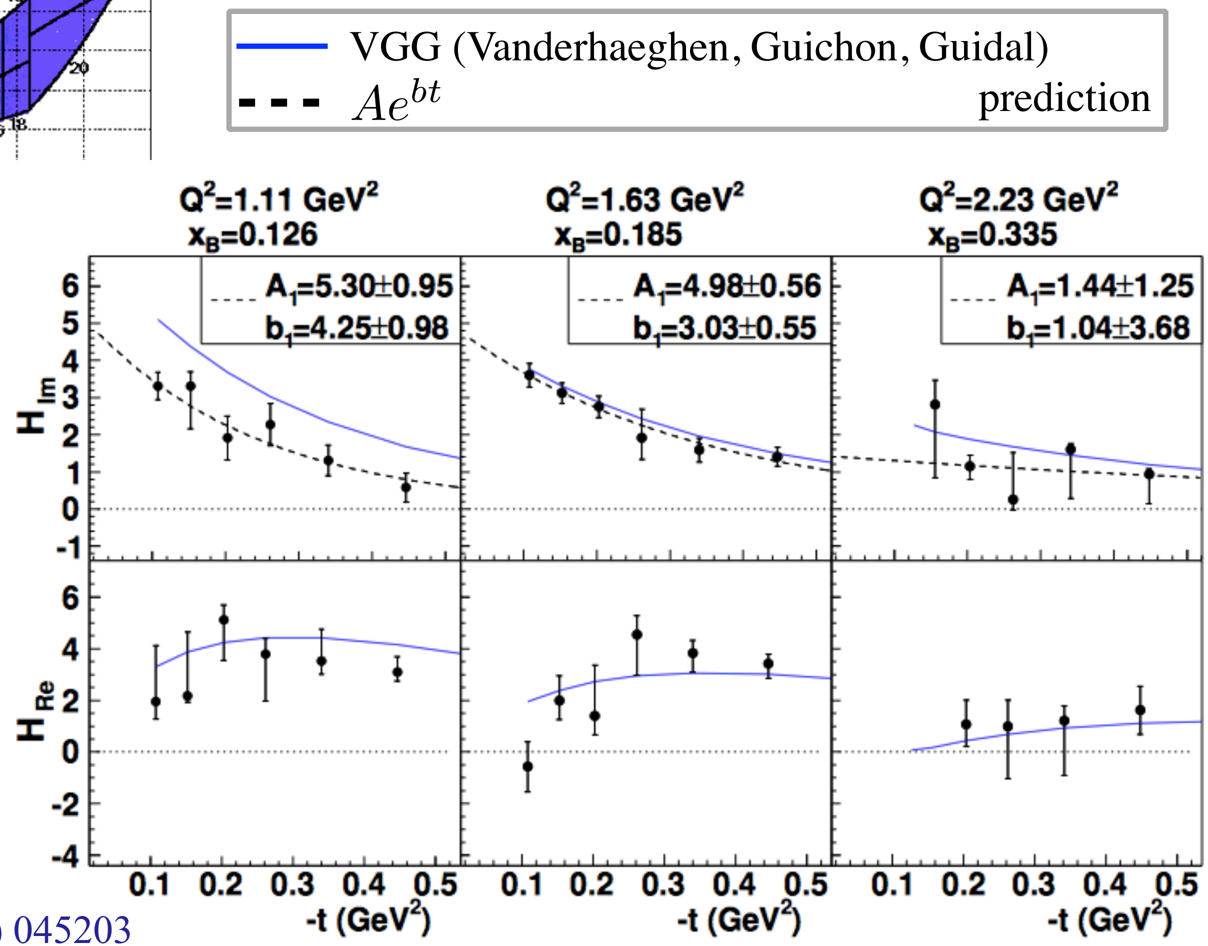

- Dominance of GPD *H* in unpolarised cross-section.

- H_{Im} slope in t becomes flatter at higher x_B

Valence quarks at centre, sea quarks spread out towards the periphery.

H.-S. Jo *et al* (CLAS), ***PRL*** **115** (2015) 212003
N. Hirlinger Saylor *et al* (CLAS), ***PRC*** **98** (2018) 045203

DVCS asymmetries @ CLAS

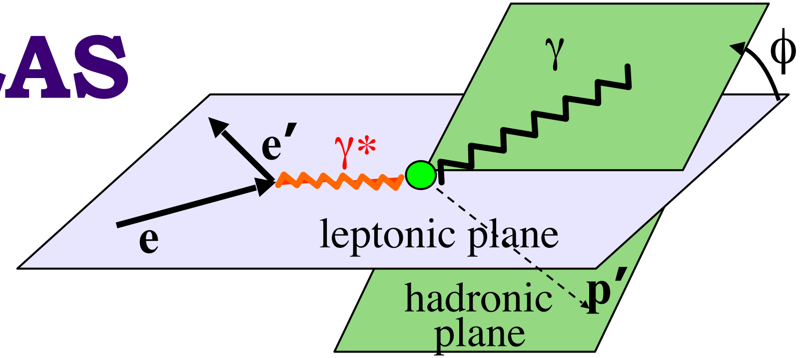

High statistics, large kinematic coverage, strong constraints on fits, simultaneous fit of BSA, TSA and DSA at common kinematics from the same dataset:

Beam-spin asymmetry (BSA): $\Delta\sigma_{LU} \sim \sin\phi\, \Im(F_1 H + \xi G_M \tilde{H} - \frac{t}{4M^2} F_2 E)\, d\phi$

Target-spin asymmetry: $\Delta\sigma_{UL} \sim \sin\phi\, \Im(F_1 \tilde{H} + \xi G_M (H + \frac{x_B}{2} E) - \xi \frac{t}{4M^2} F_2 \tilde{E} + \ldots)\, d\phi$

Double-spin asymmetry: $\Delta\sigma_{LL} \sim (A + B\cos\phi)\, \Re(F_1 \tilde{H} + \xi G_M (H + \frac{x_B}{2} E) + \ldots) d\phi$

F_1, F_2: Dirac, Pauli form factors

→ Constraints on CFFs H and $\tilde{H}$

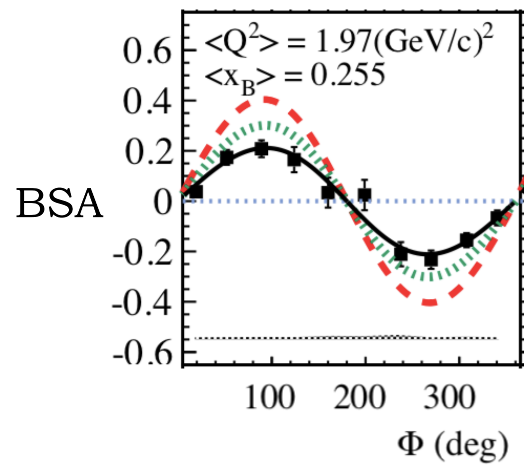

E. Seder *et al* (CLAS), ***PRL*** **114** (2015) 032001
S. Pisano *et al* (CLAS), ***PRD*** **91** (2015) 052014
F.-X. Girod *et al* (CLAS), ***PRL*** **100** (2008) 162002

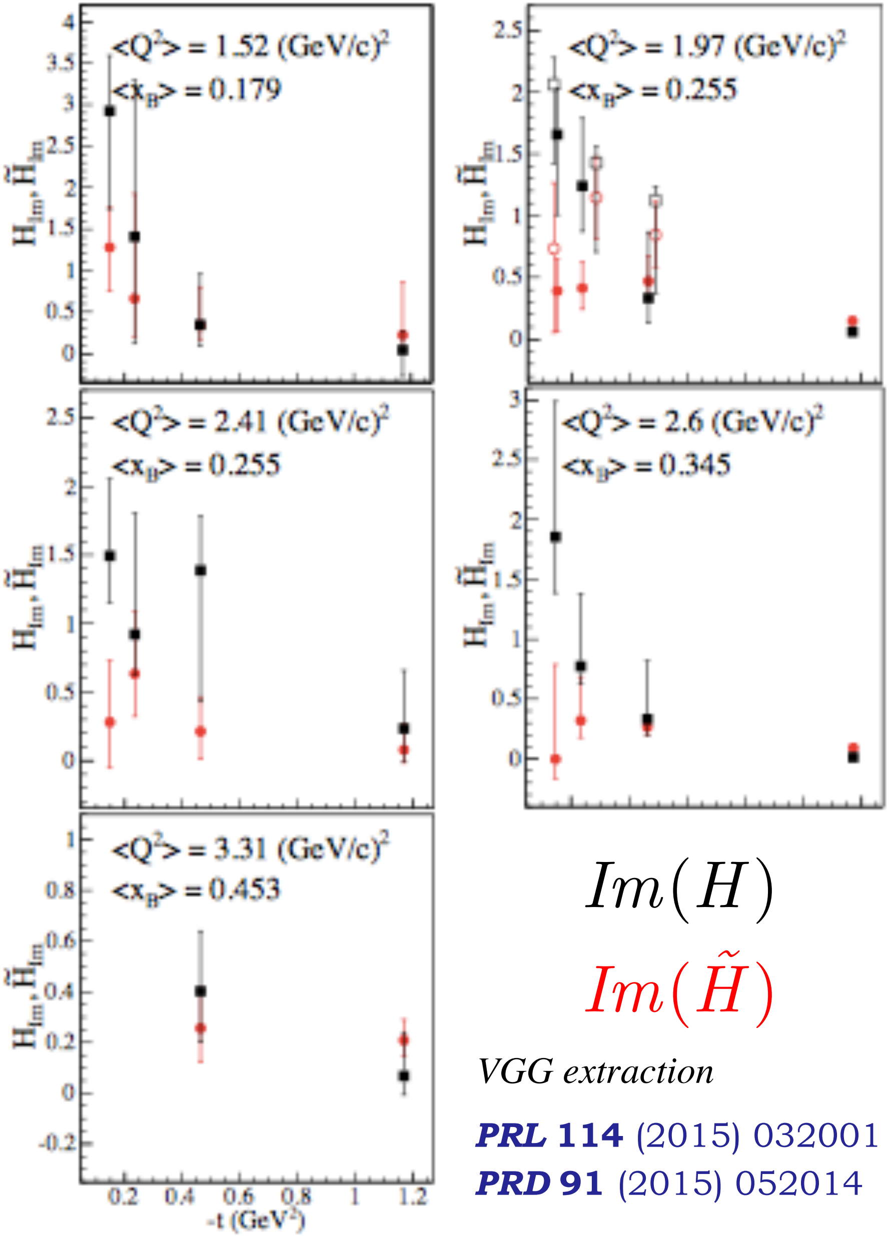

$Im(H)$

$Im(\tilde{H})$

VGG extraction

***PRL* 114** (2015) 032001
***PRD* 91** (2015) 052014

What can we learn from the asymmetries?

- Information on relative distributions of quark momenta (PDFs) and quark helicity, $\Delta q(x)$.

$$H(x,0,0) = q(x) \quad \tilde{H}(x,0,0) = \Delta q(x)$$

- Indications that axial charge is more concentrated than electromagnetic charge.

$$\int_{-1}^{+1} H dx = F_1$$

$$\int_{-1}^{+1} \tilde{H}\; dx = G_A$$

Answers will hinge on a global analysis of all available data: eg: PARTONS framework.

H. Moutarde *et al.*, Eur. Phys. J C78, 890 (2018)

GPDs and nucleon spin

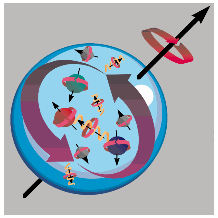

$$J_N = \frac{1}{2} = \frac{1}{2}\Sigma_q + L_q + J_g$$

- Ji's relation: $J^q = \frac{1}{2} - J^g = \frac{1}{2}\int_{-1}^{1} x dx \left\{ H^q(x,\xi,0) + E^q(x,\xi,0) \right\}$

- H^q in DVCS off the proton, first experimental constraint on E^q from neutron-DVCS beam-spin asymmetry.

M. Mazouz et al, PRL 99 (2007) 242501

- Gives constraints on orbital angular momentum of quarks: **the spin puzzle.**

- Rosenbluth separation of interference & DVCS terms underway in neutron-DVCS cross-sections: E_e = 4.5 and 5.5 GeV (experiment E08-025).

LD_2 target $\langle Q^2 \rangle$ = 1.75 GeV^2 $\langle x_B \rangle$ = 0.36

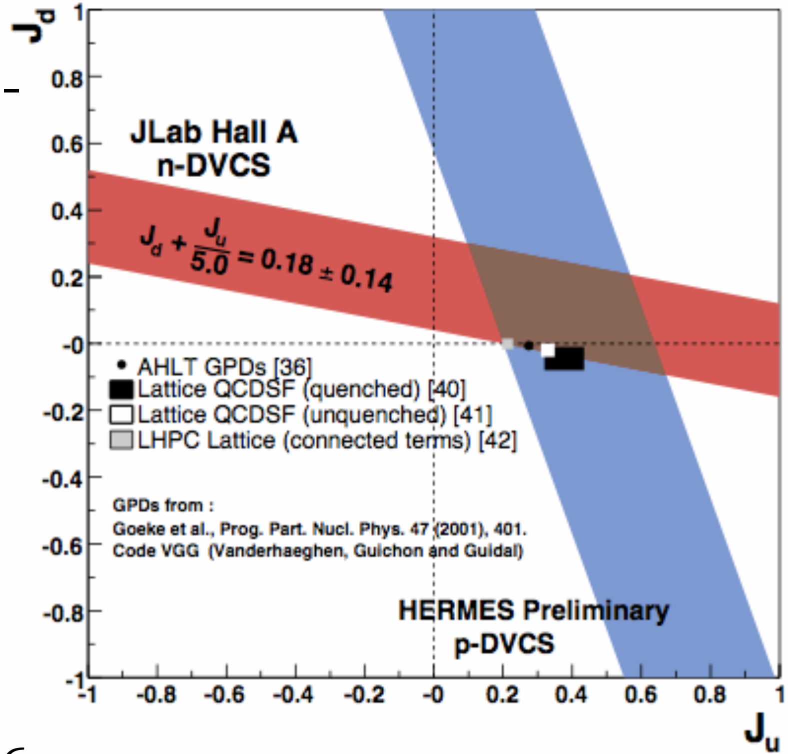

Towards nucleon tomography: local fits

Quasi model-independent extraction of CFFs based on a local fit:

- Set 8 CFFs as free parameters to fit, at each (x_B,t) point, the available observables.
- Limits imposed within +/- 5 times the VGG model predictions (Vanderhaeghen-Guichon-Guidal).
- Leading-twist DVCS amplitude parametrisation based on Double Distributions.

The best constraints in fits to CLAS data were obtained on H_{Im}.

Parametrise its dependence on t:

$$H_{Im}(\xi,t) = A(\xi)e^{B(\xi)t}$$

Relates to quark density

Inverse relation to spatial distribution

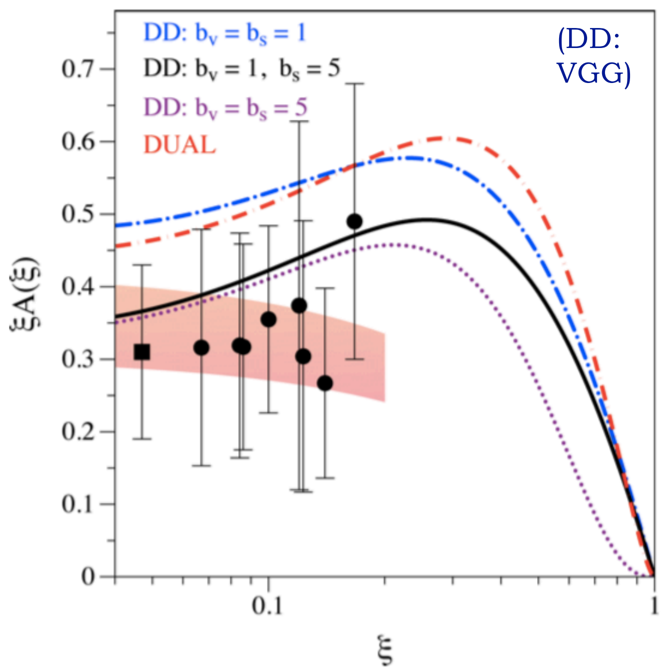

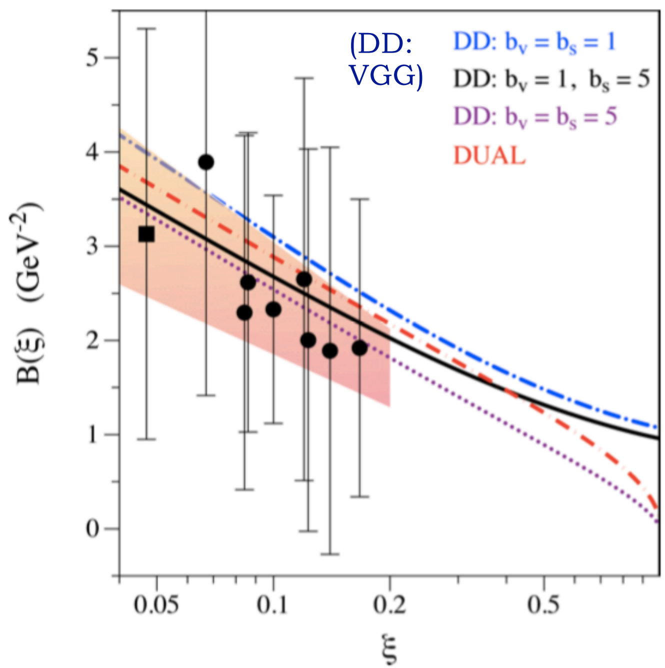

R. Dupré *et al.*, Eur. Phys. J **A 53** (2017) 171

Towards nucleon tomography: local fits

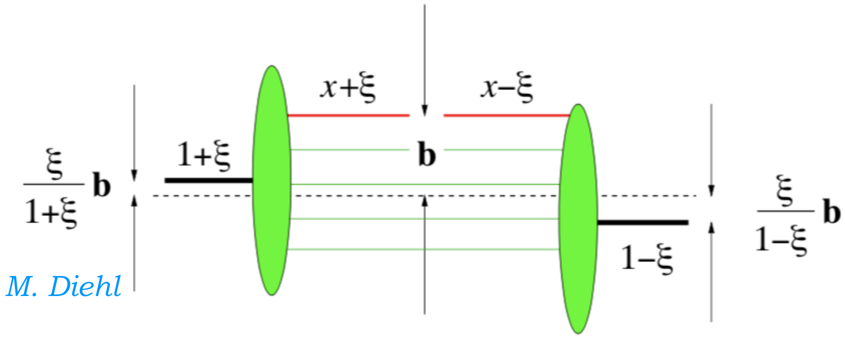

Transverse parton position interpretation only at $\xi = 0$.

Relating the impact parameter to helicity-averaged transverse distribution:

$\boxed{t = \Delta^2}$

$$\rho^q(x, \mathbf{b}_\perp) = \int \frac{d^2\boldsymbol{\Delta}_\perp}{(2\pi)^2} e^{-i\mathbf{b}_\perp\cdot\boldsymbol{\Delta}_\perp} H_-^q(x, 0, -\boldsymbol{\Delta}_\perp{}^2)$$

$$H_-^q(x, 0, t) \equiv H^q(x, 0, t) + H^q(-x, 0, t)$$

Transverse four-momentum transfer to nucleon

Assuming leading-twist and exponential dependence of GPD on t, using models to extrapolate to the zero skewness point $\xi = 0$ and assuming similar behaviour for u and d quarks there:

$$\langle b_\perp^2 \rangle^q(x) = -4 \frac{\partial}{\partial \boldsymbol{\Delta}_\perp^2} \ln H_-^q(x, 0, -\boldsymbol{\Delta}_\perp{}^2)\Big|_{\boldsymbol{\Delta}_\perp = 0}$$

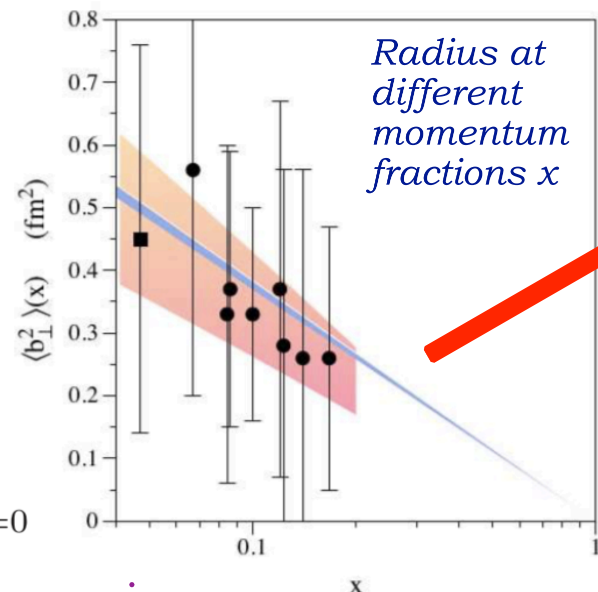

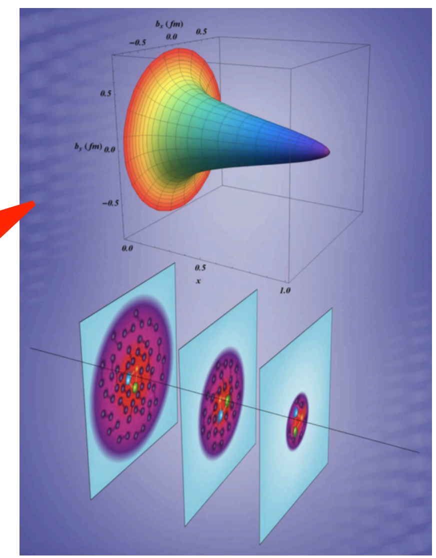

Tentative hints of 3D distributions are emerging.

We need more data from JLab @ 11 GeV!

R. Dupré *et al.*, Eur. Phys. J **A 53,** (2017) 171

Towards nucleon tomography: global fits

- PARTONS framework: global fits and neural networks to minimise model-dependence in the extraction of CFFs.

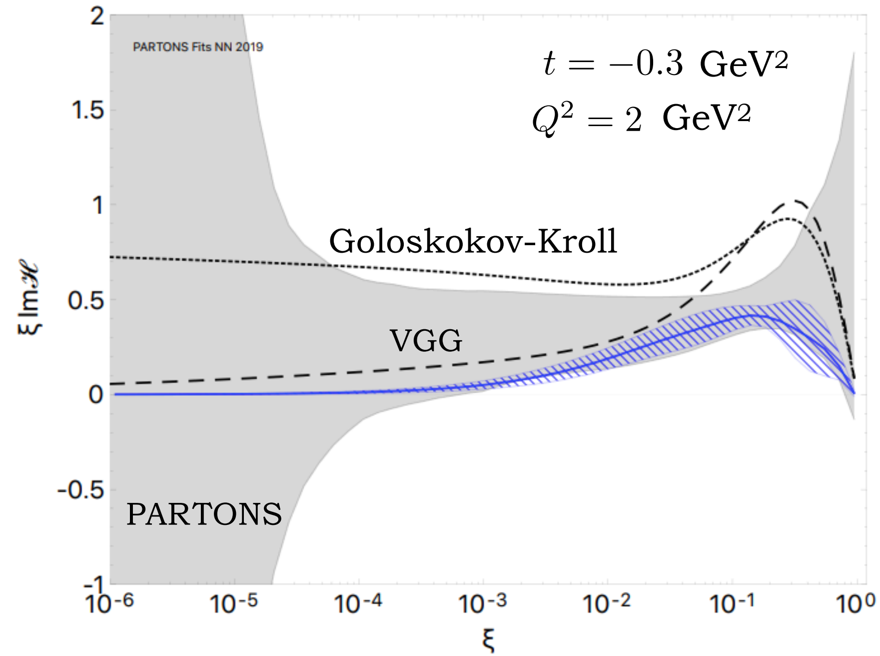

H. Moutarde *et al.*, Eur. Phys. J C79, 614 (2019)

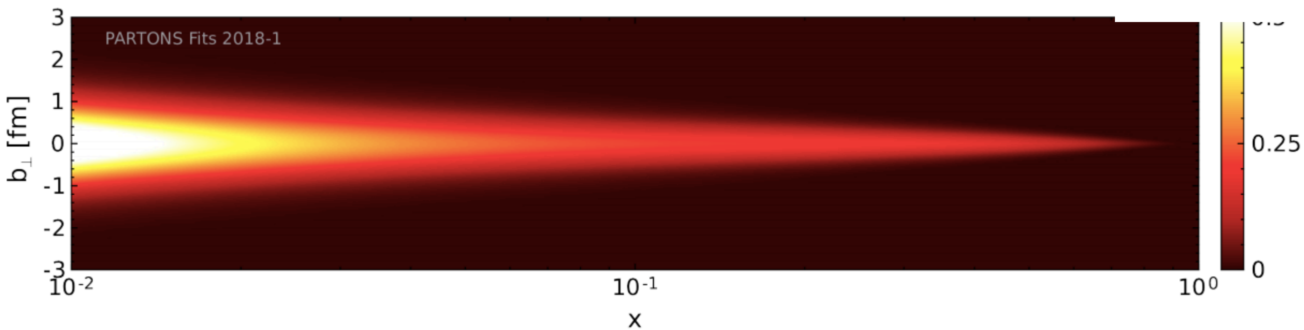

u

Inclusion of other channels into PARTONS underway.

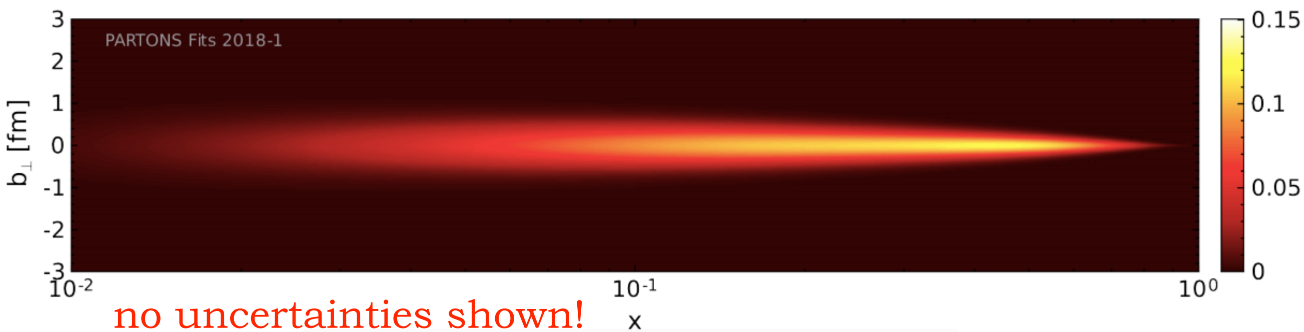

Δu_{val}

Framework in place: more data needed!

no uncertainties shown!

Image from Pawel Sznajder, IWHSS 2019

Imaging pressure within the nucleon

- GPDs provide indirect access to mechanical properties of the nucleon (encoded in the gravitational form factors, GFFs, of the energy-momentum tensor). X. D. Ji, PR**D 55**, 7114-7125 (1997) M. Polyakov, PL**B 555**, 57-62 (2016)

- Three scalar GFFs, functions of *t*: encode pressure and shear forces ($d_1(t)$), mass ($M_2(t)$) and angular momentum distributions ($J(t)$).

- Can be related to GPDs via sum rules:

$$\int x\,[H(x,\xi,t)+E(x,\xi,t)]\,\mathrm{d}x = 2J(t)$$

$$\int xH(x,\xi,t)\mathrm{d}x = M_2(t)+\frac{4}{5}\xi^2 d_1(t)$$

- Model-dependent extraction

- Neural net analysis, however: d-term almost unconstrained and consistent with zero

Possibility of extracting pressure distributions! But more data needed.

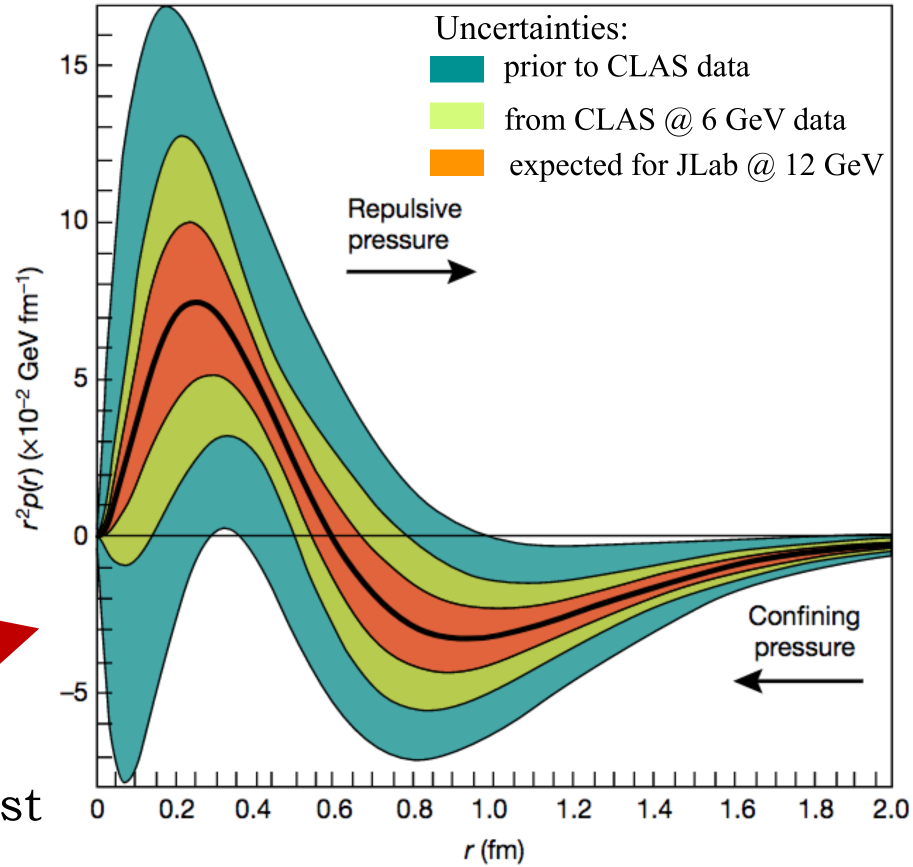

V. Burkert, L. Elouadrhiri, F.-X. Girod, Nature **557**, 396-399 (2018)

K. Kumerički, Nature **570**, E1-E2 (2019)

DVCS in Hall C

Detect electron with (Super) High Momentum Spectrometer, (S)HMS.

Detect photon in $PbWO_4$ calorimeter.

Sweeping magnet to reduce backgrounds in calorimeter.

Reconstruct recoiling proton through missing mass.

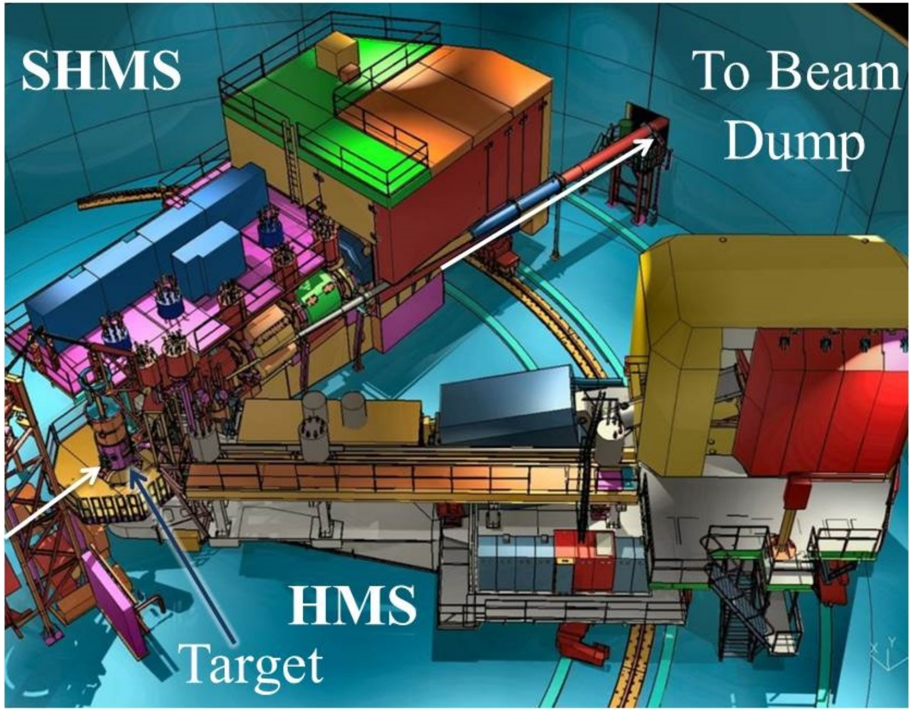

DVCS in Hall C

Detect electron with (Super) High Momentum Spectrometer, (S)HMS.

Detect photon in $PbWO_4$ calorimeter.

Sweeping magnet to red
backgrounds in cal

Reconstruct recoi
through missing m

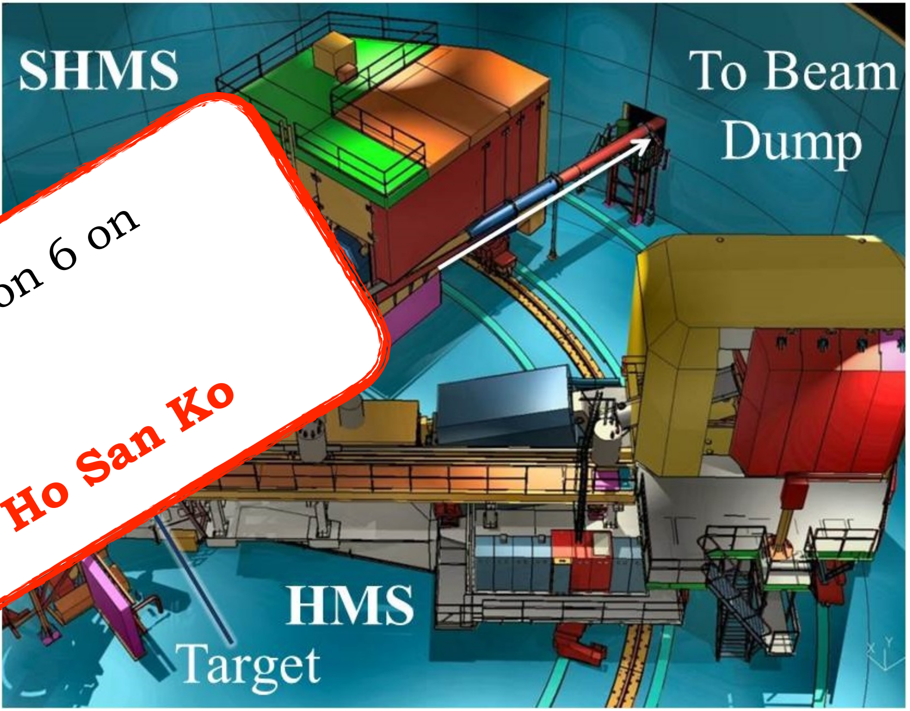

See talk in parallel session 6 on Tuesday 8.55am:

DVCS in Hall C: Ho San Ko

11 GeV era DVCS Cross-sections: Halls A and C

Experiments:
E12-06-114 (Hall A, 100 days),
E12-13-010 (Hall C, 53 days)
C. Muñoz Camacho et al.,
C. Hyde et al.

Unpolarised liquid H_2 target:

- Beam energies: 6.6, 8.8, 11 GeV
- Scans of Q^2 at fixed x_B.
- Hall A: aim for absolute cross-sections with 4% relative precision.

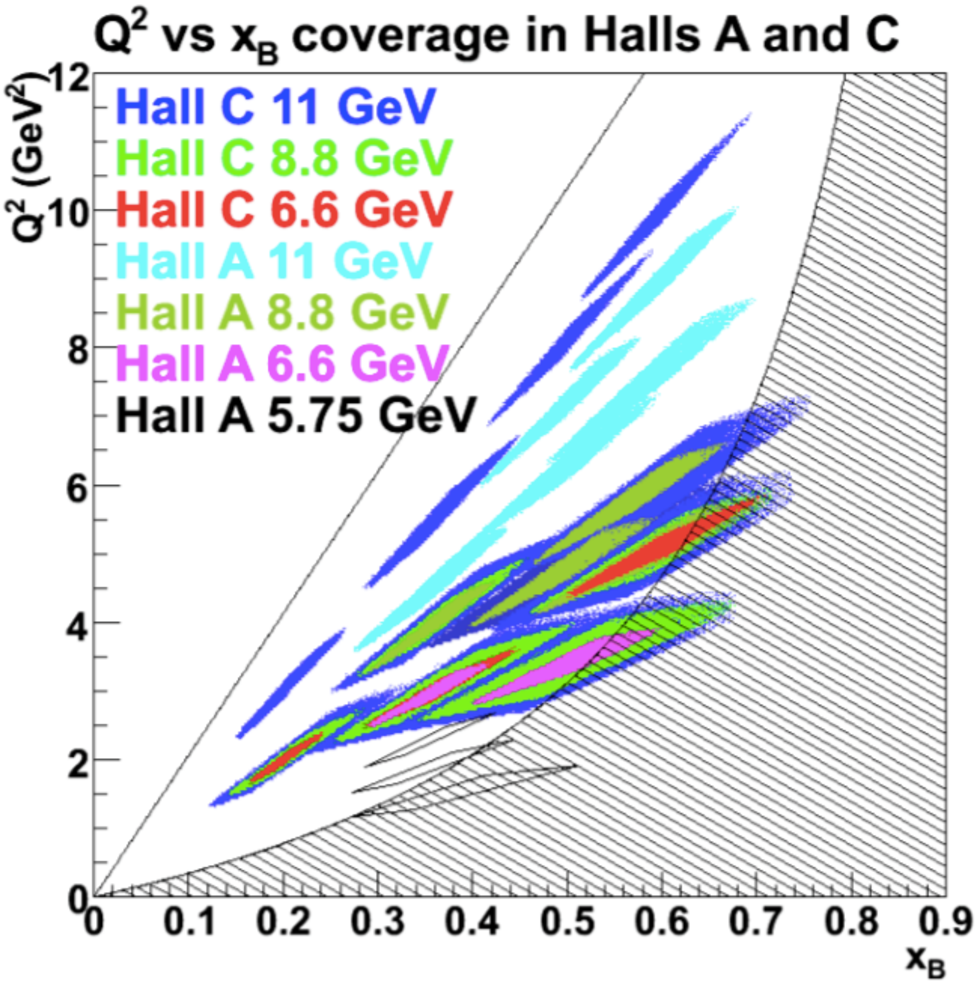

✱ Azimuthal, energy and helicity dependencies of cross-section to separate $|T_{DVCS}|^2$ and interference contributions in a wide kinematic coverage.

✱ Separate *Re* and *Im* parts of the DVCS amplitude.

11 GeV era: DVCS with CLAS12

E12-06-119: Unpolarised liquid H_2 target

Beam-spin asymmetry → $Im(H_p)$

First experiment with CLAS12! Almost complete

P_{beam} = 85%
L = 10^{35} $cm^{-2}s^{-1}$
$1 < Q^2 < 10$ GeV^2
$0.1 < x_B < 0.65$
$-t_{min} < -t < 2.5$ GeV^2

E12-16-010: Unpolarised liquid H_2 target

Beam energy: 6.6 GeV, 8.8 GeV Almost complete

E12-11-003: Unpolarised liquid D_2 target

$$e + d \rightarrow e' + \gamma + n + (p_s)$$

Beam-spin asymmetry in neutron-DVCS → $Im(E_n)$

Running this year!

E12-12-010: Transversely polarised HD target.

Target-spin asymmetries → $Im(E_p)$

~2023?

E12-06-109: Longitudinally polarised NH_3 and ND_3 targets

- Dynamic Nuclear Polarisation (DNP) of target material, cooled in a *He* evaporation cryostat.
- P_{proton} = 80%, $P_{deuteron}$ up to 50%

Target-spin asymmetry in proton- and neutron-DVCS → $Im(\widetilde{H}_p)$, $Im(H_n)$

~ 2021

DVCS with CLAS12

E12-06-119: Unpolarised liquid H_2 target

Beam-spin asymmetry → ***Im*(H_p)**

First experiment with CLAS12! Almost complete

P_{beam} = 85%
L = 10^{35} $cm^{-2}s^{-1}$
1< Q^2 < 10 GeV^2
0.1 <x_B< 0.65
$-t_{min}$< $-t$ < 2.5 GeV^2

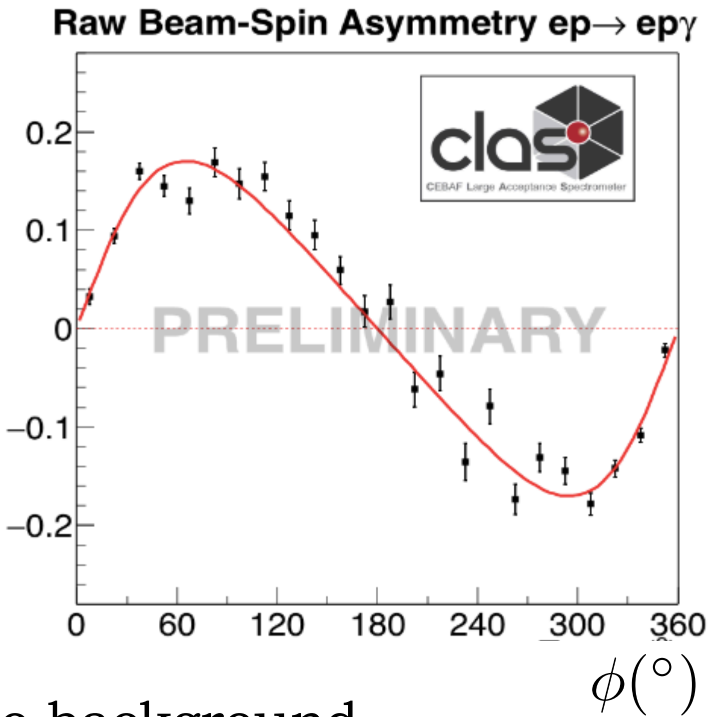

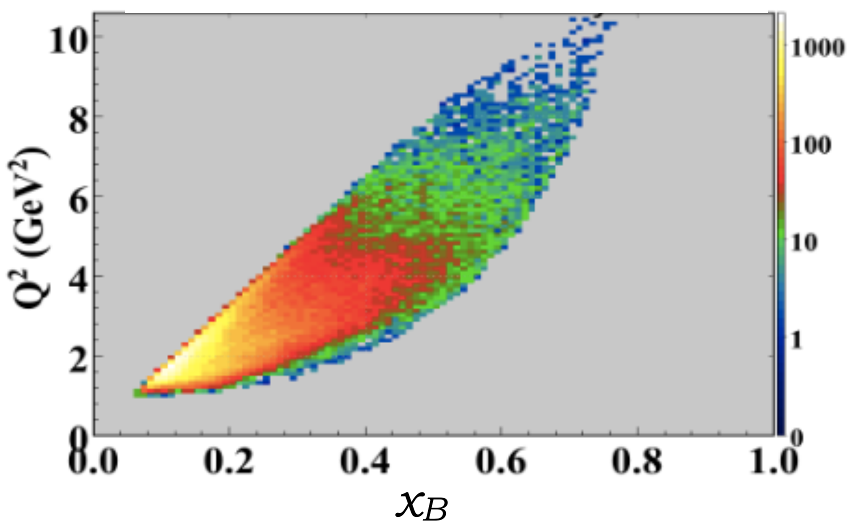

No background subtraction

Guillaume Christiaens

Neutron DVCS @ 11 GeV: sensitivity to J_q

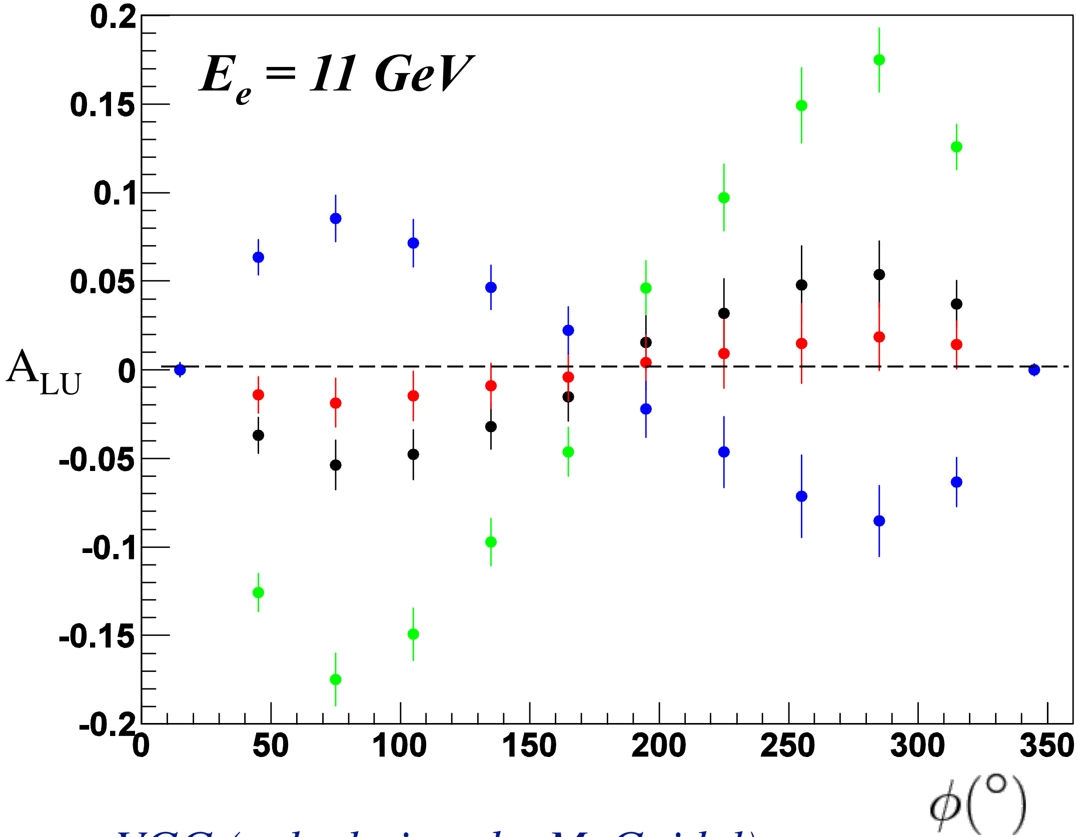

$J_u = 0.3$, $J_d = -0.1$ $J_u = 0.3$, $J_d = 0.1$

$J_u = 0.1$, $J_d = 0.1$ $J_u = 0.3$, $J_d = 0.3$

- At 11 GeV, beam spin asymmetry (A_{LU}) in neutron DVCS *is* very sensitive to J_u, J_d

- Dedicated neutron detector added to CLAS12: Central Neutron Detector

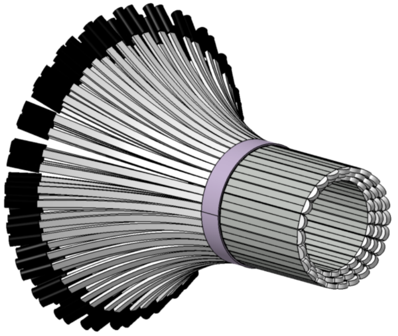

VGG (calculations by M. Guidal)

Fixed kinematics: $x_B = 0.17$ $Q^2 = 2\ \mathrm{GeV}^2$ $t = -0.4\ \mathrm{GeV}^2$

DVCS on ^{4}He: CLAS12 with ALERT

Experiment E12-17-012: Measurement of BSA in coherent DVCS from a *^{4}He* target: partonic structure of nuclei.

Z.-E. Meziani et al.

✱ Spin 0 target, so at leading twist only one chiral-even GPD: $\mathbf{H_A}$.

11 GeV beam, 80% polarised.
Gas target straw @ 3 atm
L = 6 x 10^{34} nucleon cm^{-2}s^{-1} with 1000 nA beam.

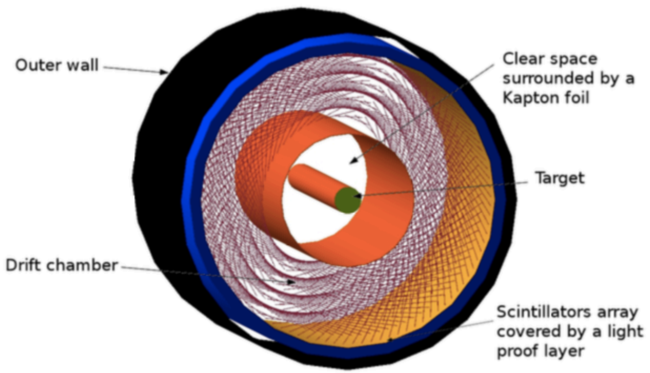

CLAS12 + ALERT: central recoil detector

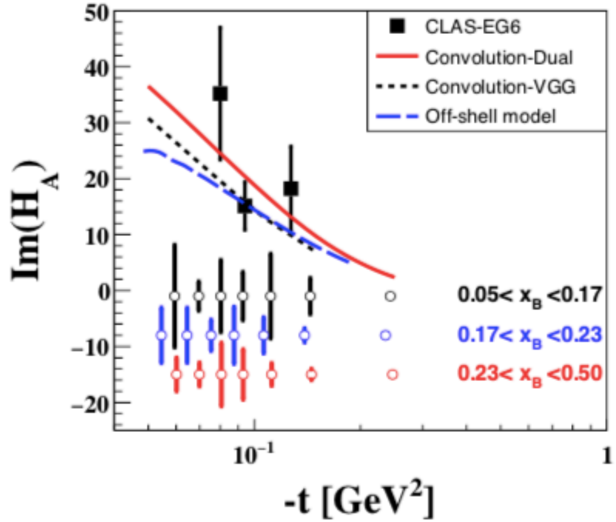

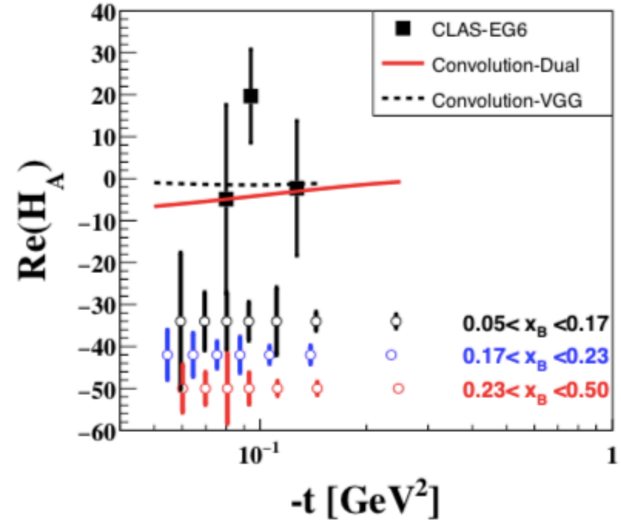

Experiment E12-17-012B
W. Armstrong et al.

Incoherent, spectator-tagged DVCS on *^{4}He* and *d*.

COMPASS @ Cern (SPS)

Compact **M**uon and **P**roton **A**pparatus for **S**tructure and **S**prectroscopy

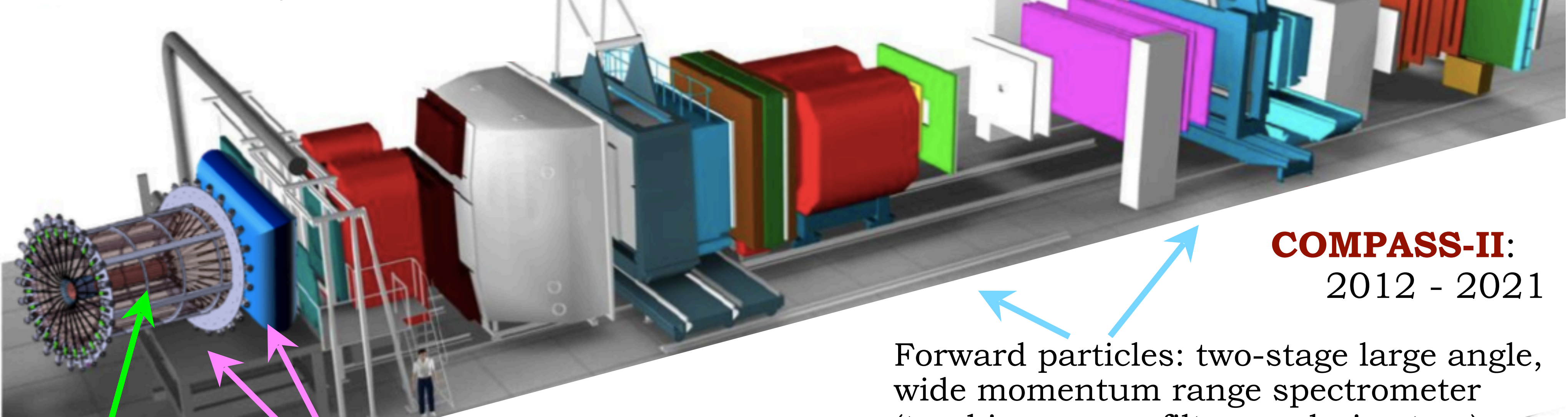

COMPASS-II: 2012 - 2021

Forward particles: two-stage large angle, wide momentum range spectrometer (tracking, muon filters, calorimeters).

2.5m liquid *H_2* target

Upgrades: new scintillator ToF CAMERA for recoil proton detection & new EM calorimeter.

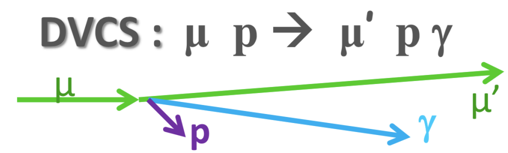

Full exclusive reconstruction

- 160 GeV 80% polarised μ^+/μ^-
- $\sim 4 \times 10^8 \mu/spill$, 9.6s/40s duty cycle

Data:
- 2008 & 2009: two v. short test runs, 40 cm LH_2 target.
- COMPASS-II: 1 month in 2012, 6 months in 2016 & 2017 each (GPD **H**).
- 2022+: transversely pol. NH_3 target (GPD **E**). LOI stage...

DVCS @ COMPASS (2012 run)

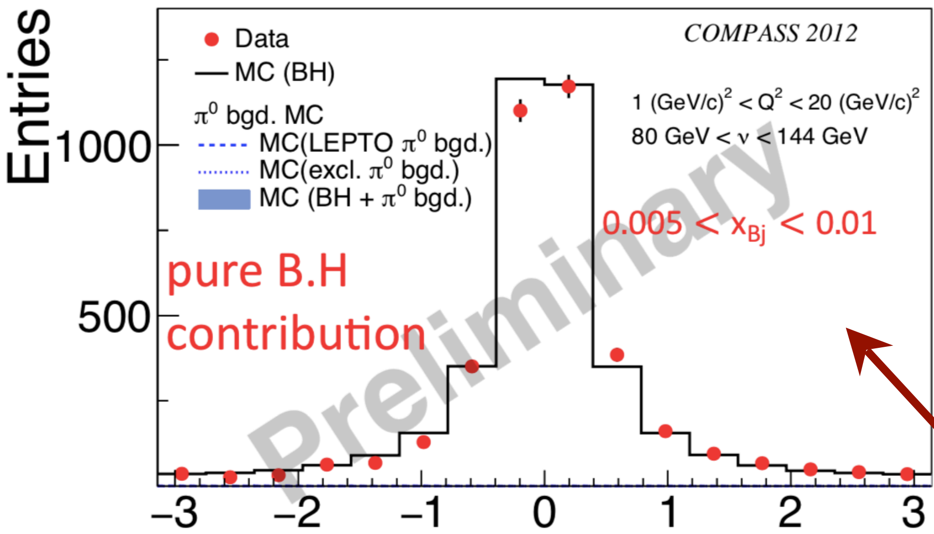

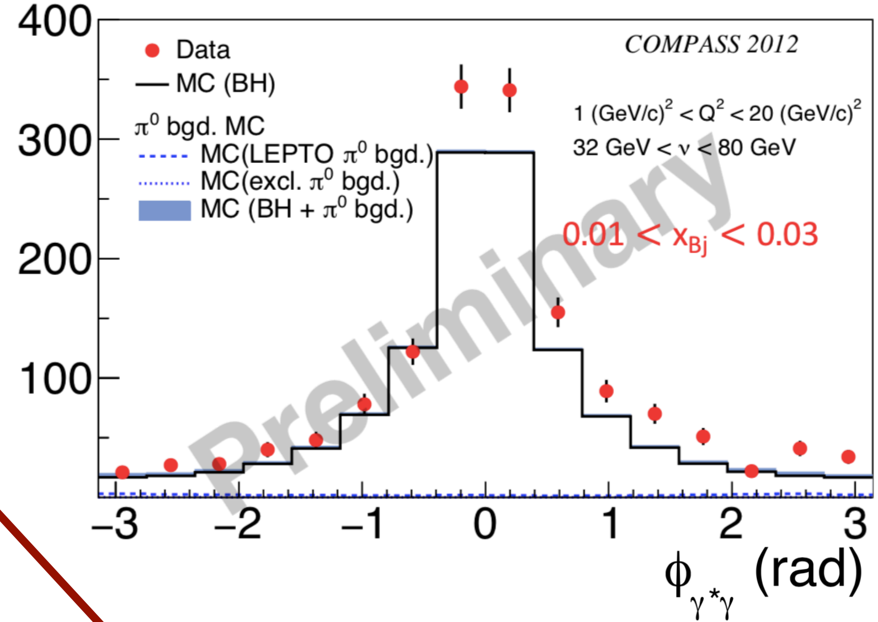

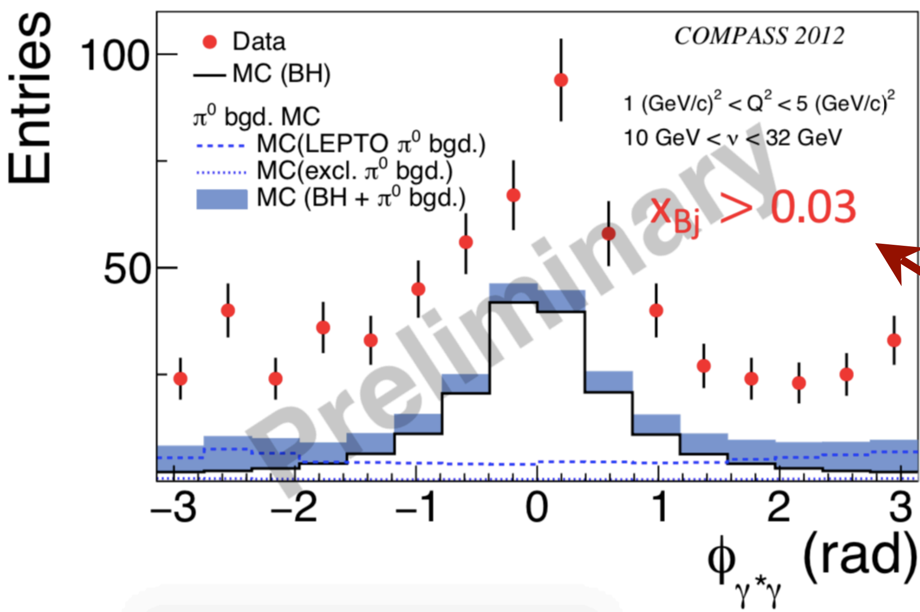

Bethe-Heitler dominates at very low x_B

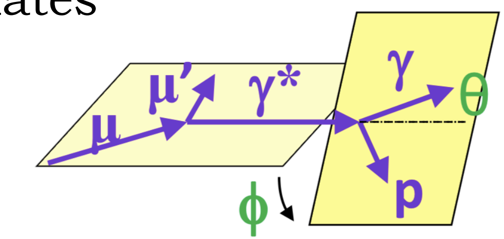

DVCS dominates at these kinematics

Slide mash-up from N. d'Hose and A. Ferrero

DVCS x-section and t-slope extraction

Kinematically constrained vertex fit applied

$d\sigma^{DVCS}/dt = e^{-B|t|}$

Slide from: A. Ferrero @ SPIN 2018

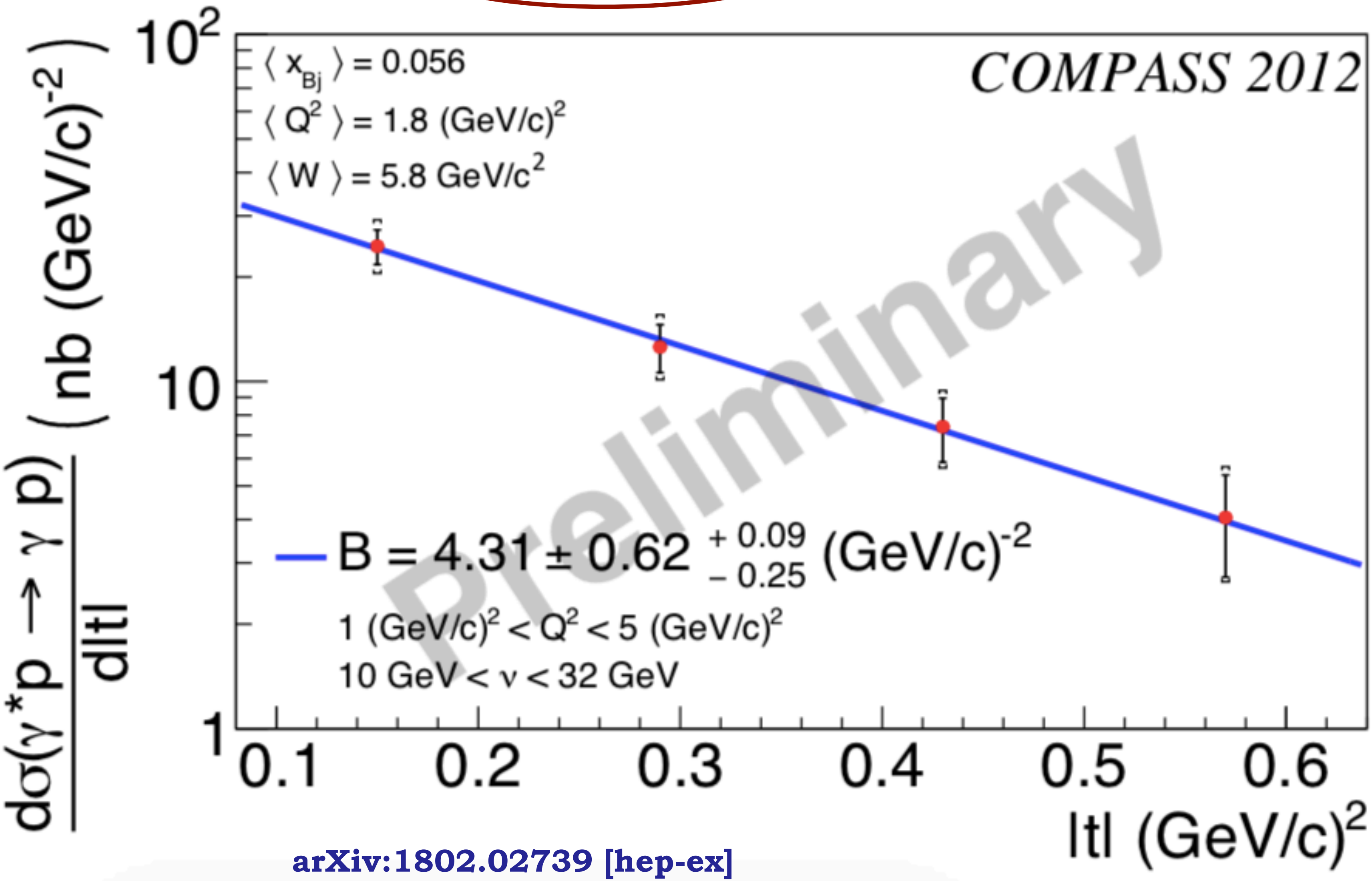

arXiv:1802.02739 [hep-ex]

Tomography of sea quarks

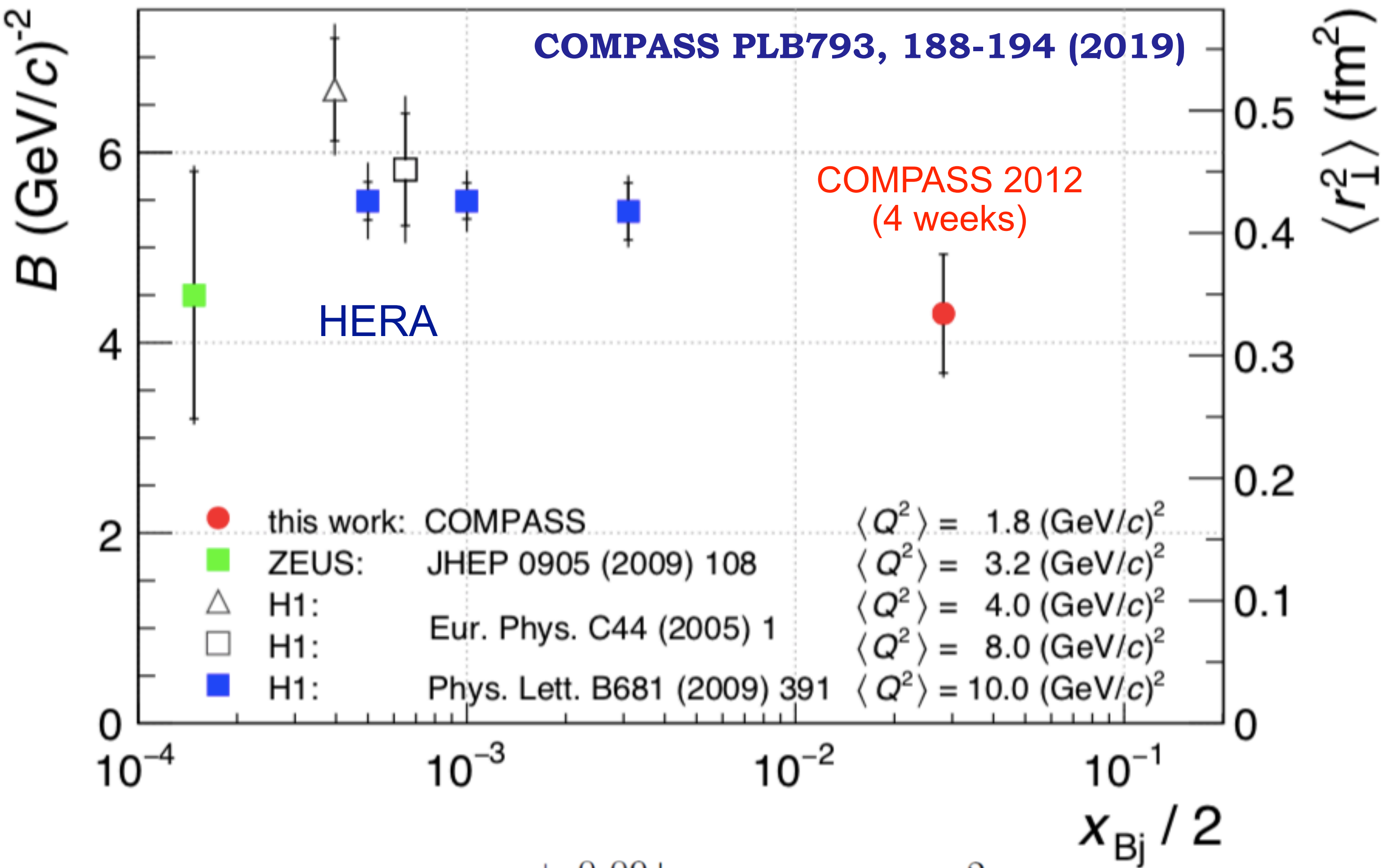

$1 < Q^2 < 5$ GeV^2

$<Q^2> = 1.8$ GeV^2

$<x_B> = 0.056$

Integrated luminosity: 42.4 pb^{-1}

10 times more stats in 2016-17 runs

$$B = (4.31 \pm 0.62_{\mathrm{stat}} \,{}^{+\,0.09}_{-\,0.25}\big|_{\mathrm{sys}})\,(\mathrm{GeV}/c)^{-2}$$

$$\sqrt{\langle r_\perp^2 \rangle} = (0.58 \pm 0.04_{\mathrm{stat}} \,{}^{+\,0.01}_{-\,0.02}\big|_{\mathrm{sys}} \pm 0.04_{\mathrm{model}})\,\mathrm{fm}$$

at average $x_B = 0.056$

$<r_\perp^2(x_B)> \approx 2B(x_B)$

for small x_B

Tomography of sea quarks

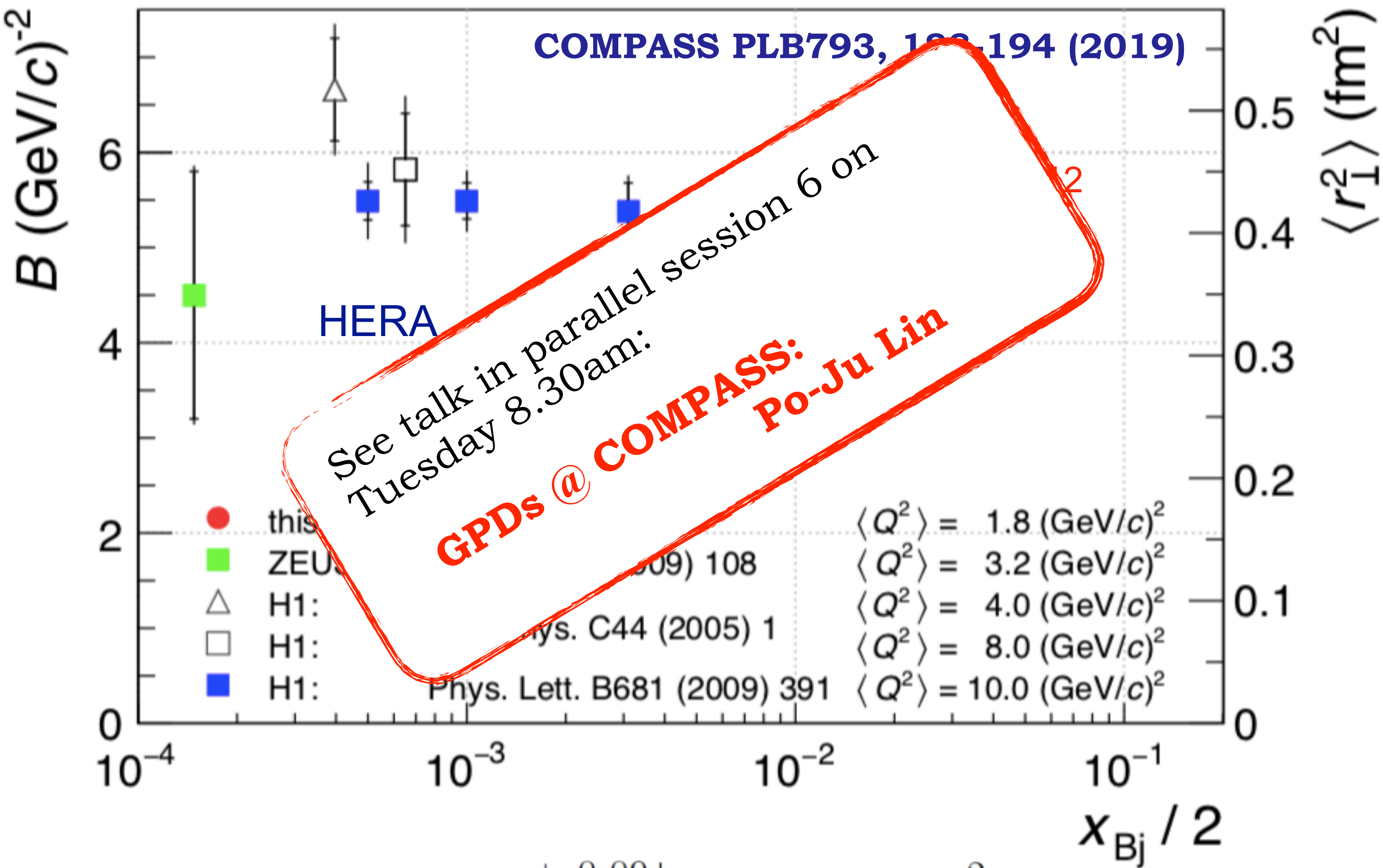

$1 < Q^2 < 5$ GeV^2

$\langle Q^2 \rangle = 1.8$ GeV^2

$\langle x_B \rangle = 0.056$

Integrated luminosity: 42.4 pb^{-1}

10 times more stats in 2016-17 runs

$$B = (4.31 \pm 0.62_{\rm stat} \,{}^{+0.09}_{-0.25}\big|_{\rm sys})\,({\rm GeV}/c)^{-2}$$

$$\sqrt{\langle r_\perp^2 \rangle} = (0.58 \pm 0.04_{\rm stat} \,{}^{+0.01}_{-0.02}\big|_{\rm sys} \pm 0.04_{\rm model})\,{\rm fm}$$

at average $x_B = 0.056$

$$\langle r_\perp^2(x_B)\rangle \approx 2B(x_B)$$

for small x_B

Deeply Virtual Meson Production

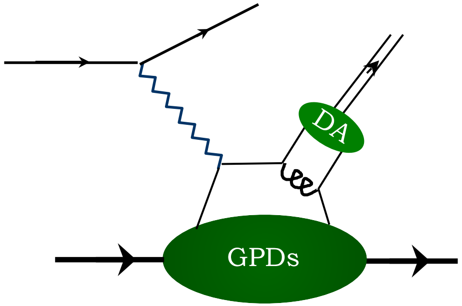

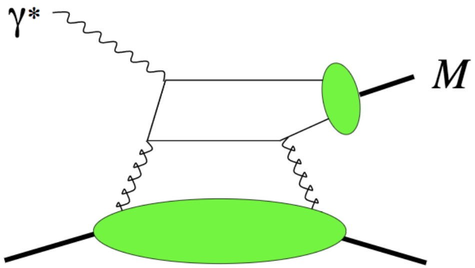

* Amplitude depends on convolution of GPDs and meson Distribution Amplitudes (DA).

* At leading order & twist, access to the four chiral-even (parton helicity-conserving) GPDs:

  - Pseudo-scalar mesons: $\tilde{H}^q, \tilde{E}^q(x, \xi, t)$
  - Vector mesons: $H^q, E^q, H^g, E^g(x, \xi, t)$

Gluon GPDs!

DVMP enables flavour decomposition of quark GPDs and gives access to gluon GPDs

Caveats:

- factorisation established only for longitudinal photons,
- factorisation sets in at a higher scale than in DVCS,
- DA not entirely understood

Extracting GPDs from DVMP is hard!

DVMP Cross-section

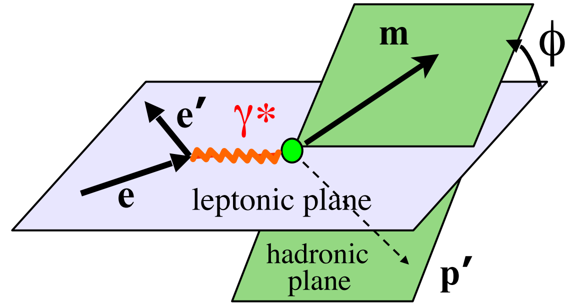

Virtual photon flux

unpolarised

$$\frac{2\pi}{\Gamma}\frac{d^4\sigma}{dQ^2 dx_B dt d\phi_{meson}} = \boxed{\sigma_T + \epsilon\sigma_L + \epsilon\sigma_{TT}\cos 2\phi + \sqrt{\epsilon(1+\epsilon)}\sigma_{LT}\cos\phi}$$

polarised beam $\rightarrow$ $\boxed{+P_b\sqrt{\epsilon(1-\epsilon)}\sigma_{LT'}\sin\phi}$

longitudinally polarised target $\rightarrow$ $\boxed{+P_{tg}\left(\sqrt{\epsilon(1+\epsilon)}\sigma_{UL}^{\sin\phi}\sin\phi + \epsilon\sigma_{UL}^{\sin 2\phi}\sin 2\phi\right)}$

Target and beam longitudinally polarised $\rightarrow$ $\boxed{+P_b P_{tg}\left(\sqrt{1-\epsilon^2}\sigma_{LL} + \sqrt{\epsilon(1-\epsilon)}\sigma_{LL}^{\cos\phi}\cos\phi\right)}$

ϵ: ratio of the fluxes of longitudinally (L) and transversely (T) polarised virtual photons.

σ_i: structure functions, related to scattering amplitudes (i = L,T,LT, ...), *eg:*

$$\frac{d\sigma_L}{dt} = \frac{4\pi\alpha}{k'}\frac{1}{Q^6}\left\{(1-\xi^2)|\langle\tilde{H}\rangle|^2 - 2\xi^2\mathrm{Re}[\langle\tilde{H}\rangle^*\langle\tilde{E}\rangle] - \frac{t'}{4m^2}\xi^2|\langle\tilde{E}\rangle|^2\right\}$$

where $\langle F\rangle \equiv \sum_\lambda \int_{-1}^{1} dx\,\underbrace{\mathcal{H}_{\mu'\lambda'\mu\lambda}}_{\text{hard-scattering kernel}}\,\underbrace{F}_{\text{GPD}}$

Transversity GPDs

- For pseudo-scalar mesons, access four chiral-odd (parton helicity-flipping) transversity GPDs (via convolutions of leading-twist GPDs with twist-3 meson DA): $E_T^q, \tilde{E}_T^q, H_T^q, \tilde{H}_T^q(x,\xi,t)$

  Appear in DVMP amplitude when virtual photon has transverse polarisation — not accessible at LT in DVCS.

- $\tilde{E}_T$ can be related to the transverse anomalous magnetic moment:
$$\kappa_T = \int_{-1}^{+1} \tilde{E}_T(x,\xi,t=0)\,dx$$

- and H_T to the transversity distribution: $H_T(x,0,0) = h_1(x)$

  which describes distribution of transverse partons in a transverse nucleon

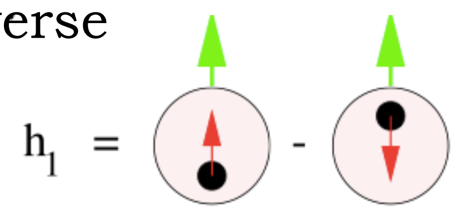

- The combination $\bar{E}_T = 2\tilde{H}_T + E_T$
  is related to spatial density of transversely polarised quarks in an unpolarised nucleon.

DVMP @ JLab

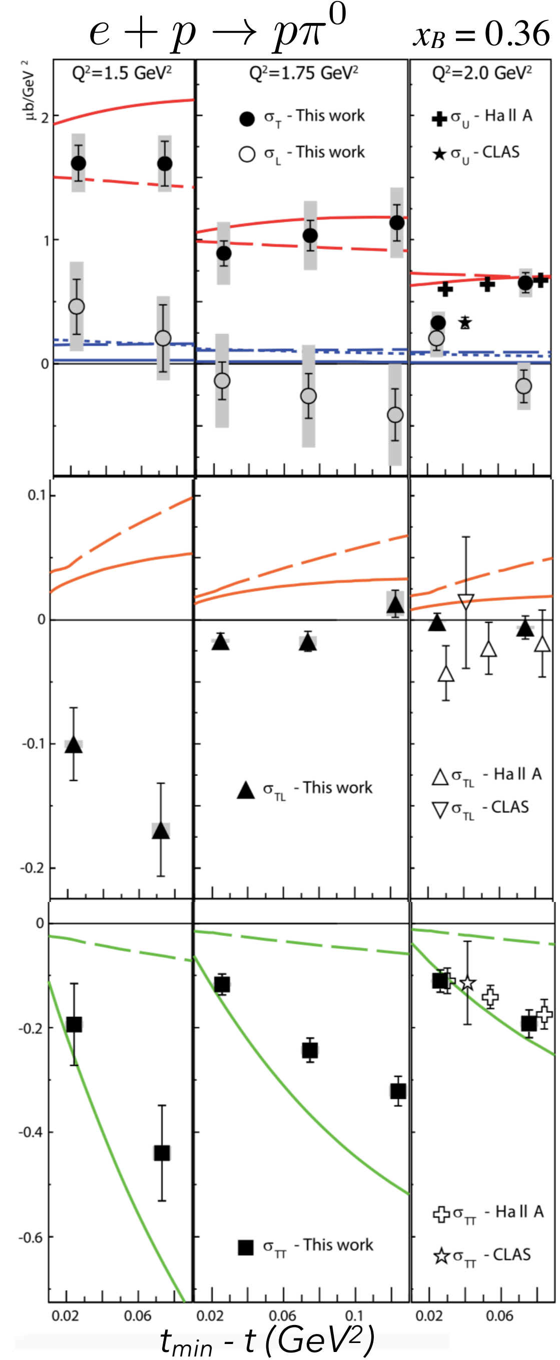

Vector mesons:

- L/T contributions to cross-sections separated by using helicity conservation between virtual photon and meson: strong deviations from leading-twist GPD formalism (higher-twist? evolution effects? meson-size corrections?)

- Gluonic GPD H^g dominates at small x: gluonic radius.

  → GPD extraction much cleaner for heavier quarks: J/Ψ

Too close to threshold @ JLab12, ideal for the Electron-Ion Collider!

Pseudo-scaler mesons:

- Separation of L/T contributions to cross-sections through Rosenbluth-like techniques / simultaneous fits at different kinematics.

- Strong transverse contribution observed in charged and neutral pion / K+ cross-sections: possible access to transversity GPDs.

—— Goloskokov Kroll (EPJ A47, 112 (2011))
- - - Goldstein, Hernandez, Liuti (PRD 84, 034007 (2011))

M. Defurne *et al*, ***PRL* 117** (2016) 262001

- Attempt at GPD flavour-separation using π^0 and η BSA.

Meson production at JLab 12 GeV

Cross-sections and spin asymmetries in the 11 GeV kinematics:

- Hard exclusive electroproduction of η and π^0 (E12-06-108, CLAS12)
- Exclusive ϕ meson electroproduction (E12-12-007, CLAS12)
- DVCS and neutral pion cross-sections (E12-13-010, Hall C)
- Scaling study of the L-T separated pion electroproduction cross-section (E12-07-105, Hall C)
- Studies of the L-T separated kaon electroproduction cross-section from 5-11 GeV (E12-09-011, Hall C)
- Near-threshold electroproduction of J/Ψ (E12-12-006, Hall A)
- Time-like Compton scattering and J/Ψ electroproduction (E12-12-001, CLAS12)

Meson production at COMPASS

Unpolarised target:

e p → e π^0 p $\quad \boxed{\dfrac{d^2\sigma}{dt\,d\phi_\pi} = \dfrac{1}{2\pi}\left[\boxed{\left(\dfrac{d\sigma_T}{dt} + \epsilon \dfrac{d\sigma_L}{dt}\right)} + \epsilon \cos 2\phi_\pi \boxed{\dfrac{d\sigma_{TT}}{dt}} + \sqrt{2\epsilon(1+\epsilon)}\cos\phi_\pi \boxed{\dfrac{d\sigma_{LT}}{dt}}\right]}$

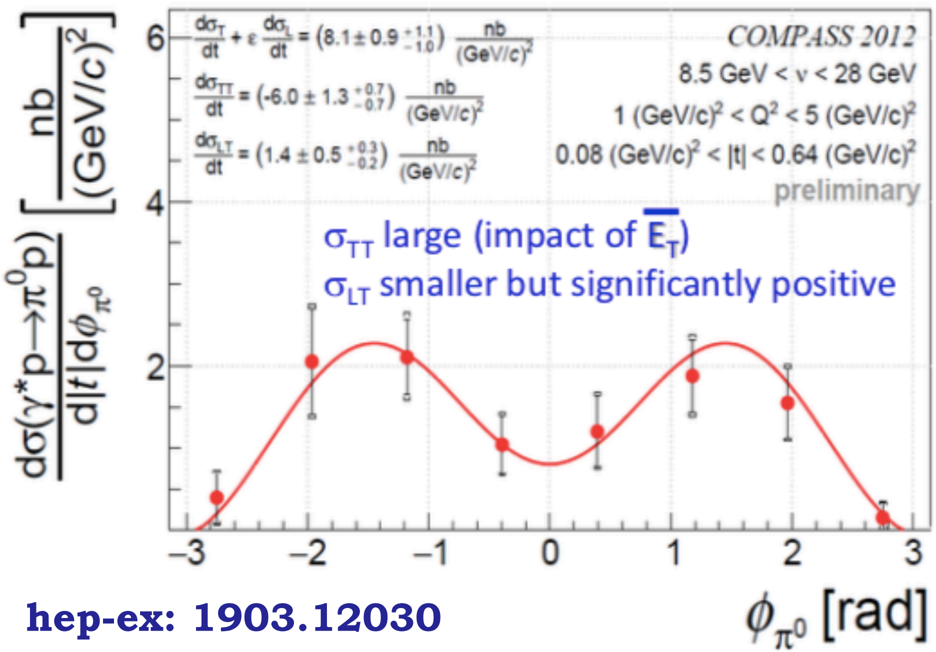

A dip at small t would indicate a large impact of $\overline{E}_T$

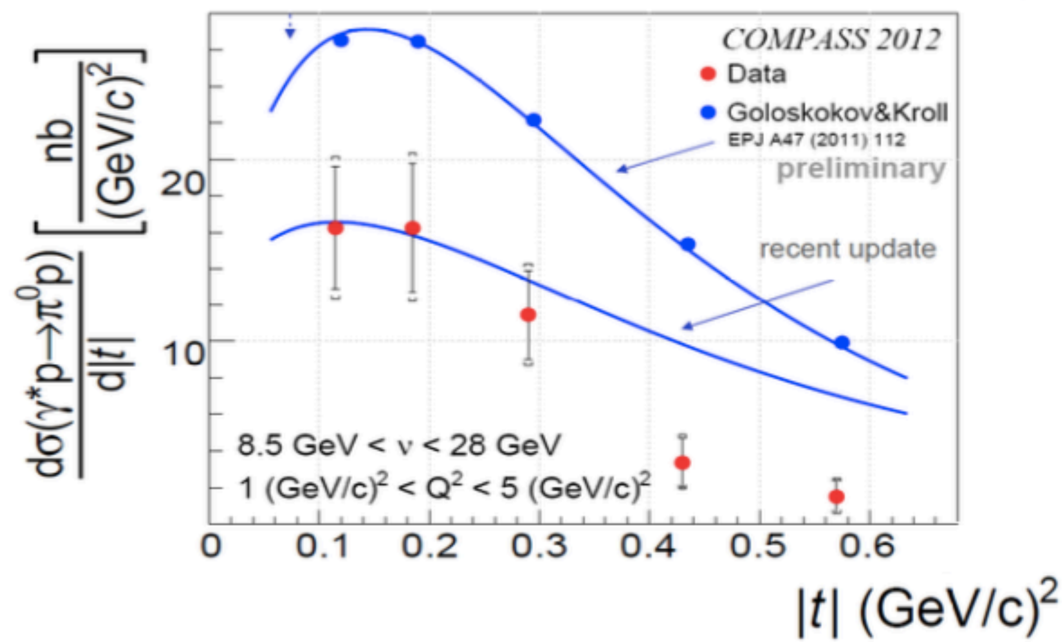

hep-ex: 1903.12030

Transversely-polarised target: ρ^0 and ω

Sensitivity to $\mathbf{H_T}$

NPB865, 1-20 (2012)
PLB731, 19 (2014)
NPB915, 454-475 (2017)

Slide from Po-Ju Lin, IWHSS 2019

Meson production at COMPASS

Unpolarised target:

$e\,p \rightarrow e\,\pi^0\,p$

$$\frac{d^2\sigma}{dt\,d\phi_\pi} = \frac{1}{2\pi}\left[\boxed{\left(\frac{d\sigma_T}{dt}+\epsilon\frac{d\sigma_L}{dt}\right)}+\epsilon\cos 2\phi_\pi \boxed{\frac{d\sigma_{TT}}{dt}}+\sqrt{2\epsilon(1+\epsilon)}\cos\phi_\pi\boxed{\frac{d\sigma_{LT}}{dt}}\right]$$

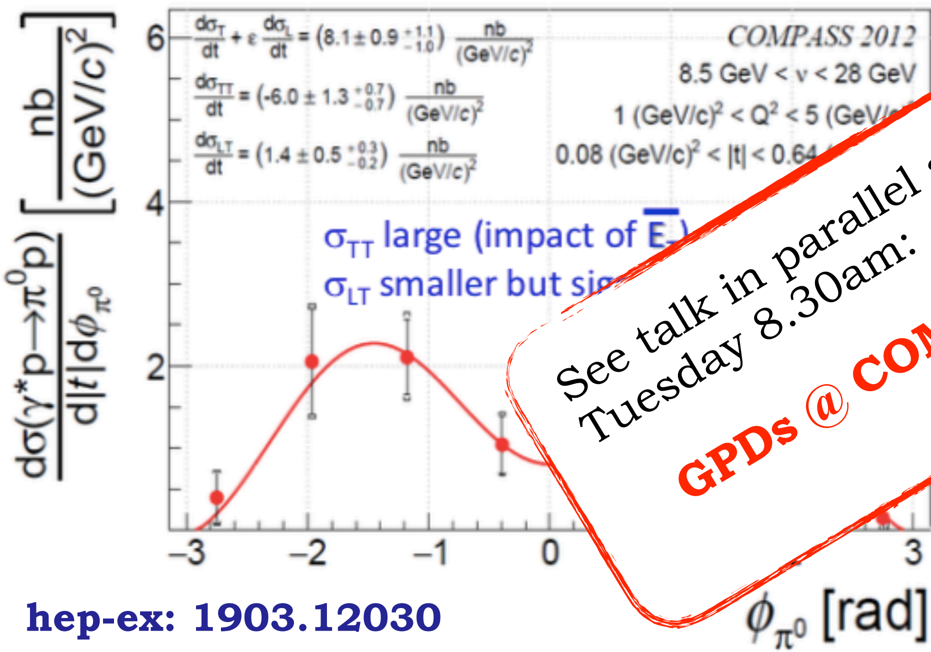

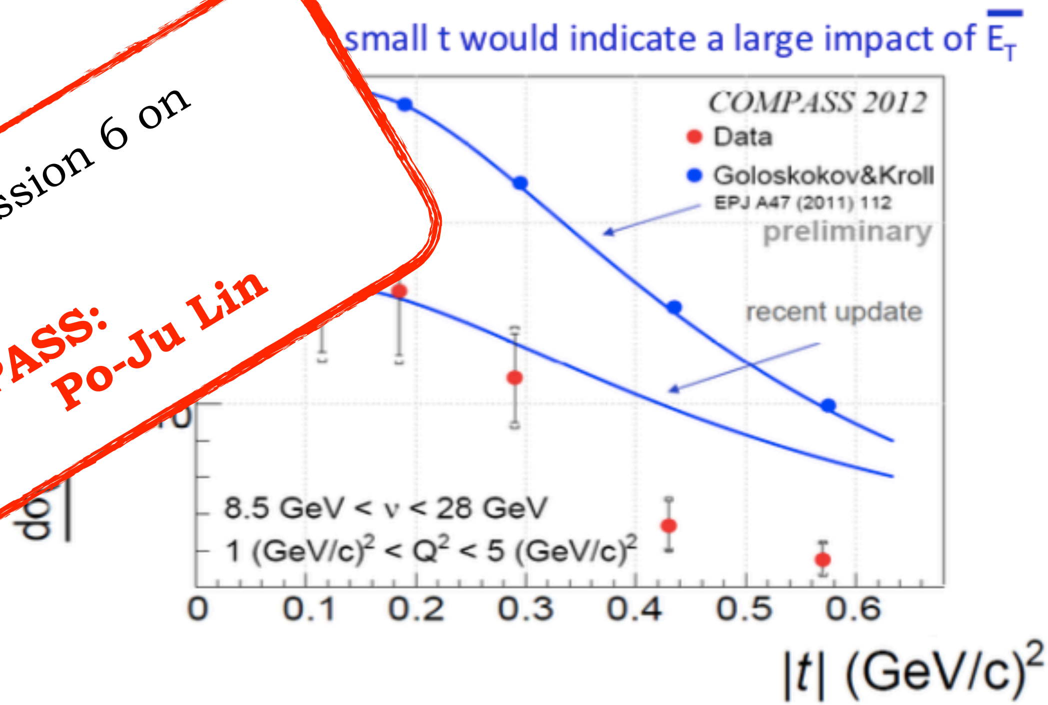

See talk in parallel session 6 on
Tuesday 8.30am:
GPDs @ COMPASS:
Po-Ju Lin

hep-ex: 1903.12030

Transversely-polarised target: ρ^0 and ω

Sensitivity to $\mathbf{H_T}$

NPB865, 1-20 (2012)
PLB731, 19 (2014)
NPB915, 454-475 (2017)

Slide from Po-Ju Lin, IWHSS 2019

Summary

- Valence quark region at Jefferson Lab, sea quarks at Hermes and COMPASS. Very low-x gluons await the Electron-Ion Collider.
- Factorisation appears to be applicable at JLab kinematics for DVCS, situation for HEMP/DVMP not so straight-forward.
- Constraints for GPD models, most strongly for H and $\tilde{H}$
- First attempts at tomography -- framework in place, more data needed!
- Possibility of extracting pressure distributions of the nucleon.
- GPDs in the nuclear medium.
- Need measurements across a wide range of channels: DVCS, Double-DVCS, TCS, HEMP/DVMP, meson-photon production, …

Thank you!

Back-up

John Bercow, Speaker of the House
(*Tagesschau*)

Order and Twist

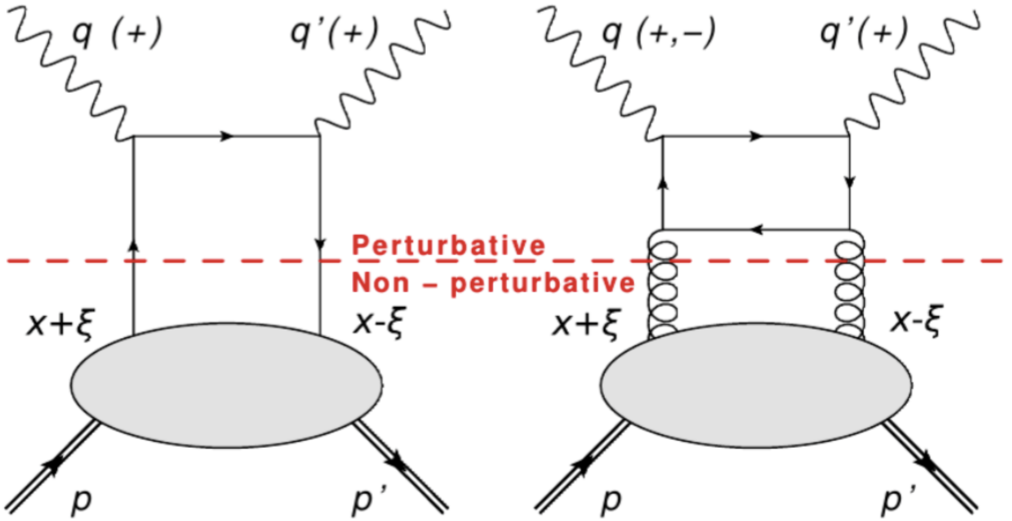

- Twist: powers of $\frac{1}{\sqrt{Q^2}}$ in the DVCS amplitude. Leading-twist (LT) is twist-2.

- Order: introduces powers of α_s

- Leading Order (LO) requires $Q^2 >> M^2$ (M: target mass)

DVCS with transversely polarised target @ COMPASS

$$\mathcal{D}_{CS,T} \equiv \Delta\sigma_T(\mu^{+\downarrow}) - \Delta\sigma_T(\mu^{-\uparrow})$$

$$\rightarrow Im(F_2\mathcal{H} - F_1\mathcal{E}) \sin(\phi - \phi s) \cos \phi$$

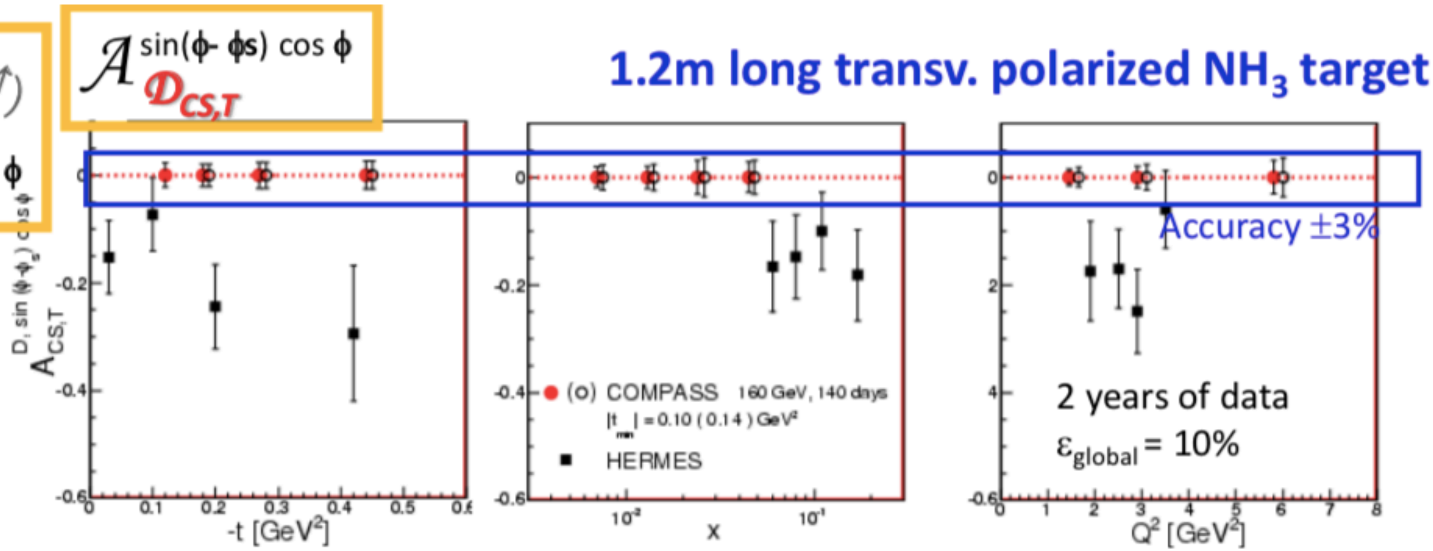

Indications of statistical accuracy.

Slide from: N. d'Hose @ Getting to Grips with QCD, Primosten 2018

DVCS in Hall A

Detect electron in the Left High Resolution Spectrometer (HRS-L): 0.01% momentum resolution

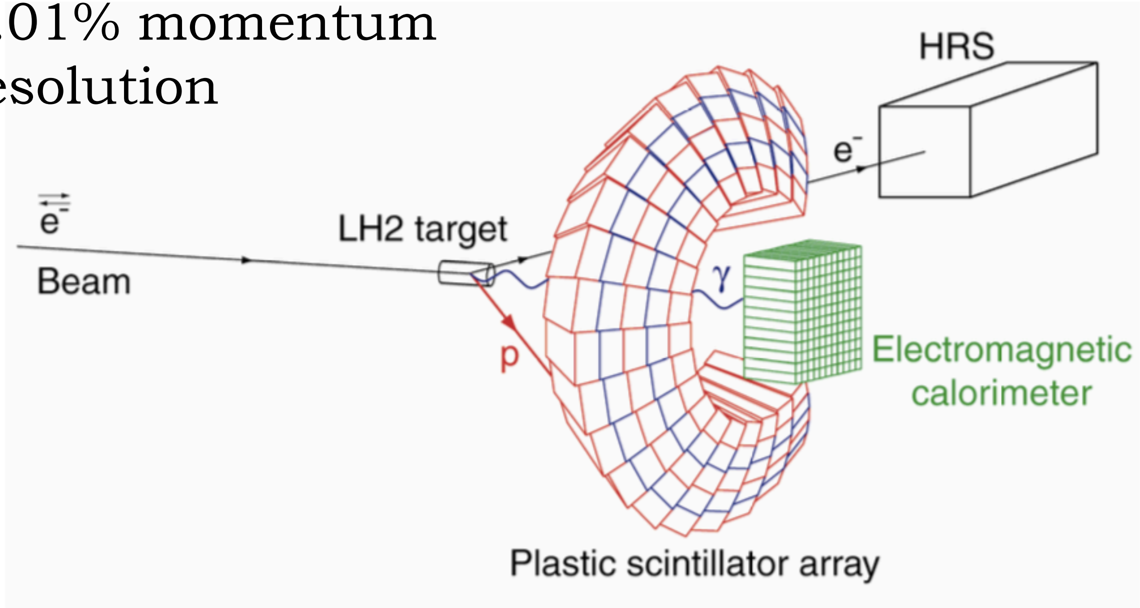

Detect photon in PbF_2 calorimeter: < 3% energy resolution

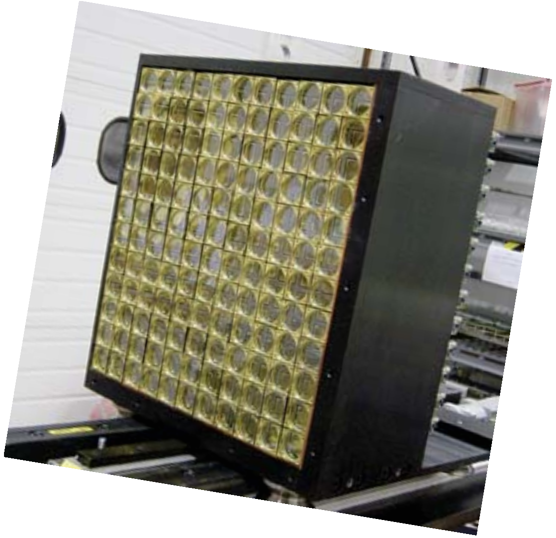

Detect recoil proton in plastic scintillator array.

Large kinematic coverage: CLAS

- Unpolarised DVCS cross-sections and helicity-dependent cross-section differences in a wide kinematic range:

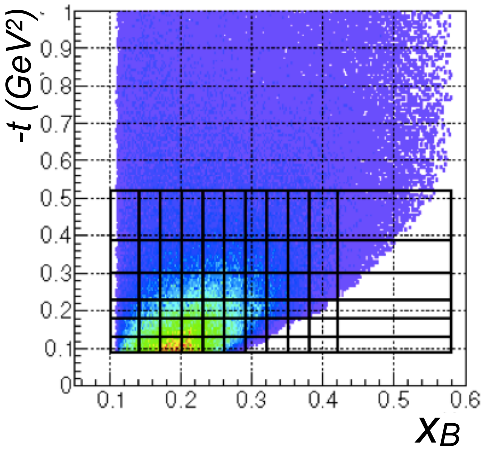

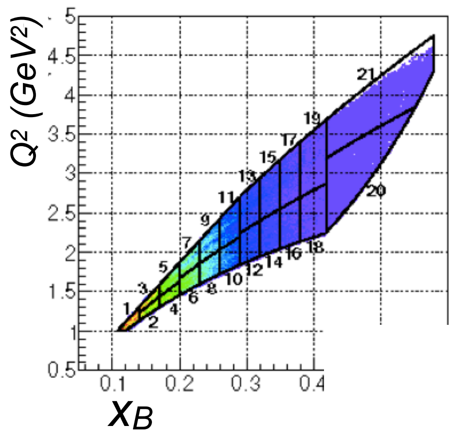

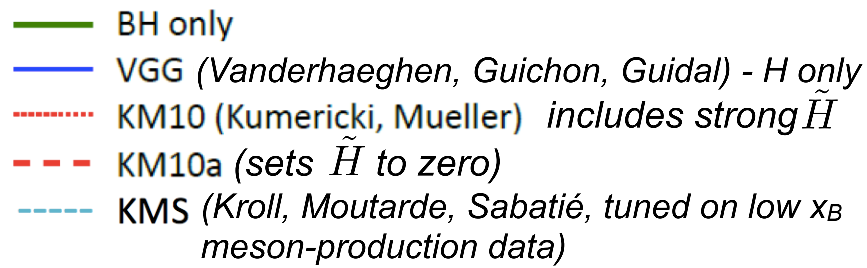

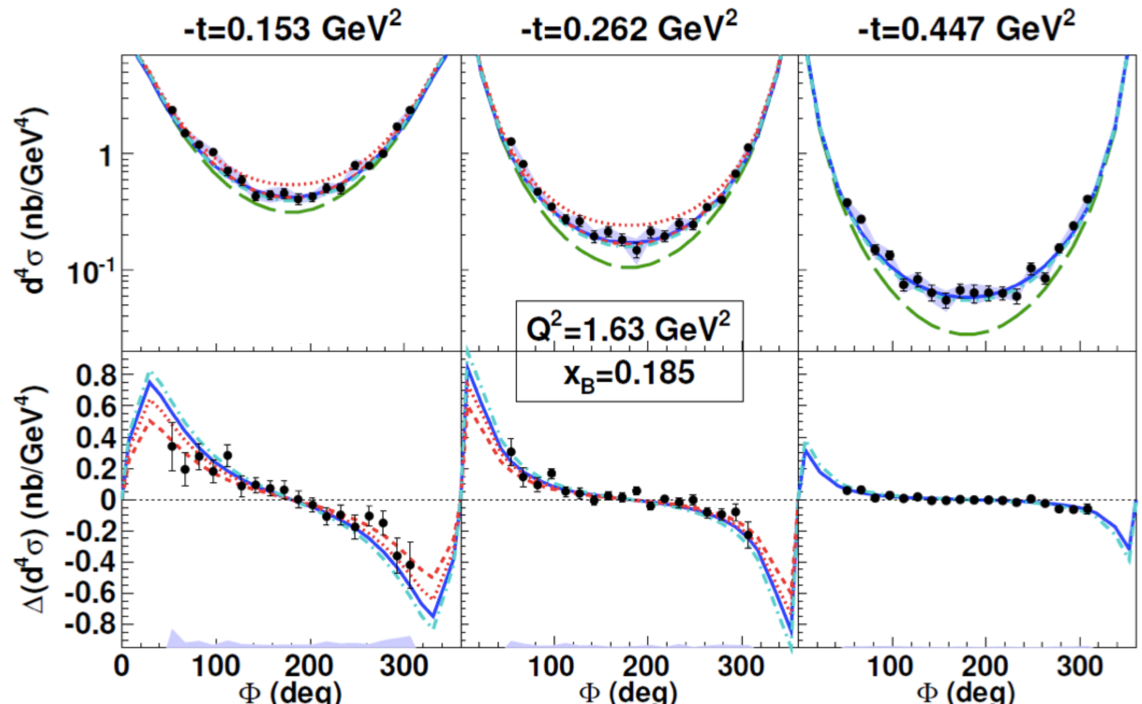

- Widest phase space coverage in valence quark region: CFF constraints.

H.-S. Jo *et al* (CLAS), ***PRL* 115** (2015) 212003
N. Hirlinger Saylor *et al* (CLAS), ***PRC* 98** (2018) 045203

Which DVCS experiment?

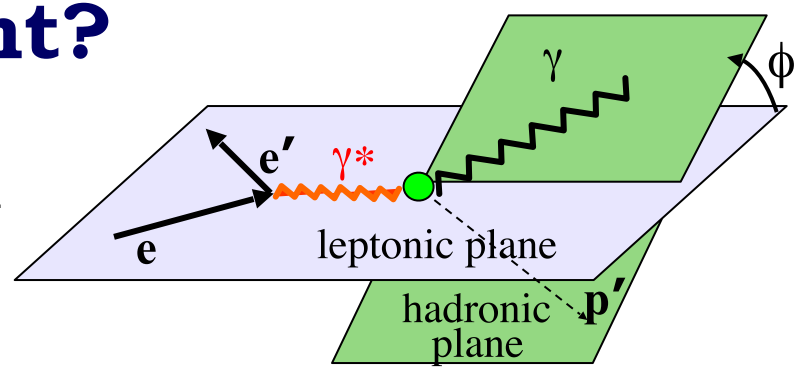

Real parts of CFFs accessible in cross-sections, beam-charge and double polarisation asymmetries,

imaginary parts of CFFs in single-spin asymmetries.

Beam, target polarisation

For example:

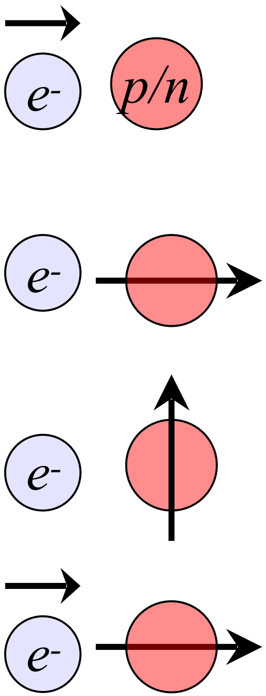

	Proton	Neutron
$$\Delta\sigma_{LU} \sim \sin\phi\, \Im(F_1 H + \xi G_M \tilde{H} - \frac{t}{4M^2} F_2 E)\, d\phi$$	$Im\{\boldsymbol{H}_{\mathbf{p}}, \tilde{H}_{\mathrm{p}}, E_{\mathrm{p}}\}$	$Im\{H_{\mathrm{n}}, \tilde{H}_{\mathrm{n}}, \boldsymbol{E}_{\mathbf{n}}\}$
$$\Delta\sigma_{UL} \sim \sin\phi\, \Im(F_1 \tilde{H} + \xi G_M (H + \frac{x_B}{2} E) - \xi \frac{t}{4M^2} F_2 \tilde{E} + \ldots)\, d\phi$$	$Im\{\boldsymbol{H}_{\mathbf{p}}, \tilde{\boldsymbol{H}}_{\mathbf{p}}\}$	$Im\{\boldsymbol{H}_{\mathbf{n}}, E_{\mathrm{n}}, \tilde{E}_{\mathrm{n}}\}$
$$\Delta\sigma_{UT} \sim \cos\phi\, \Im(\frac{t}{4M^2}(F_2 H - F_1 E) + \ldots) d\phi$$	$Im\{\boldsymbol{H}_{\mathbf{p}}, \boldsymbol{E}_{\mathbf{p}}\}$	$Im\{\boldsymbol{H}_{\mathbf{n}}\}$
$$\Delta\sigma_{LL} \sim (A + B\cos\phi)\, \Re(F_1 \tilde{H} + \xi G_M (H + \frac{x_B}{2} E) + \ldots) d\phi$$	$Re\{\boldsymbol{H}_{\mathbf{p}}, \tilde{\boldsymbol{H}}_{\mathbf{p}}\}$	$Re\{\boldsymbol{H}_{\mathbf{n}}, E_{\mathrm{n}}, \tilde{E}_{\mathrm{n}}\}$

What do GPDs tell us?

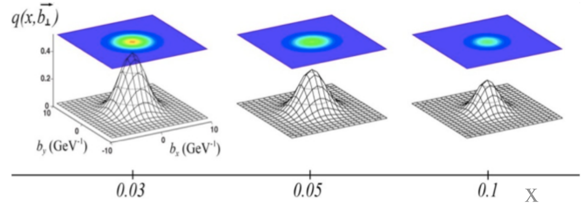

* **Tomography** of the nucleon: transverse spacial distributions of quarks and gluons in longitudinal momentum space.

* For small *x* can image the pion cloud: chiral symmetry breaking.

* Provide information on the orbital angular momentum contribution to nucleon spin: **the spin puzzle**.

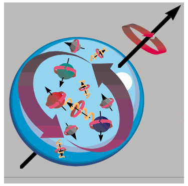

* Using transversely polarised targets can map transverse shift of partons due to the polarisation: combine with TMDs to access **spin-orbit correlations** of quarks and gluons, study non-perturbative interactions of partons.

* Indirect access to mechanical properties of the nucleon: possibilities of extracting **pressure distributions** within the nucleon.

CLAS

Beam-spin Asymmetry (A_{LU})

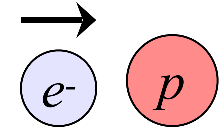

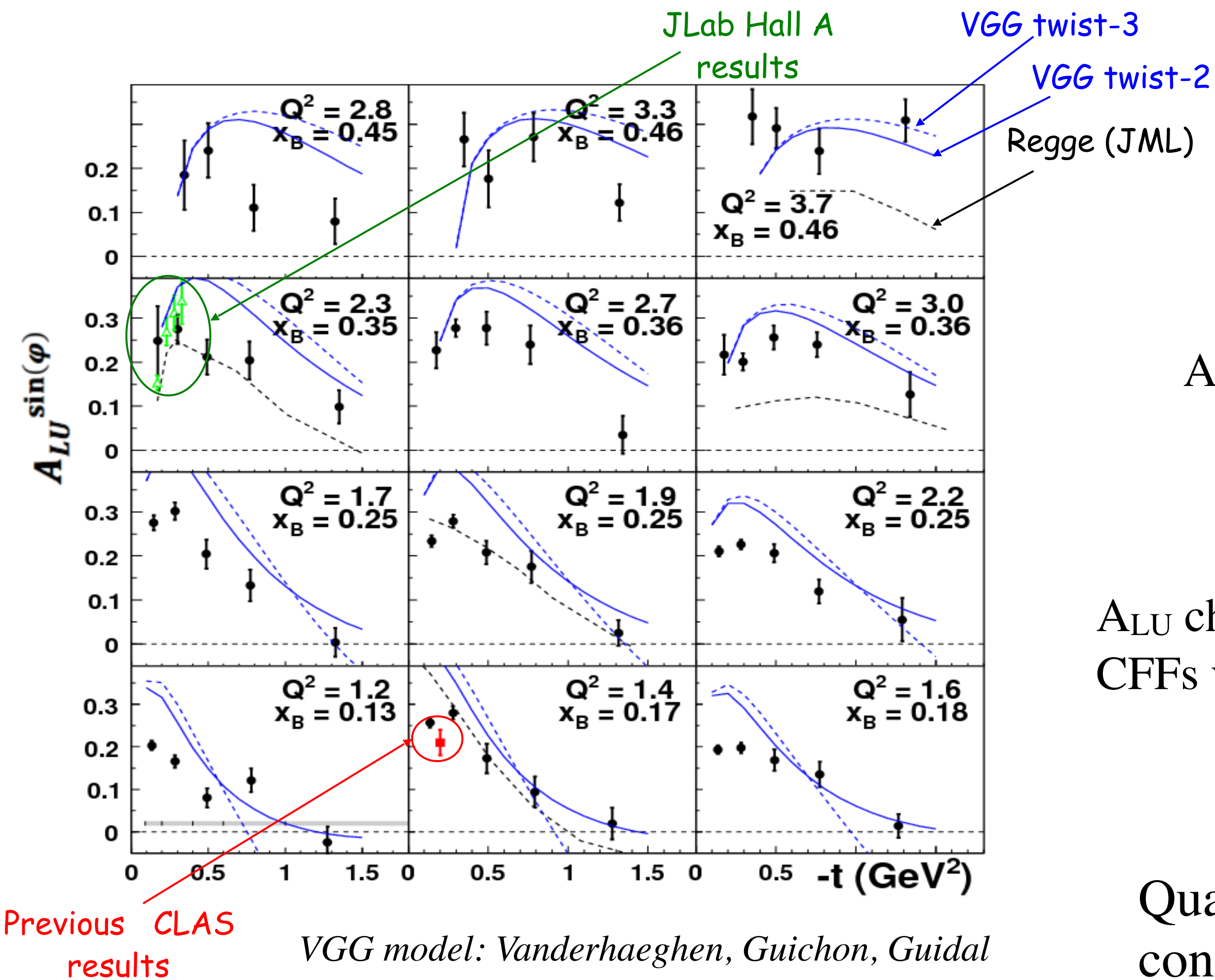

VGG model: Vanderhaeghen, Guichon, Guidal

Follows first CLAS measurement:
S. Stepanyan *et al* (CLAS), ***PRL* 87** (2001) 182002

A_{LU} from fit to asymmetry:

$$A_i = \frac{\alpha_i \sin\phi}{1 + \beta_i \cos\phi}$$

A_{LU} characterised by imaginary parts of CFFs via:
$$F_1 H + \xi G_M \tilde{H} - \frac{t}{4M^2} E$$

Qualitative agreement with models, constraints on fit parameters.

F.-X. Girod *et al* (CLAS), ***PRL* 100** (2008) 162002.

Target-spin Asymmetry (A_{UL})

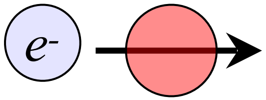

Follows first CLAS measurement:
S. Chen *et al* (CLAS), ***PRL* 97** (2006) 072002

A_{UL} from fit to asymmetry:

$$A_i = \frac{\alpha_i \sin\phi}{1 + \beta_i \cos\phi}$$

A_{UL} characterised by imaginary parts of CFFs via:

$$F_1 \tilde{H} + \xi G_M \left(H + \frac{x_B}{2} E\right) - \frac{\xi t}{4M^2} F_2 \tilde{E} + \ldots$$

High statistics, large kinematic coverage, strong constraints on fits, simultaneous fit with BSA and DSA from the same dataset.

E. Seder *et al* (CLAS), ***PRL* 114** (2015) 032001

S. Pisano *et al* (CLAS), ***PRD* 91** (2015) 052014

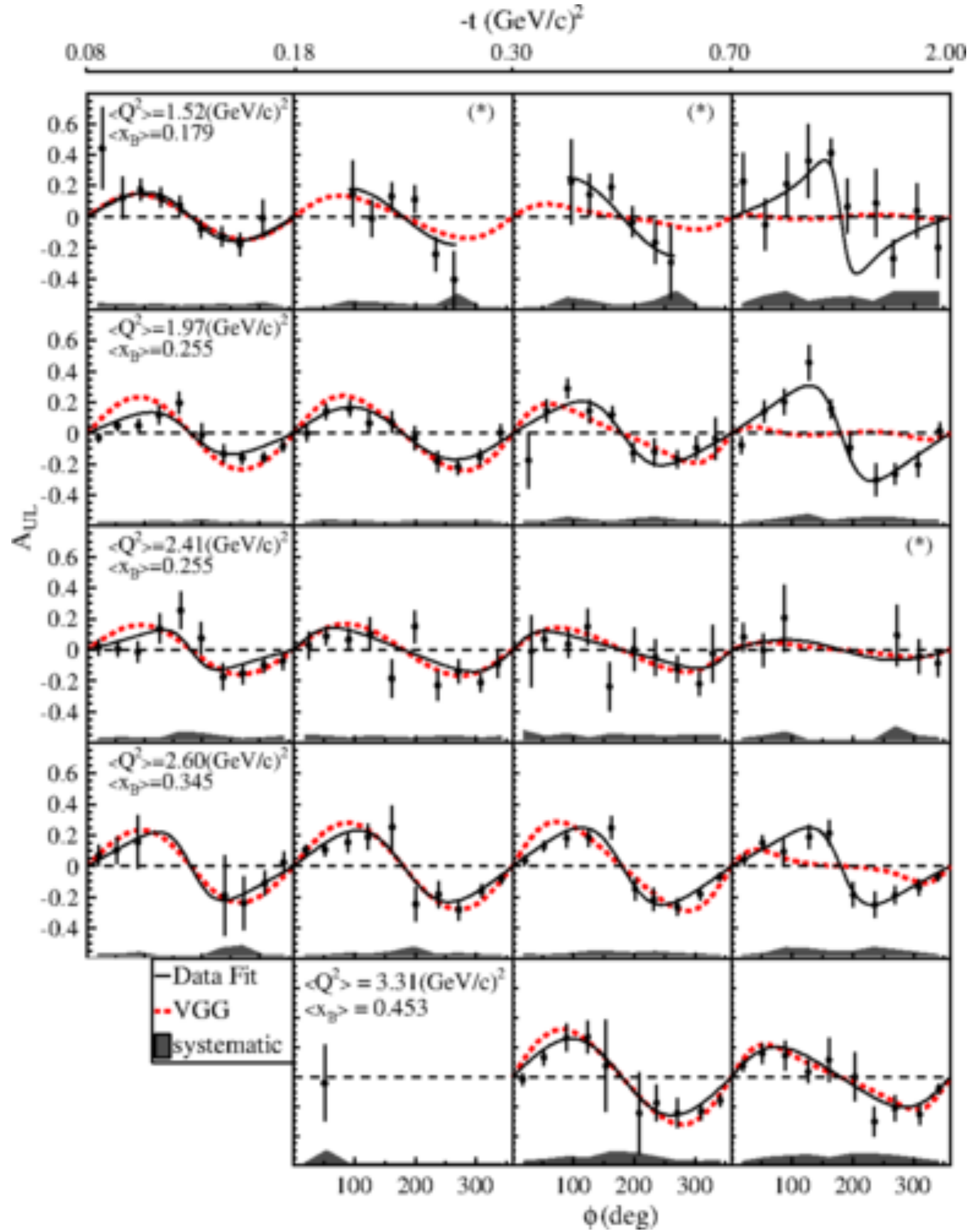

Beam- and target-spin asymmetries

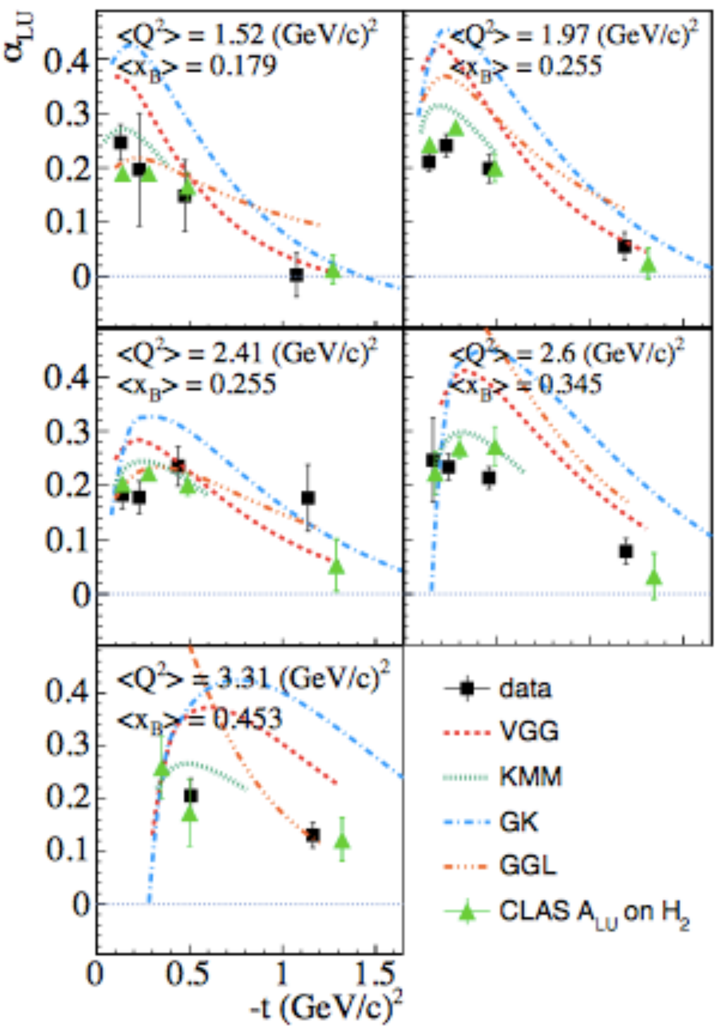

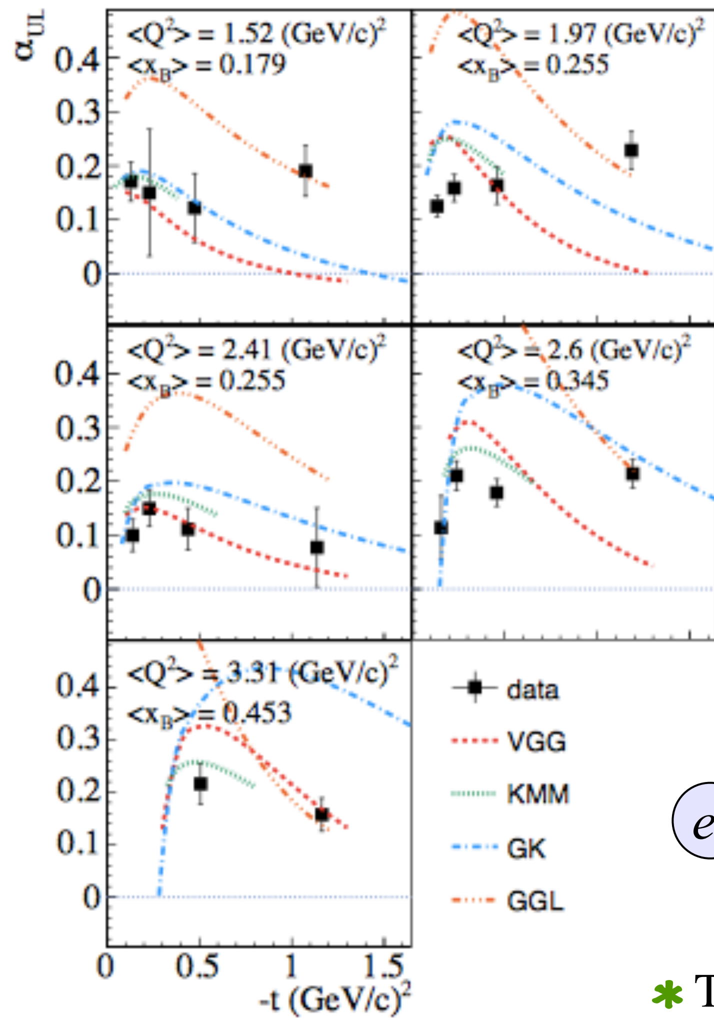

$$A = \frac{\alpha sin\phi}{1+\beta cos\phi}$$

GGL: Goldstein, Gonzalez, Liuti

GK: Kroll, Moutarde, Sabatié

KMM: Kumericki, Mueller, Murray

VGG: Vanderhaeghen, Guichon, Guidal

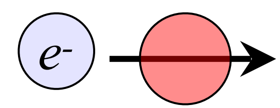

* TSA shows a flatter distribution in *t* than BSA.

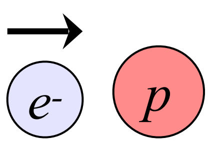

S. Pisano *et al* (CLAS), ***PRD* 91** (2015) 052014

E. Seder *et al* (CLAS), ***PRL* 114** (2015) 032001

Double-spin asymmetry

At leading twist, double-spin asymmetry (DSA) can be expressed as:

$$A_{\mathrm{LL}}(\phi) \sim \frac{c_{0,\mathrm{LP}}^{\mathrm{BH}} + c_{0,\mathrm{LP}}^{\mathcal{I}} + (c_{1,\mathrm{LP}}^{\mathrm{BH}} + c_{1,\mathrm{LP}}^{\mathcal{I}})\cos\phi}{c_{0,\mathrm{unp}}^{\mathrm{BH}} + (c_{1,\mathrm{unp}}^{\mathrm{BH}} + c_{1,\mathrm{unp}}^{\mathcal{I}} + \ldots)\cos\phi\ldots}$$

$$c_{0,\mathrm{LP}}^{\mathcal{I}}, c_{1,\mathrm{LP}}^{\mathcal{I}} \propto \Re\mathrm{e}[F_1\widetilde{\mathcal{H}} + \xi(F_1+F_2)(\mathcal{H} + \frac{x_B}{2}\mathcal{E}) - \xi(\frac{x_B}{2}F_1 + \frac{t}{4M^2}F_2)\widetilde{\mathcal{E}}]$$

At CLAS kinematics, leading-twist dominance of these CFFs

* Fit function for the phi-dependence of the asymmetry: $\frac{\kappa_{\mathrm{LL}} + \lambda_{\mathrm{LL}}\cos\phi}{1+\beta\cos\phi}$

Shares denominator with BSA and TSA!
If measurements at same kinematics, can do a simultaneous fit.

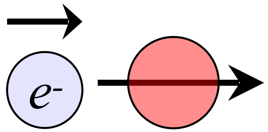

Double-spin Asymmetry (A_{LL})

CLAS

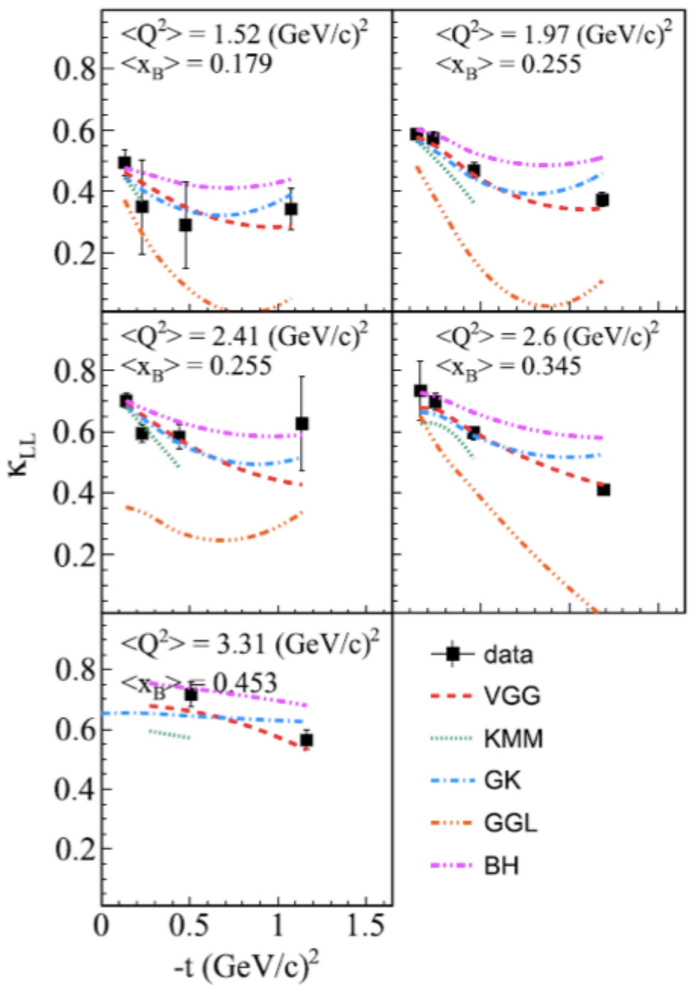

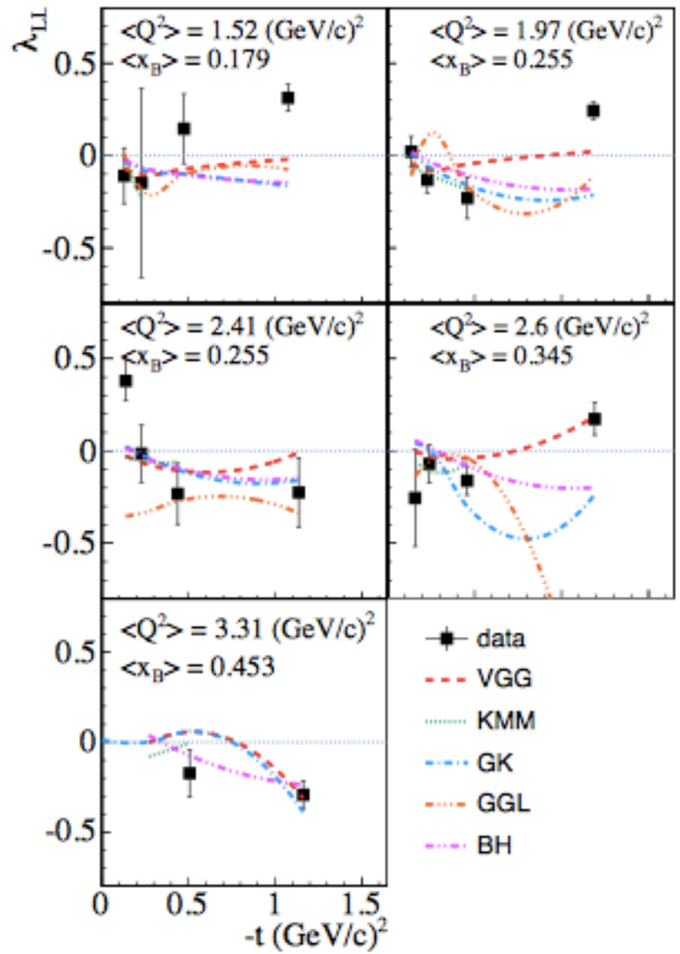

A_{LL} from fit to asymmetry:

$$\frac{\kappa_{\rm LL} + \lambda_{\rm LL}\cos\phi}{1+\beta\cos\phi}$$

A_{LL} characterised by real parts of CFFs via:

$$F_1\tilde{H} + \xi G_M\left(H + \frac{x_B}{2}E\right) + \ldots$$

- Fit parameters extracted from a simultaneous fit to BSA, TSA and DSA.
- Constant term dominates and is almost entirely BH.

E. Seder *et al* (CLAS), ***PRL* 114** (2015) 032001

S. Pisano *et al* (CLAS), ***PRD* 91** (2015) 052014

CFF extraction from three spin asymmetries at common kinematics.

Projected sensitivities to *Im(H)* CFF

$Q^2 = 2.6\ GeV^2,\ x_B = 0.23$ $Q^2 = 5.9\ GeV^2,\ x_B = 0.35$

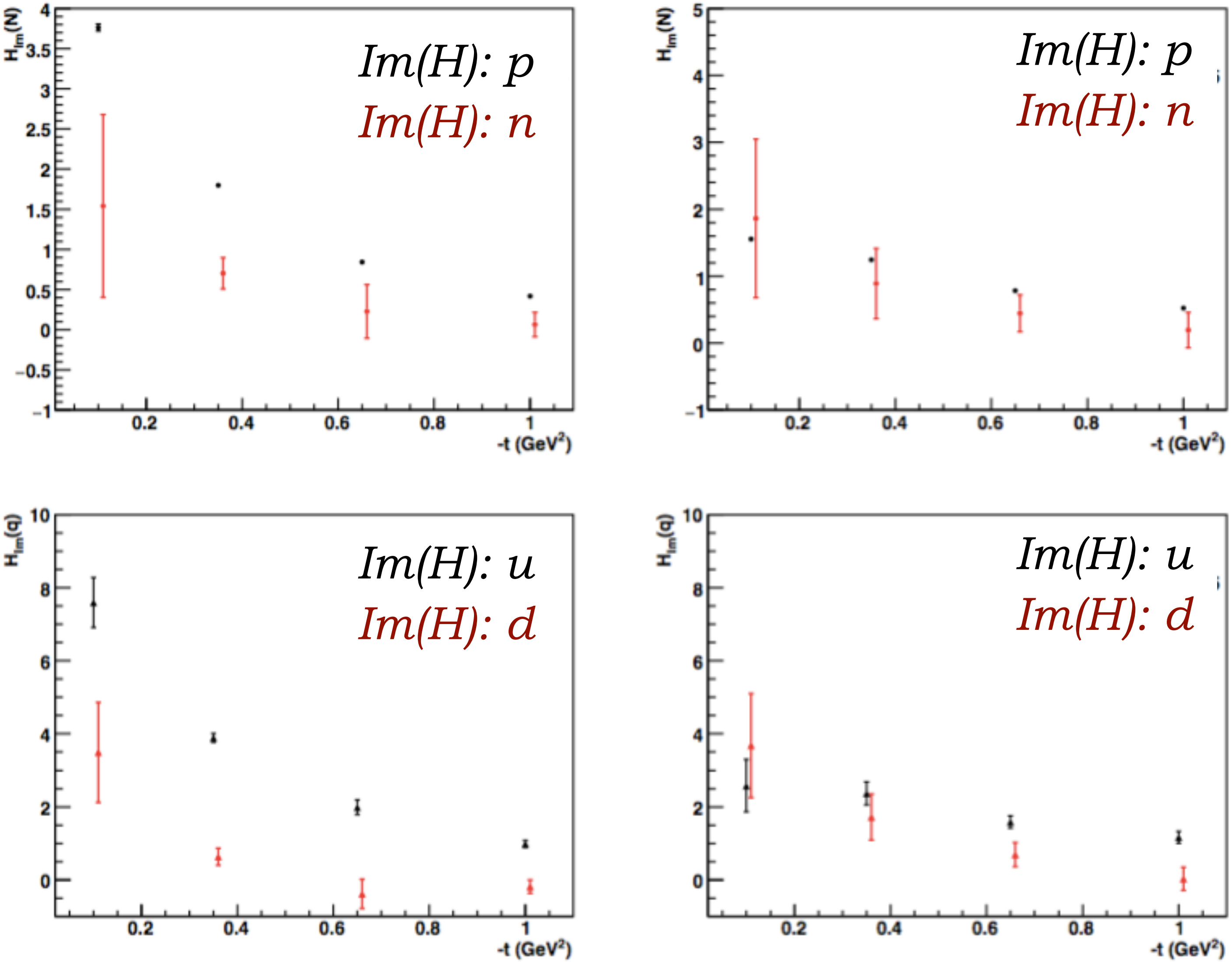

Projections for *Im(H)* neutron and proton and up and down CFFs extracted from approved CLAS12 experiments.

VGG fit (M. Guidal)

Projected sensitivities to *Im(E)* CFF

CLAS12

Q^2 = 2.6 GeV^2, x_B = 0.23 $\qquad$ Q^2 = 5.9 GeV^2, x_B = 0.35

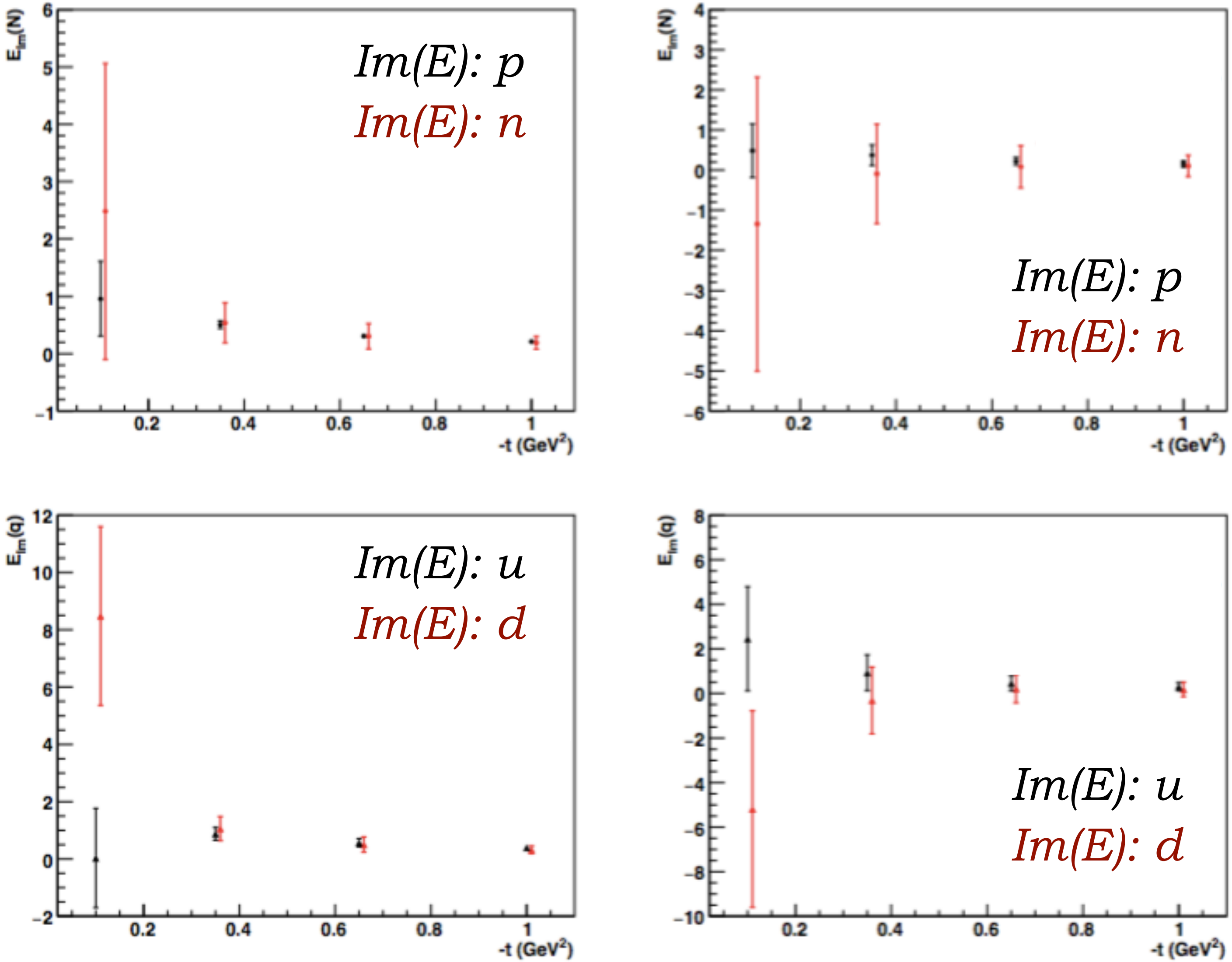

Projections for *Im(E)* neutron and proton and up and down CFFs extracted from approved and conditionally-approved CLAS12 experiments.

VGG fit (M. Guidal)

DVCS on the bound proton

CLAS

- Beam spin asymmetry in DVCS from bound protons in ^{4}He.

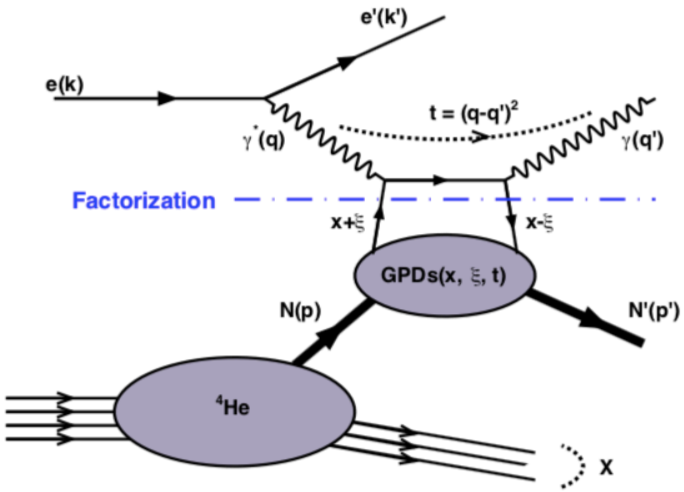

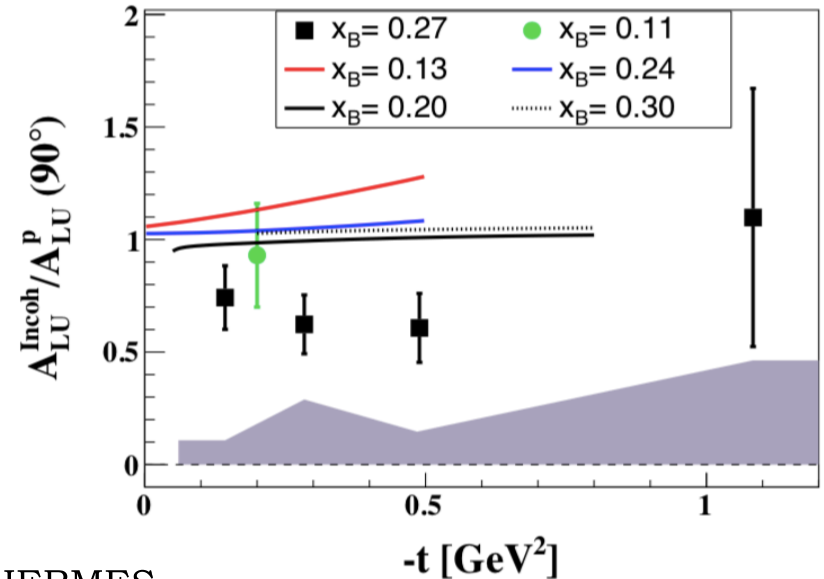

HERMES

Off-shell: S. Liuti, K. Taneja, PRC72, 032201 (2005)

On-shell: V. Guzey, A. Thomas, K. Tsushima, PLB673, 9 (2009)

- 25% - 40% lower asymmetries for bound proton compared to free, no strong dependence on t.
- Medium-modification effects, initial/final state interactions?

M. Hattawy *et al*, arXiv:1812.07628

Nuclear GPDs: coherent DVCS on ^4He

CLAS

- ^4He is spin-0, so only one GPD at leading twist, $\mathbf{H_A}$.

$$\Re e(\mathcal{H}_A) = \mathcal{P}\int_0^1 dx[H_A(x,\xi,t) - H_A(-x,\xi,t)]\,C^+(x,\xi)$$

$$\Im m(\mathcal{H}_A) = -\pi(H_A(\xi,\xi,t) - H_A(-\xi,\xi,t))$$

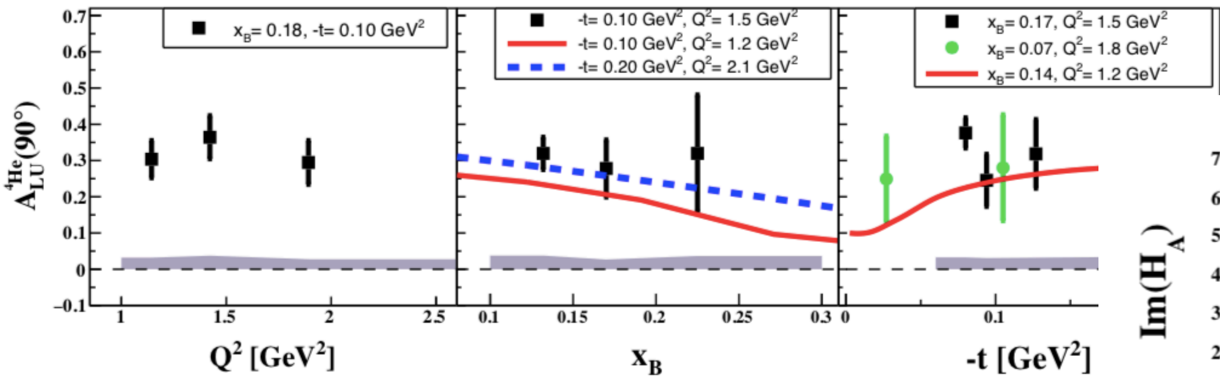

HERMES

S. Liuti, K. Taneja, PRC72, 032201 (2005)

- Beam spin asymmetry in coherent DVCS from ^4He: CLAS and a radial time projection chamber (RTPC) for detection of recoiling helium, data taken in 2009.

- Paves the way for measurements at 11 GeV.

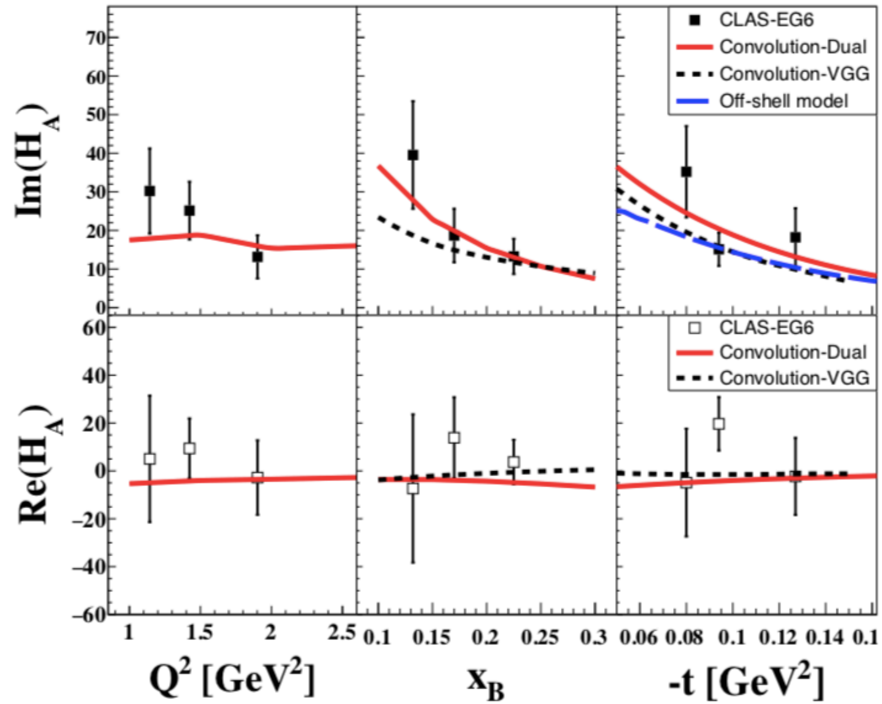

V. Guzey, PRC78, 025211 (2008)

M. Guidal *et al*, PRD72, 054013 (2005)

J. Gonzalez-Hernandez *et al*, PRC88, 065206 (2013)

M. Hattawy *et al*, PRL 119 (2017) 202004.

First DVCS cross-sections in valence region

Hall A

- E00-110: Hall A, ran in 2004, high precision, narrow kinematic range.

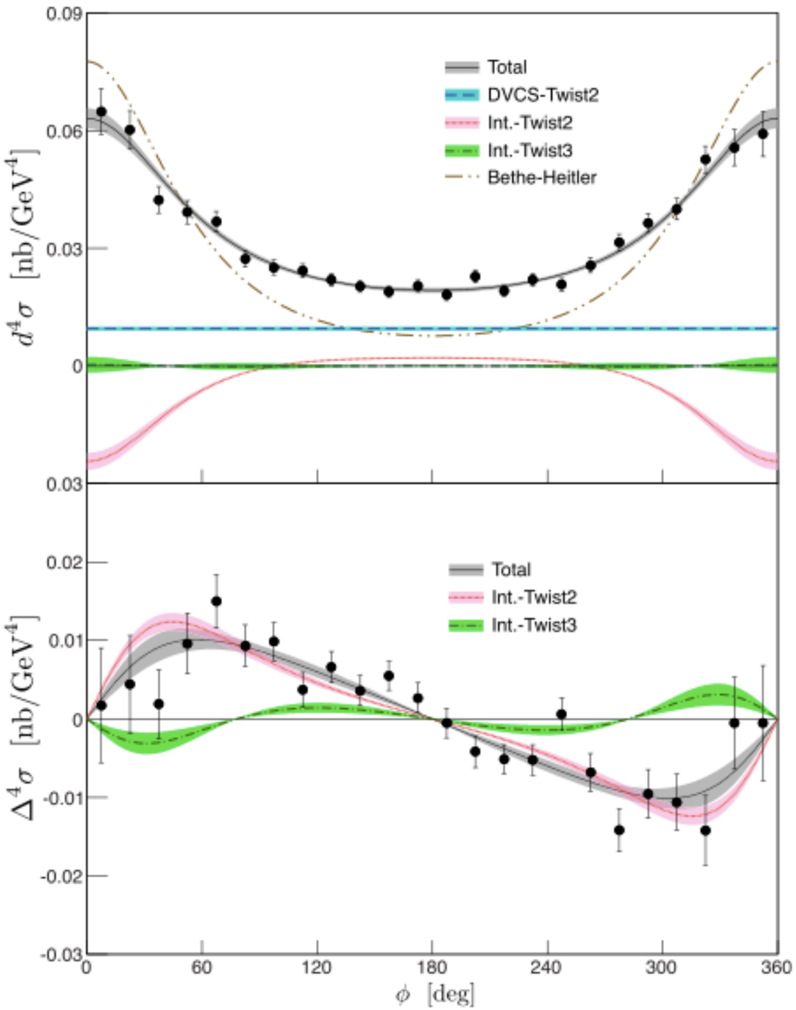

$$x_B = 0.36, Q^2 = 2.3\ GeV^2, -t = 0.32\ GeV^2$$

- Luminosity $=10^{37}$ cm^{-2}s^{-1}.
- Measure Q^2-dependence (Q^2: 1.5, 1.9, 2.3 GeV^2) of DVCS-BH cross-sections at fixed x_B (0.36).
- Also x_B dependence at constant Q^2.
- CFFs show scaling in DVCS: leading twist (twist-2) dominance at this moderate Q^2.

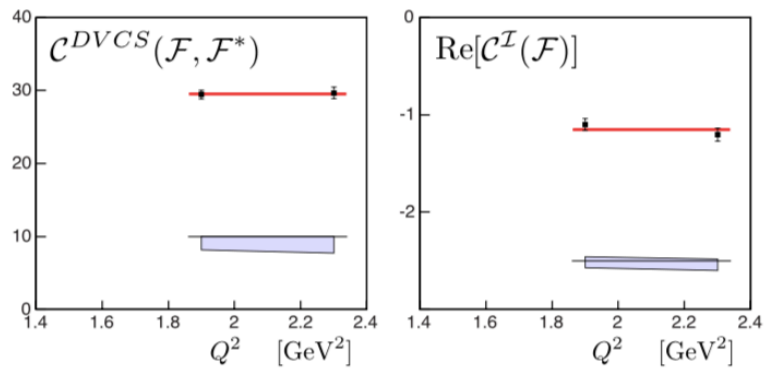

M. Defurne *et al*, ***PRC* 92** (2015) 055202.

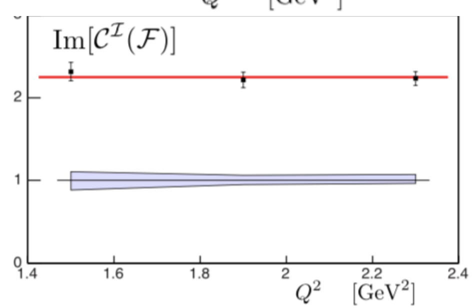

- Strong deviation of unpolarised DVCS cross-section from BH: extraction of $|T_{DVCS}|^2$ amplitude as well as interference terms.

First DVCS cross-sections in valence region

Hall A

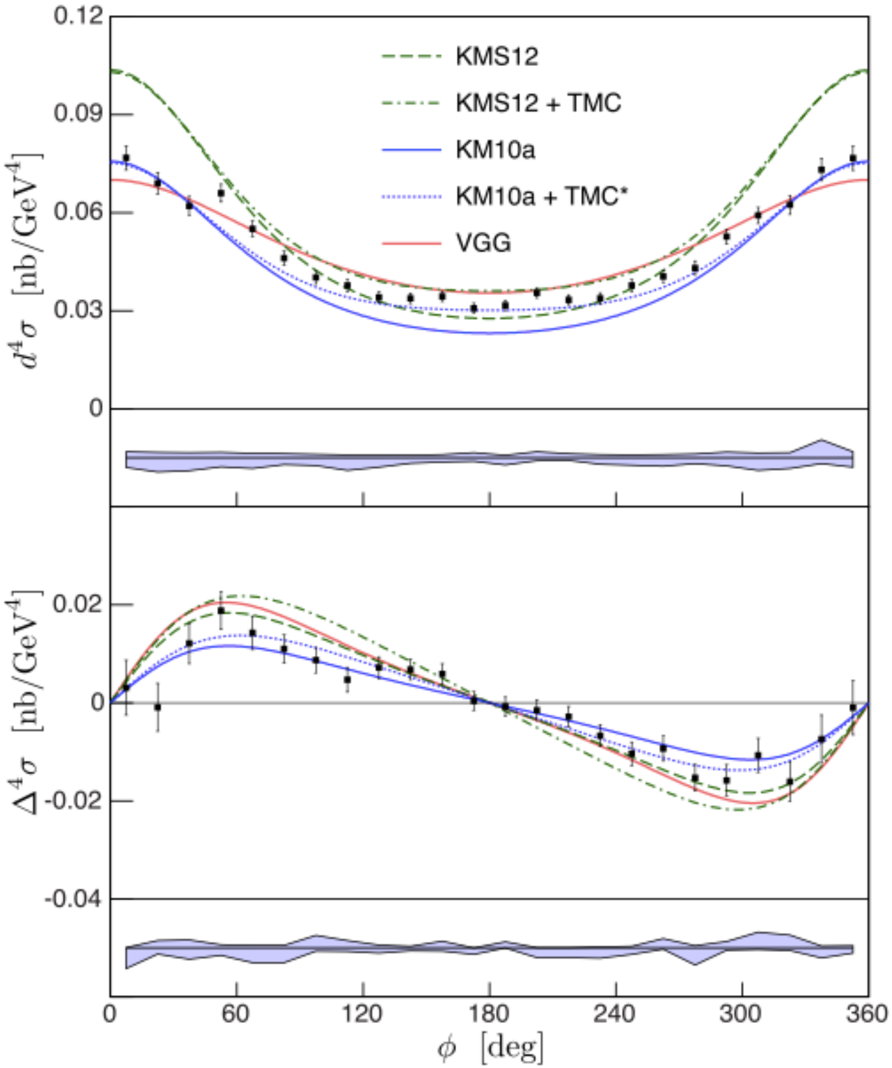

$x_B = 0.36, Q^2 = 1.9\ GeV^2, -t = 0.32\ GeV^2$

- High precision of the data: sensitivity to subtle differences in model predictions.

VGG model: Vanderhaeghen, Guichon, Guidal

KMS model: Kroll, Moutarde, Sabatié

KM model: Kumericki, Mueller

TMC: kinematic twist-4 target-mass and finite-t corrections, calculated for proton DVCS and estimated for KMS12.

- KMS parameters tuned on very low x_B meson-production data: not adapted to valence quarks.

→ TMC*: TMC extracted from the KMS12 model and applied to KM10a.

- TMC improve agreement for KM10a model, especially at $\phi = 180^\circ$. Higher-twist effects?

The devil is in the detail…

M. Defurne *et al*, ***PRC* 92** (2015) 055202.

Here comes the twist...

- Twist: powers of $\frac{1}{\sqrt{Q^2}}$ in the DVCS amplitude. Leading-twist (LT) is twist-2.
- Order: introduces powers of α_s
- LO requires $Q^2 >> M^2$ (M: target mass)

  Bold assumption for JLab 6 GeV kinematics!

- CFFs can be classified according to real and virtual photon helicity:

$\mathcal{F}_{++}$

helicity of real produced photon

helicity of virtual incoming photon

- Helicity-conserved CFFs — $\mathcal{F}_{++}$
- Helicity-flip (transverse) — $\mathcal{F}_{-+}$
- Longitudinal to transverse flip — $\mathcal{F}_{0+}$

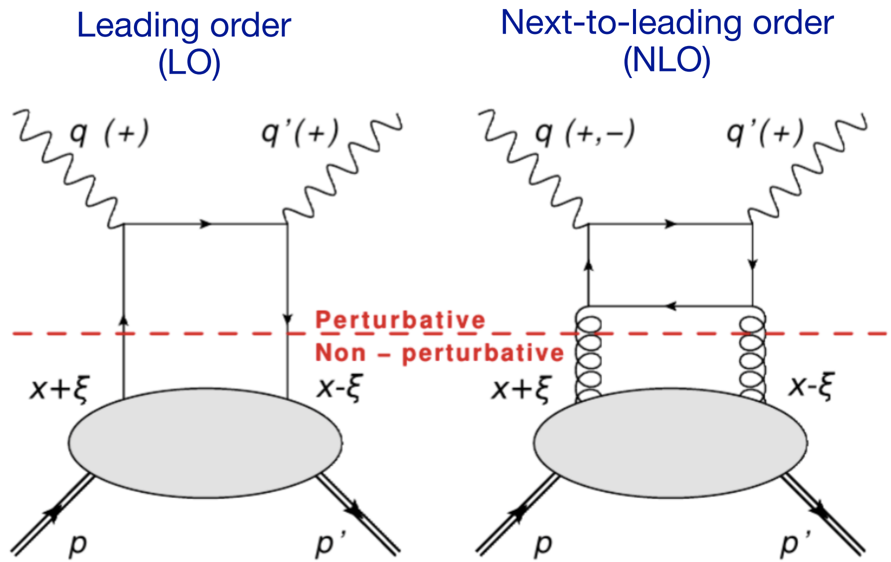

- CFFs contributing to the scattering amplitude:
  - LT in LO: only $\mathcal{F}_{++}$
  - LT in NLO: both $\mathcal{F}_{++}$ and $\mathcal{F}_{-+}$
  - Twist-3: $\mathcal{F}_{0+}$

Here comes the twist…

- At finite Q^2 and non-zero t there's ambiguity in defining the light-cone axis:
  - Traditional GPD phenomenology uses the Belitsky convention, in plane of q and P:
    A. Belitsky *et al*, ***Nucl. Phys. B878*** (2014), 214
  - New, Braun definition using q and q': more natural.
    V. Braun *et al*, ***Phys. Rev. D89*** (2014), 074022

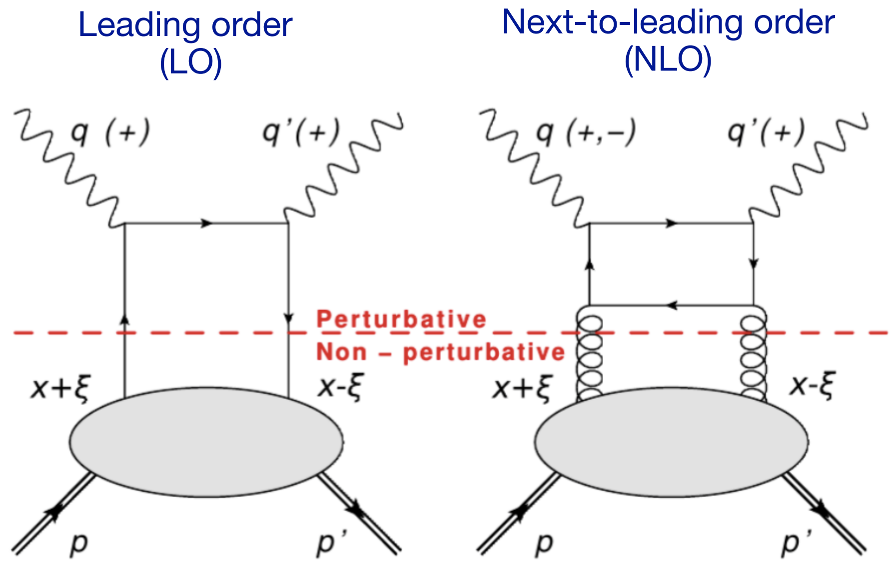

Reformulating CFFs in this frame absorbs most kinematic power corrections (TMC):

$$\mathcal{F}_{++} = \mathbb{F}_{++} + \frac{\chi}{2}\left[\mathbb{F}_{++} + \mathbb{F}_{-+}\right] - \chi_0 \mathbb{F}_{0+}$$
$$\mathcal{F}_{-+} = \mathbb{F}_{-+} + \frac{\chi}{2}\left[\mathbb{F}_{++} + \mathbb{F}_{-+}\right] - \chi_0 \mathbb{F}_{0+}$$
$$\mathcal{F}_{0+} = -(1+\chi)\mathbb{F}_{0+} + \chi_0\left[\mathbb{F}_{++} + \mathbb{F}_{-+}\right]$$

Belitsky CFFs

Braun CFFs

Assuming LO and LT in the Braun frame:

$$\begin{aligned} \mathcal{F}_{++} &= (1+\tfrac{\chi}{2})\mathbb{F}_{++} \\ \mathcal{F}_{-+} &= \tfrac{\chi}{2}\mathbb{F}_{++} \\ \mathcal{F}_{0+} &= \chi_0 \mathbb{F}_{++} \end{aligned}$$

HT/HO contributions in the Belitsky frame, scaled by kinematic factors χ and χ_0.

Non-negligible at the Q^2 and x_B of the Hall A cross-section measurement:

$\chi_0 = 0.25,\ \chi = 0.06$ for $Q^2 = 2\ \mathrm{GeV}^2,\ x_B = 0.36,\ t = -0.24\ \mathrm{GeV}^2$

M. Defurne *et al*, ***Nature Communications 8*** (2017) 1408

Hints of higher twist or higher orders

Hall A

- Including either higher order or higher twist effects (HT) improves the match with data:

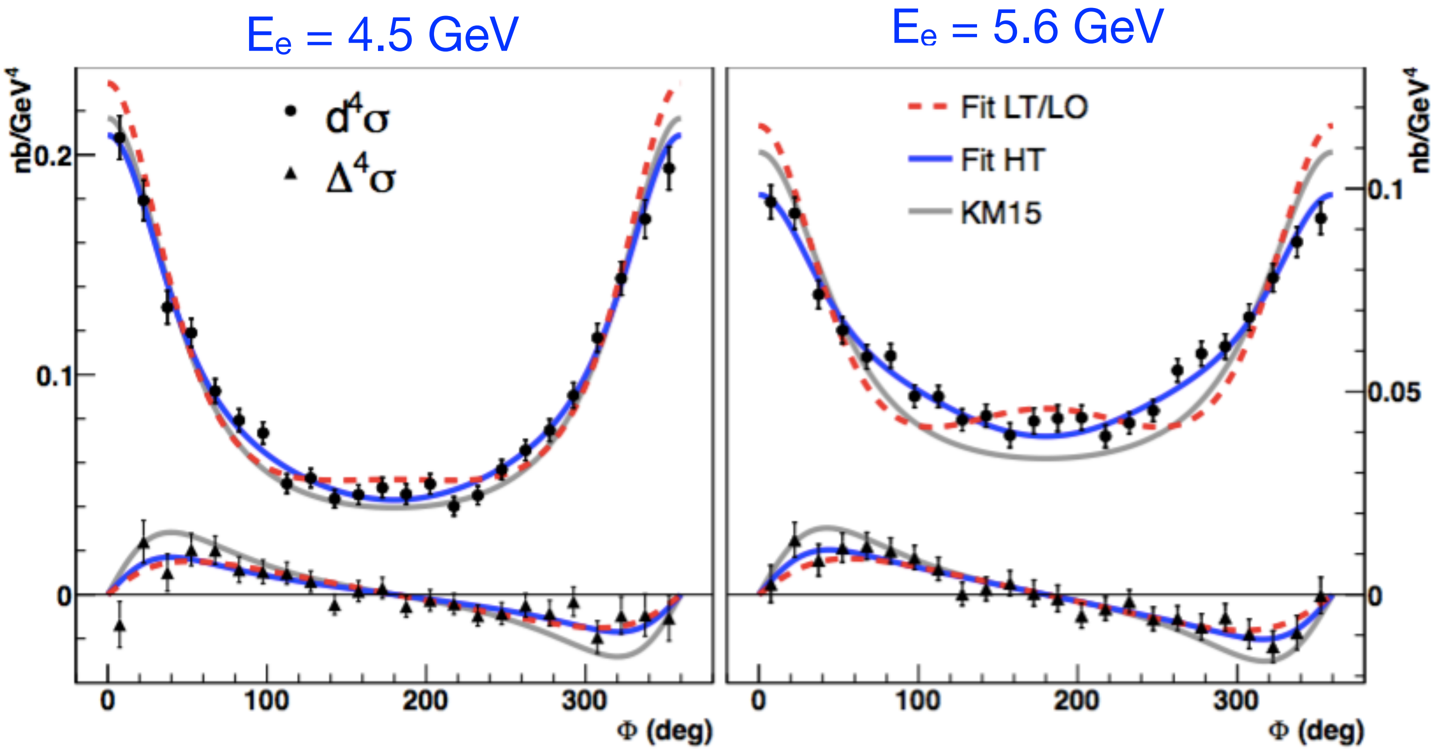

Higher-order and / or higher-twist terms are important! A glimpse of gluons.

Wider range of beam energy needed to identify the dominant effect → **JLab at 11 GeV.**

M. Defurne *et al*, ***Nature Communications* 8** (2017) 1408.

Rosenbluth separation of DVCS² and BH-DVCS terms

Hall A

- Generalised Rosenbluth separation of the DVCS² (scales as E_e^2) and the BH-DVCS interference (scales as E_e^3) terms in the cross-section is possible but NLO and/or higher-twist required: experiment E07-007 @ two beam energies: 4.5 and 5.6 GeV.

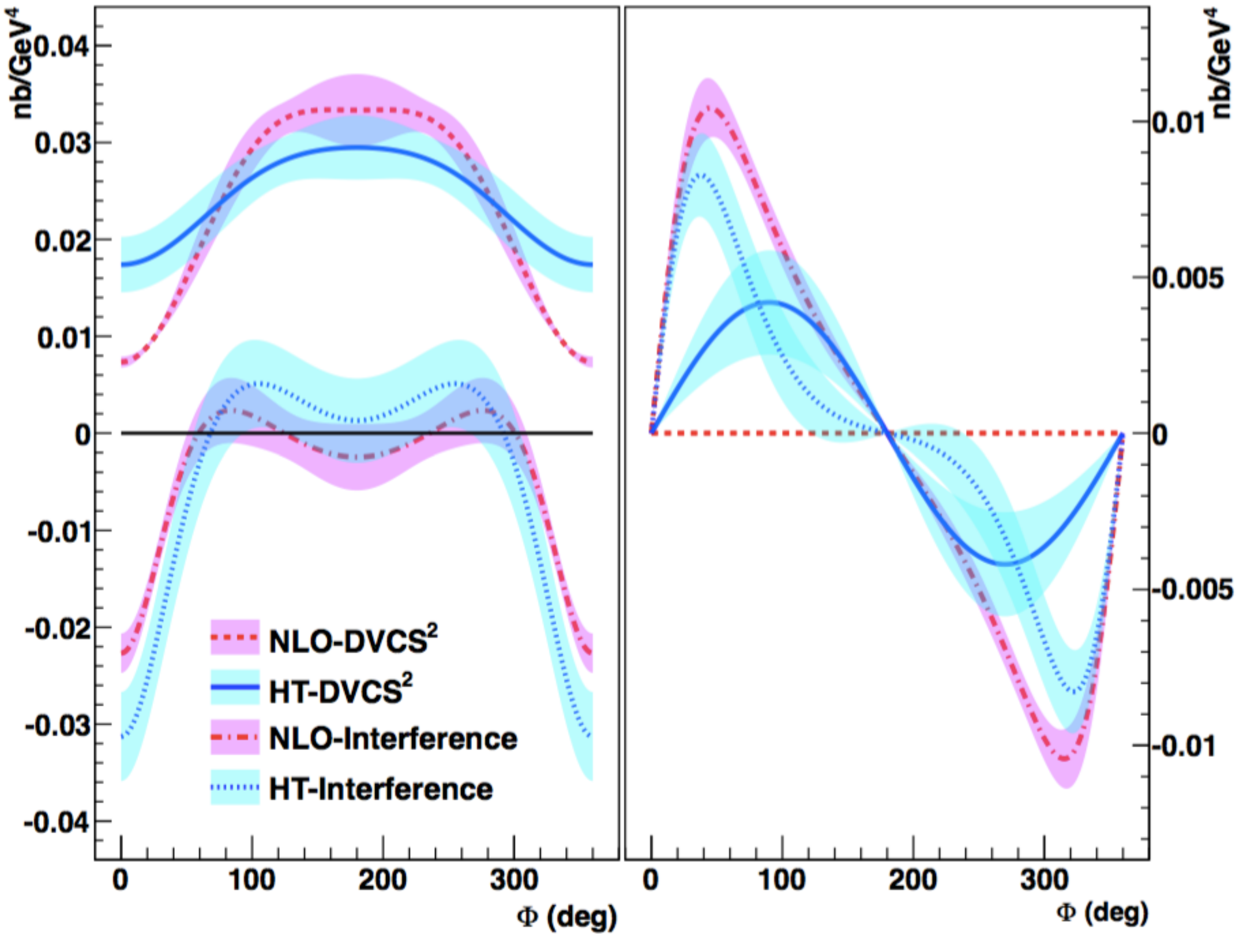

- Significant differences between pure DVCS and interference contributions.
- Helicity-dependent cross-section has a sizeable DVCS² contribution in the higher-twist scenario.
- Separation of HT and NLO effects requires scans across wider ranges of Q^2 and beam energy: JLab12!

M. Defurne *et al*, ***Nature Communications* 8** (2017) 1408.

CLAS unpolarised cross-sections

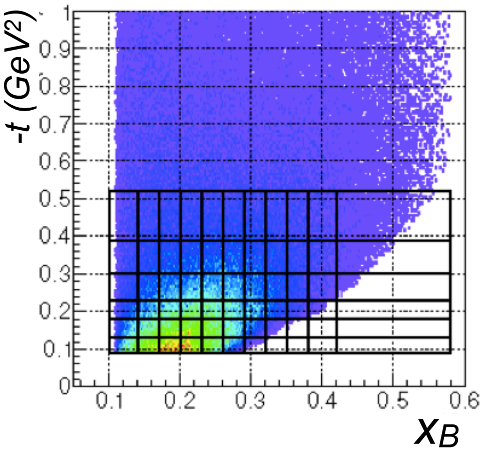

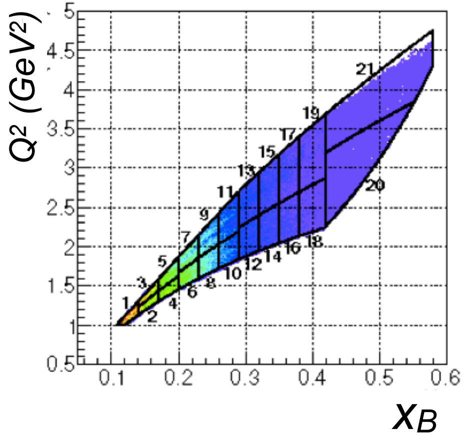

- BH only
- VGG *(Vanderhaeghen, Guichon, Guidal) - H only*
- KM10 (Kumericki, Mueller) *includes strong* $\tilde{H}$
- KM10a *(sets* $\tilde{H}$ *to zero)*
- KMS *(Kroll, Moutarde, Sabatié, tuned on low* x_B *meson-production data)*

* Widest phase space coverage in valence quark region: CFF constraints.
* Dominance of GPD *H* in unpolarised cross-section.

$$\frac{d^4\sigma_{ep\to ep\gamma}}{dQ^2 dx_B dt d\Phi}$$

$$\frac{1}{2}\left(\frac{d^4\overrightarrow{\sigma}_{ep\to ep\gamma}}{dQ^2 dx_B dt d\Phi} - \frac{d^4\overleftarrow{\sigma}_{ep\to ep\gamma}}{dQ^2 dx_B dt d\Phi}\right)$$

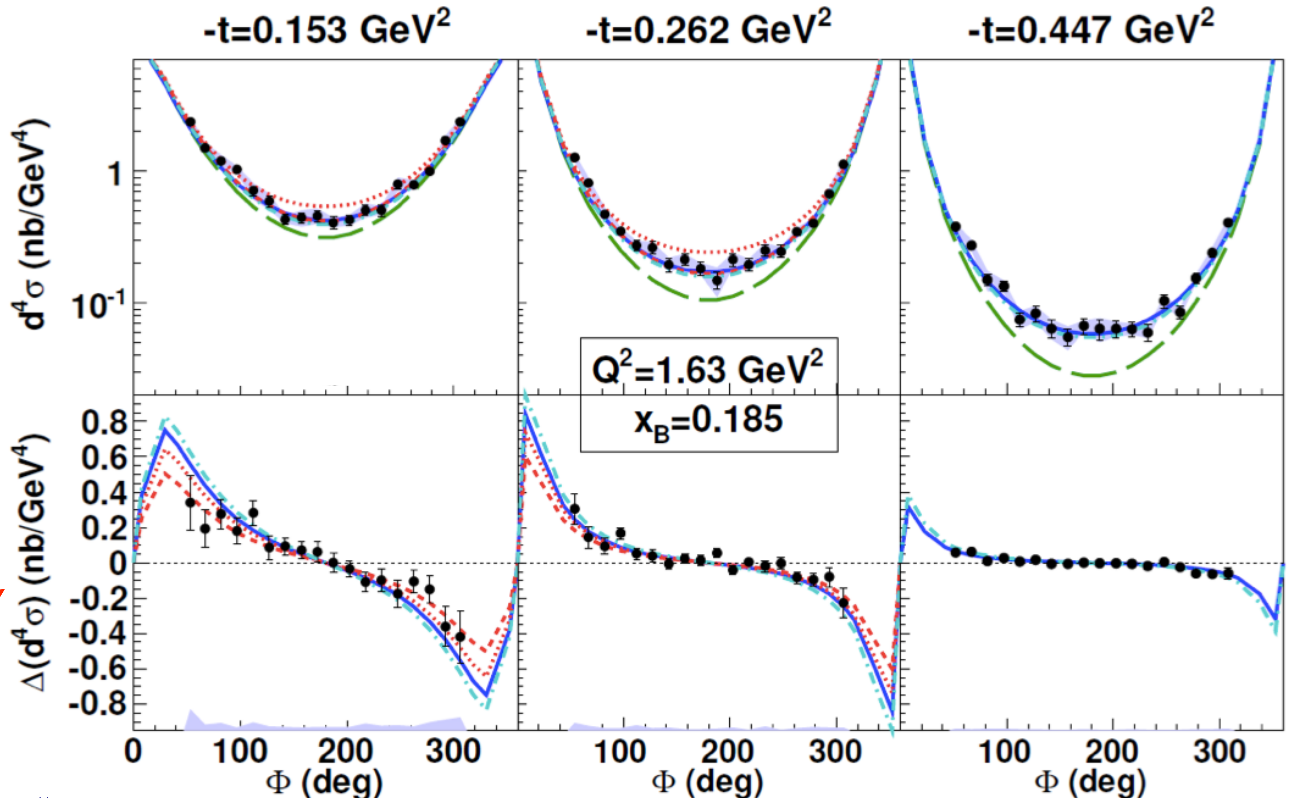

H.-S. Jo *et al* (CLAS), ***PRL* 115** (2015) 212003

Nucleon Tomography from GPDs

* At a fixed Q^2, x_B, slope of GPD with t is related, via a Fourier Transform, to the transverse spatial spread.

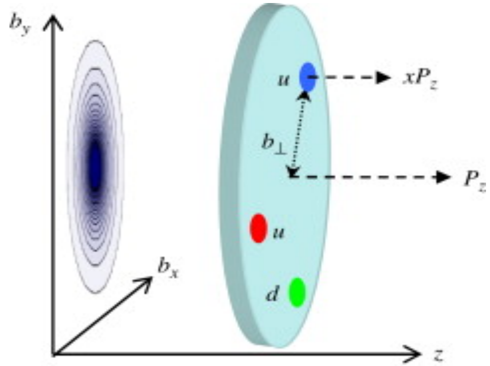

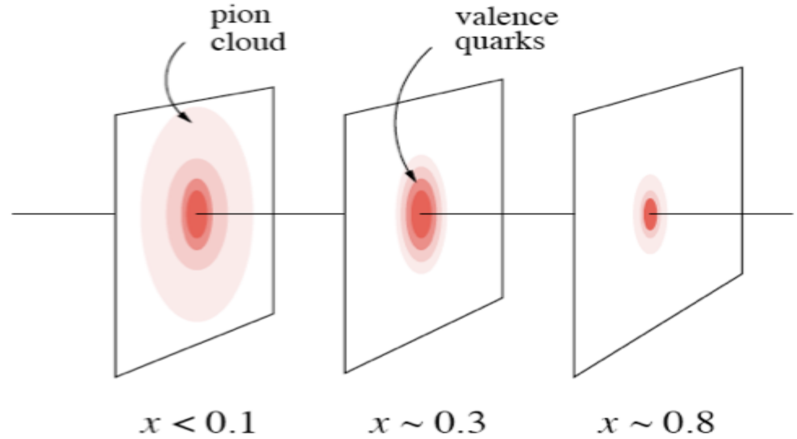

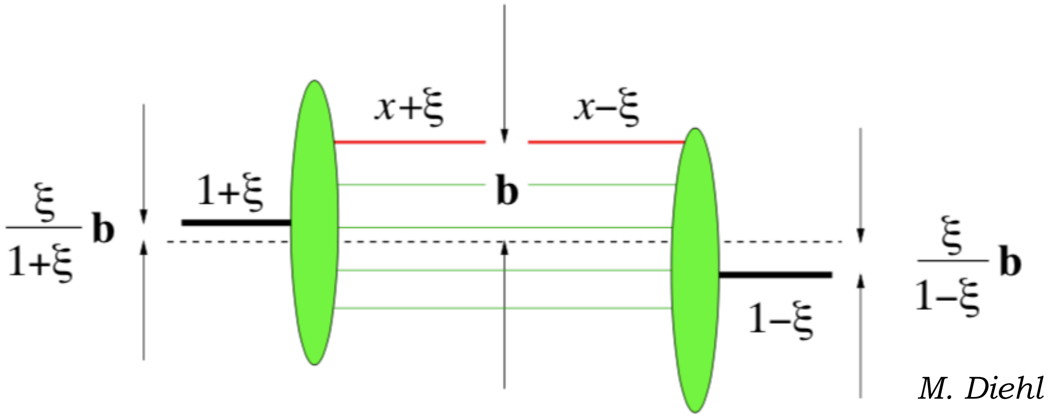

*Formally, the radial separation, **b**, between the struck parton and the centre of momentum of the remaining spectators.*

* Experimentally, fit the t-dependence of structure functions or CFFs with an exponential.

eg: $$\frac{d\sigma_U}{dt} = Ae^{Bt}$$

GPDs and nucleon spin

$$J_N = \frac{1}{2} = \frac{1}{2}\Sigma_q + L_q + J_g$$

* Ji's relation: $J^q = \frac{1}{2} - J^g = \frac{1}{2}\int_{-1}^{1} xdx\,\left\{H^q(x,\xi,0) + E^q(x,\xi,0)\right\}$

Second Mellin moments of the GPDs contain information on the total angular momentum carried by quarks.

Note that the contribution from GPD *H* is given by the quark momentum, already known from PDFs:

$$2J^q = \int_0^1 \mathrm{d}x\, x[q(x) + \bar{q}(x)] + \int_{-1}^{+1} \mathrm{d}x\, x E^q(x,0,0)$$

Compton Form Factors in DVCS

Experimentally, DVCS amplitude is proportional to Compton Form Factors (CFFs) — sums of GPD integrals over x:

$$\int_{-1}^{1} dx F(\mp x, \xi, t) \left[\frac{1}{x - \xi + i\epsilon} \pm \frac{1}{x + \xi - i\epsilon} \right]$$

GPD

Plus sign for unpolarised GPDs, minus for polarised.

Can be decomposed into real and imaginary parts:

Cauchy's principal value integral

$$\Re\mathrm{e}\mathcal{F} = \mathcal{P} \int_{-1}^{1} dx \left[\frac{1}{x - \xi} \mp \frac{1}{x + \xi} \right] F(x, \xi, t)$$

$$\Im\mathrm{m}\mathcal{F}(\xi, t) = -\pi [F(\xi, \xi, t) \mp F(-\xi, \xi, t)]$$

* Both parts are accessible in different experimental observables

Other reactions to get at GPDs

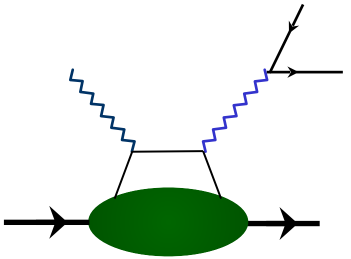

- **Time-like Compton scattering**: virtual photon is time-like. At leading order, access same integrals of GPDs. At higher orders, they differ.

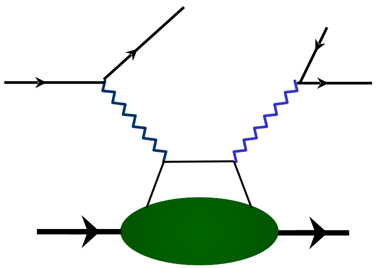

- **Double Deeply Virtual Compton scattering**: two virtual photons: the second vertex provides a second variable Q'^2. This allows direct access to x, but cross-sections are suppressed by another factor of α.

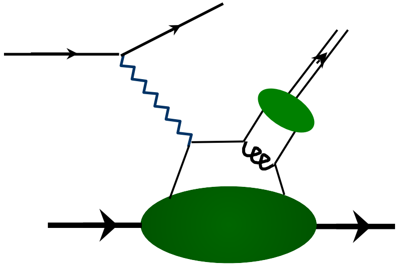

- **Deeply Virtual Meson Production**: the meson vertex provides flavour information. Amplitude now depends on GPDs and the meson Distribution Amplitudes. In light mesons, more sensitive to higher order and higher twist.

In vector mesons, gluon GPDs appear at lowest order!

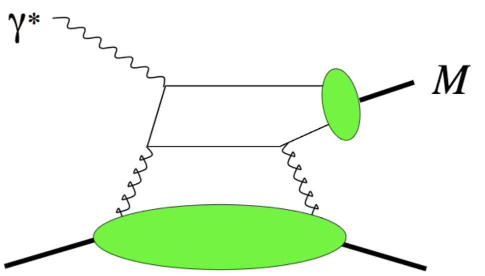

Nucleon Tomography from GPDs

- Flavour separation is possible in DVCS using different targets (proton and neutron), and in DVMP with different mesons.

  For example, compare measurements of π^0 and η DVMP:

$$H_T^{\pi^0} = (e_u H_T^u - e_d H_T^d)/\sqrt{2}, \qquad H_T^{\eta} = (e_u H_T^u + e_d H_T^d)/\sqrt{6},$$

$$\bar{E}_T^{\pi^0} = (e_u \bar{E}_T^u - e_d \bar{E}_T^d)/\sqrt{2}, \qquad \bar{E}_T^{\eta} = (e_u \bar{E}_T^u + e_d \bar{E}_T^d)/\sqrt{6}.$$

Up-quark charge

(Goloskokov-Kroll model)

- Different GPDs represent different aspects of the parton distributions: EM charge, axial charge, transversity, etc….

- Sensitivity to gluon distributions through gluon GPDs.

  Particularly cleanly accessible for heavier q: J/Ψ

Extracting asymmetries

Number of DVCS/BH events for each kinematic bin:

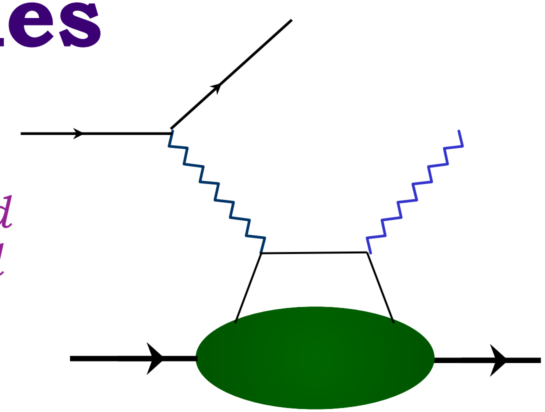

$$N^{bt} = (1 - B^{bt}_{\pi^0}) \cdot \frac{N^{bt}_{ep\gamma}}{FC^{bt}}$$

Number of detected events in identified reaction

Polarisation state of beam, target

Background due to π^0 contamination

Normalisation by beam current (in Faraday Cup)

* Beam-spin asymmetry:

$$A_{\mathrm{LU}} = \frac{P_t^-(N^{++} - N^{-+}) + P_t^+(N^{+-} - N^{--})}{P_b(P_t^-(N^{++} + N^{-+}) + P_t^+(N^{+-} + N^{--}))}$$

Beam, target polarisation

* Target-spin asymmetry:

$$A_{\mathrm{UL}} = A^{\mathrm{lab}}_{\mathrm{UL}} + c_{A_{\mathrm{UT}}}$$

Correction for electron / virtual photon axes

$$A^{\mathrm{lab}}_{\mathrm{UL}} = \frac{N^{++} + N^{-+} - N^{+-} - N^{--}}{D_f(P_t^-(N^{++} + N^{-+}) + P_t^+(N^{+-} + N^{--}))}$$

Dilution factor due to unpolarised background

* Double-spin asymmetry:

$$A_{\mathrm{LL}} = A^{\mathrm{lab}}_{\mathrm{LL}} + c_{A_{\mathrm{LT}}}$$

$$A^{\mathrm{lab}}_{\mathrm{LL}} = \frac{N^{++} + N^{--} - N^{+-} - N^{-+}}{P_b \cdot D_f(P_t^-(N^{++} + N^{-+}) + P_t^+(N^{+-} + N^{--}))}$$

The DVCS/BH amplitude

$$\mathcal{T}^2 = |\mathcal{T}_{\rm BH}|^2 + |\mathcal{T}_{\rm DVCS}|^2 + \mathcal{I}$$

Interference term for DVCS/BH

$$|\mathcal{T}_{\rm BH}|^2 = \frac{e^6}{x_B^2 y^2 (1+\epsilon^2)^2 t\, \mathcal{P}_1(\phi)\mathcal{P}_2(\phi)} [c_0^{\rm BH} + \sum_{n=1}^{2} c_n^{\rm BH} \cos n\phi + s_1^{\rm BH} \sin\phi]$$

$$|\mathcal{T}_{\rm DVCS}|^2 = \frac{e^6}{y^2 \mathcal{Q}^2} \{c_0^{\rm DVCS} + \sum_{n=1}^{2} [c_n^{\rm DVCS} \cos n\phi + s_n^{\rm DVCS} \sin n\phi]\}$$

$$\mathcal{I} = \frac{e^6}{x_B y^3 t \mathcal{P}_1(\phi)\mathcal{P}_2(\phi)} \{c_0^{\mathcal{I}} + \sum_{n=1}^{3} [c_n^{\mathcal{I}} \cos n\phi + s_n^{\mathcal{I}} \sin n\phi]\}$$

Intermediate lepton propagators

Coefficients depending on Compton Form Factors

From asymmetries to CFFs

At leading twist, beam-spin asymmetry (BSA) can be expressed as:

$$A_{\mathrm{LU}}(\phi) \sim \frac{s^{\mathcal{I}}_{1,\mathrm{unp}} \sin\phi}{c^{\mathrm{BH}}_{0,\mathrm{unp}} + (c^{\mathrm{BH}}_{1,\mathrm{unp}} + c^{\mathcal{I}}_{1,\mathrm{unp}} + \ldots)\cos\phi \ldots}$$ *higher-twist terms…*

The leading coefficient is related to the imaginary part of the Compton Form Factors:

$$s^{\mathcal{I}}_{1,\mathrm{unp}} \propto \Im\mathrm{m}[F_1 \mathcal{H} + \xi(F_1 + F_2)\widetilde{\mathcal{H}} - \frac{t}{4M^2} F_2 \mathcal{E}]$$

At CLAS kinematics, this dominates

F_1, F_2: Dirac, Pauli form factors

Likewise, for the target-spin asymmetry (TSA):

$$A_{\mathrm{UL}}(\phi) \sim \frac{s^{\mathcal{I}}_{1,\mathrm{LP}} \sin\phi}{c^{\mathrm{BH}}_{0,\mathrm{unp}} + (c^{\mathrm{BH}}_{1,\mathrm{unp}} + c^{\mathcal{I}}_{1,\mathrm{unp}} + \ldots)\cos\phi + \ldots}$$

$$s_{1,\mathrm{LP}} \propto \Im\mathrm{m}[F_1 \widetilde{\mathcal{H}} + \xi(F_1 + F_2)(\mathcal{H} + \frac{x_B}{2}\mathcal{E}) - \xi(\frac{x_B}{2} F_1 + \frac{t}{4M^2} F_2)\widetilde{\mathcal{E}}]$$

At CLAS kinematics, these CFFs dominate

* Obtain coefficients from fitting the phi-dependence of the asymmetry:

$$A_i = \frac{\alpha_i \sin\phi}{1 + \beta_i \cos\phi}$$

Proton DVCS @ 11 GeV

CLAS12

Impact of CLAS12 unpolarised target proton-DVCS data on the extraction of Re(H) and Im(H).

Re(H)

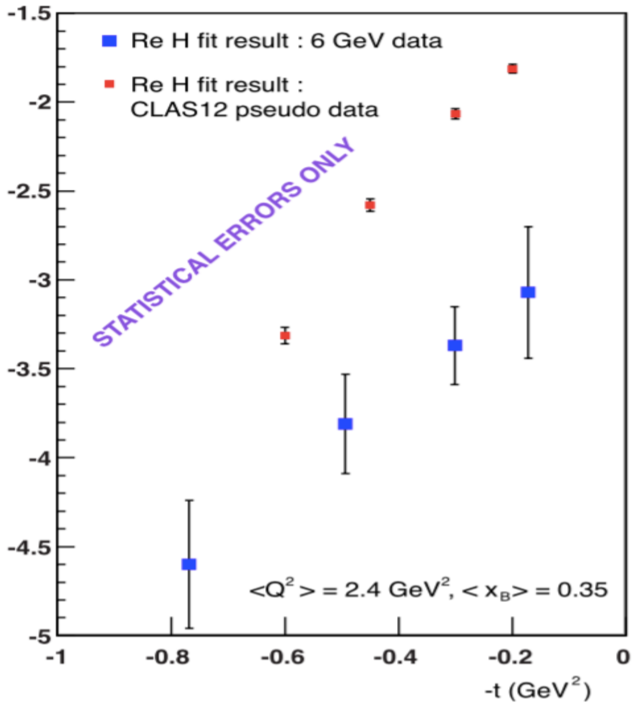

Im(H)

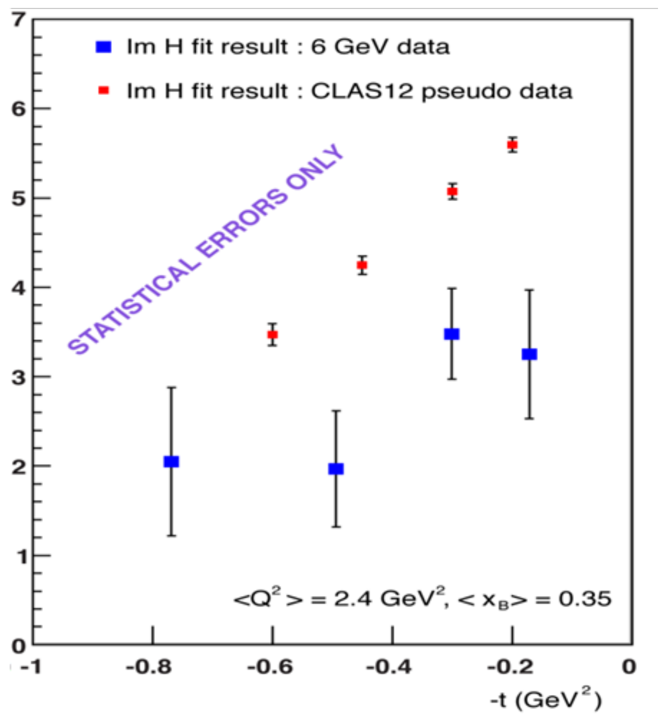

(CLAS 6 GeV extraction H. Moutarde)

DVCS @ JLab12

- Scheduled experiments to measure cross-sections and spin asymmetries with unpolarised and longitudinally polarised liquid H_2 and D_2 targets using CLAS12. → $Im(E_n)$, $Im(H_p)$, $Im(\widetilde{H}_p)$, $Re(H_p)$

- Dynamic Nuclear Polarisation (DNP) of target material, cooled in a *He* evaporation cryostat.
- P_{proton} = 80%,
- $P_{deuteron}$ up to 50%

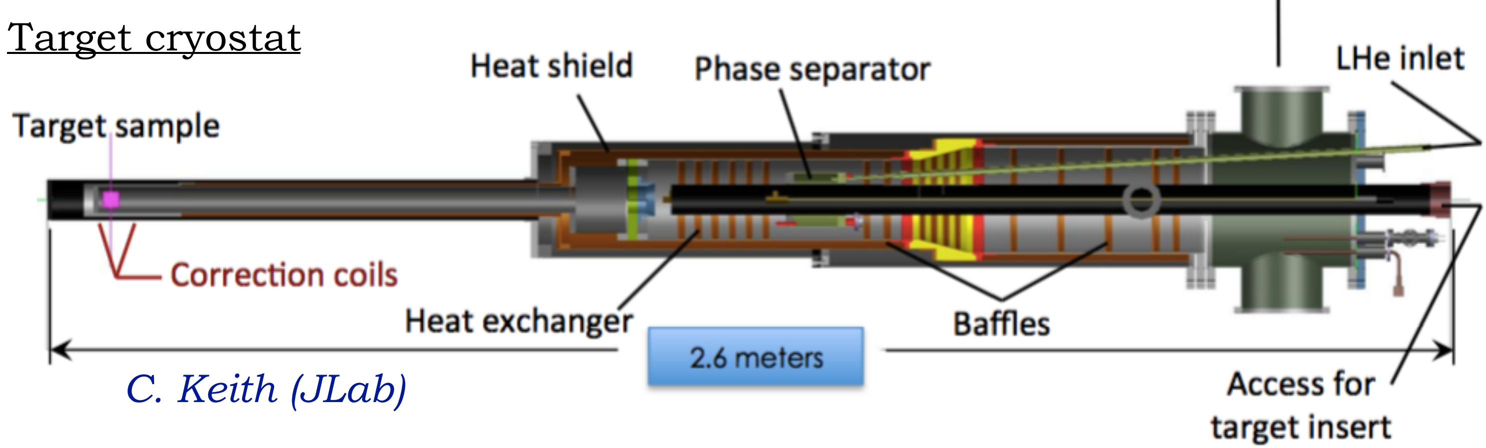

C. Keith (JLab)

- Measurements of cross-sections at 10.6, 8.8 and 6.6 GeV (allows separation of pure DVCS amplitude and the DVCS/Bethe-Heitler interference terms) in Halls A, B and C.

- Transversely-polarised target (HD) for use with electron beams is under development (Hall B). → $Im(E_p)$

- Measurement of beam-spin asymmetry in coherent DVCS from a ^4He target (CLAS12 + recoil detector ALERT): partonic structure of nuclei. → $Im(H_A)$

JLab 6 GeV era DVCS X-sections: kinematics

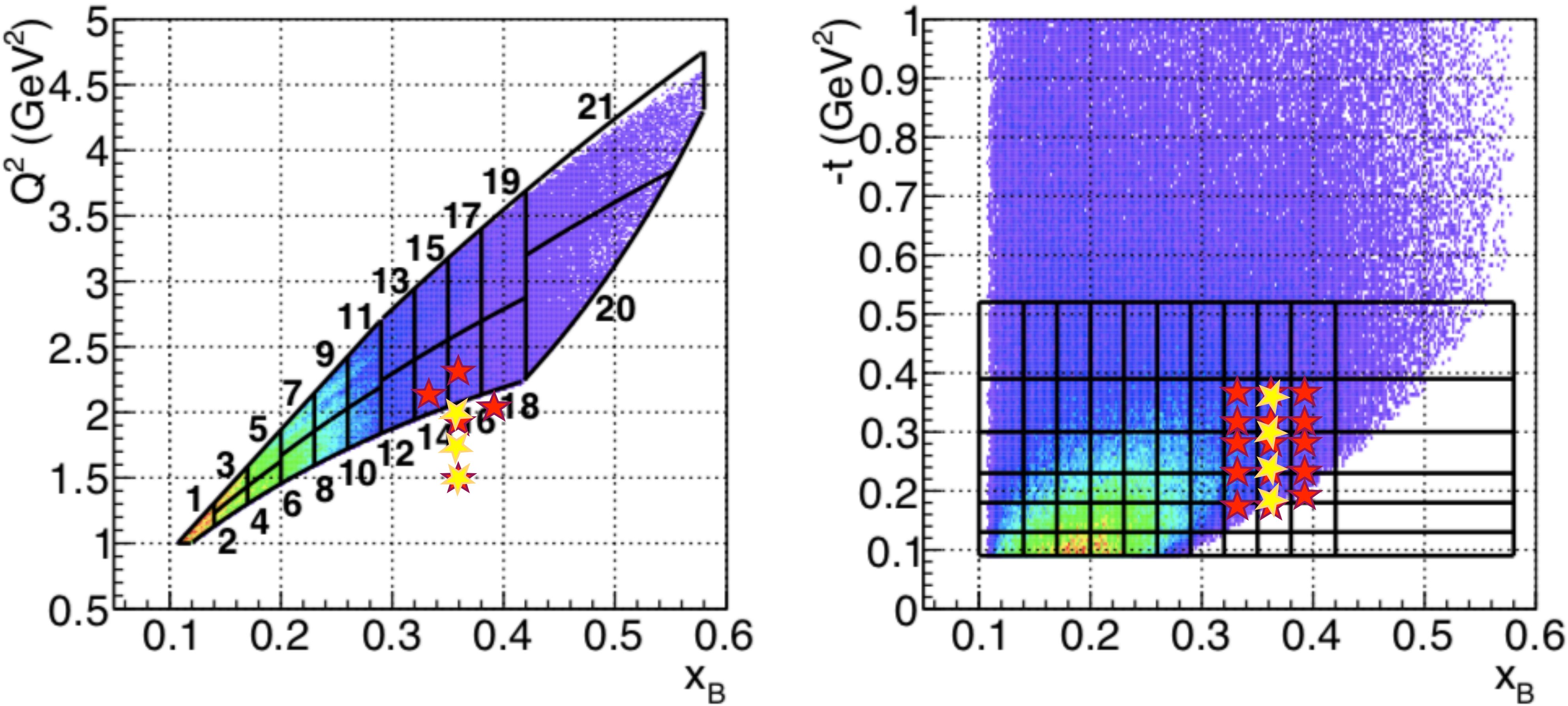

CLAS 2D distributions: H.-S. Jo *et al* (CLAS), ***PRL* 115** (2015) 212003

Hall A

★ M. Defurne *et al*, ***PRC* 92** (2015) 055202

★ M. Defurne *et al*, ***Nature Communications* 8** (2017) 1408

Proton DVCS @ 11 GeV

CLAS12

Experiment E12-06-119

F. Sabatié et al.

P_{beam} = 85%
$L = 10^{35}$ cm^{-2}s^{-1}
$1 < Q^2 < 10$ GeV^2
$0.1 < x_B < 0.65$
$-t_{min} < -t < 2.5$ GeV^2

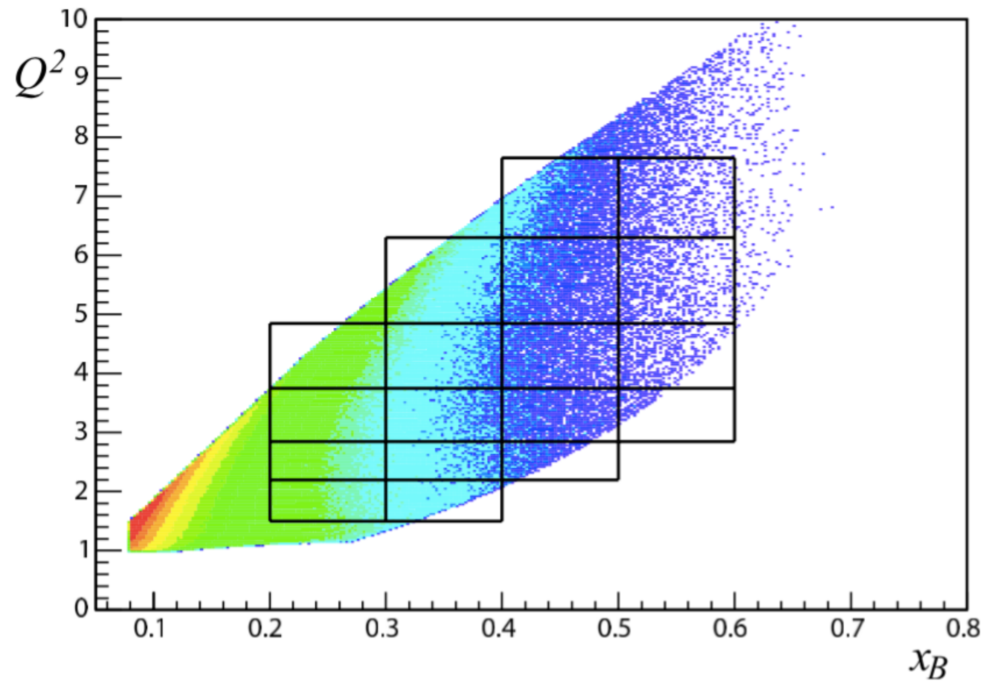

Kinematics similar for all proton DVCS @ 11 GeV with CLAS12 experiments

First experiment with CLAS12

Unpolarised liquid H_2 target:

- Statistical error: 1% - 10% on sinφ moments
- Systematic uncertainties: ~ 6 - 8%

Started this February!

A_{LU} characterised by imaginary parts of CFFs via:

$$F_1 H + \xi G_M \tilde{H} - \frac{t}{4M^2} E \longrightarrow \mathit{Im}(\mathrm{H_p})$$

DVCS at lower energies with CLAS12

CLAS12

Experiment E12-16-010B
F.-X. Girod et al.

Unpolarised liquid H_2 target:

- Beam energies: 6.6, 8.8 GeV
- Simultaneous fit to beam-spin and total cross-sections.

✱ Rosenbluth separation of interference and $|T_{DVCS}|^2$ terms in the cross-section

✱ Scaling tests of the extracted CFFs

✱ Model-dependent determination of the D-term in the Dispersion Relation between *Re* and *Im* parts of CFFs: sensitivity to Gravitational Form Factors.

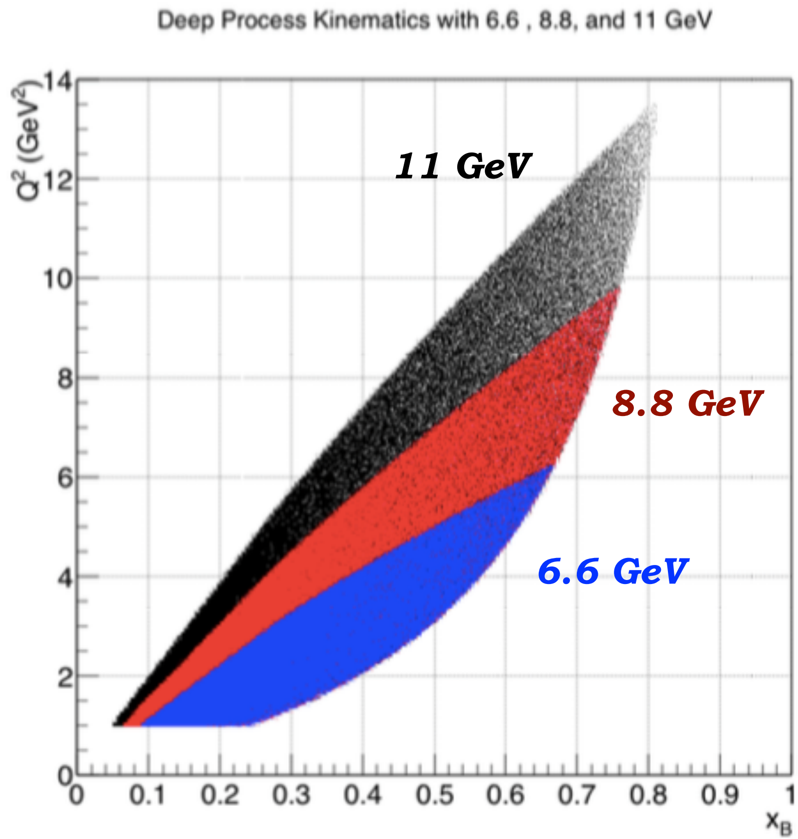

Compare with measurements from Halls A and C: cross-check model and systematic uncertainties.

DVCS at lower energies with CLAS12

Projected extraction of CFFs (red) compared to generated values (green). Three curves on the *Re(H)* show three different scenarios for the D-term.

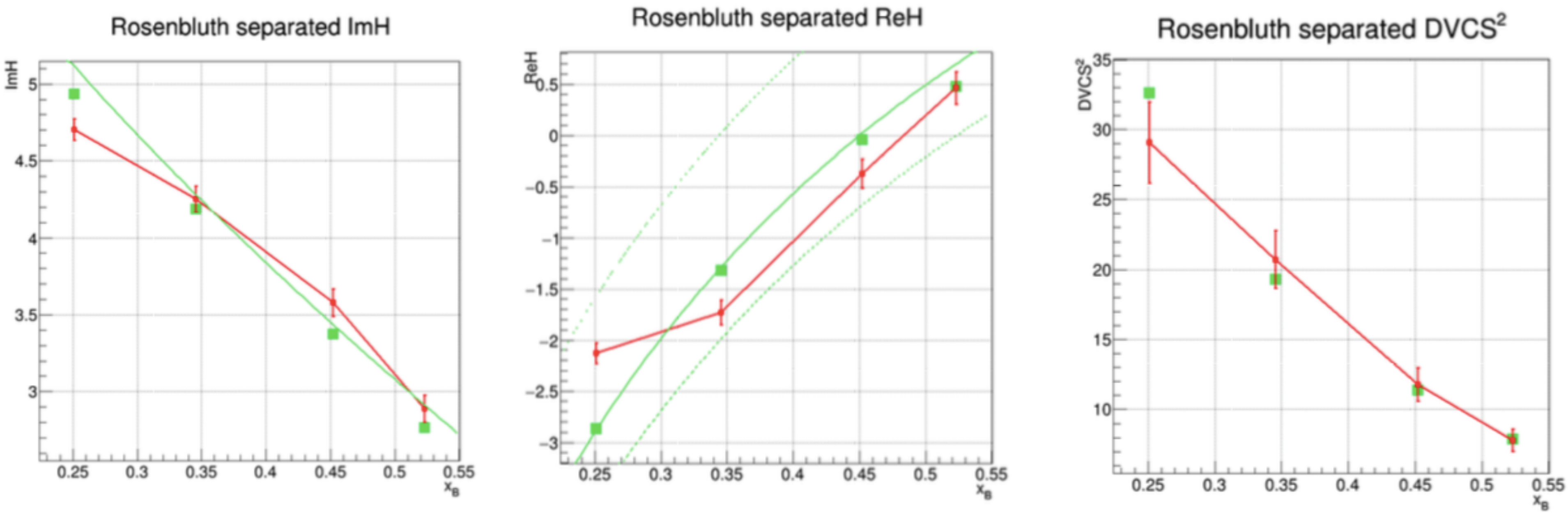

F.-X. Girod et al.

Neutron DVCS @ 11 GeV

CLAS12

Experiment E12-11-003

S. Niccolai, D. Sokhan et al.

$$\Delta\sigma_{LU} \sim \sin\phi\ \mathbf{Im}\{F_1 H + \xi(F_1+F_2)\tilde{H} - kF_2 E\}d\phi$$

Im (E_n) dominates.

Simulated statistical sample:

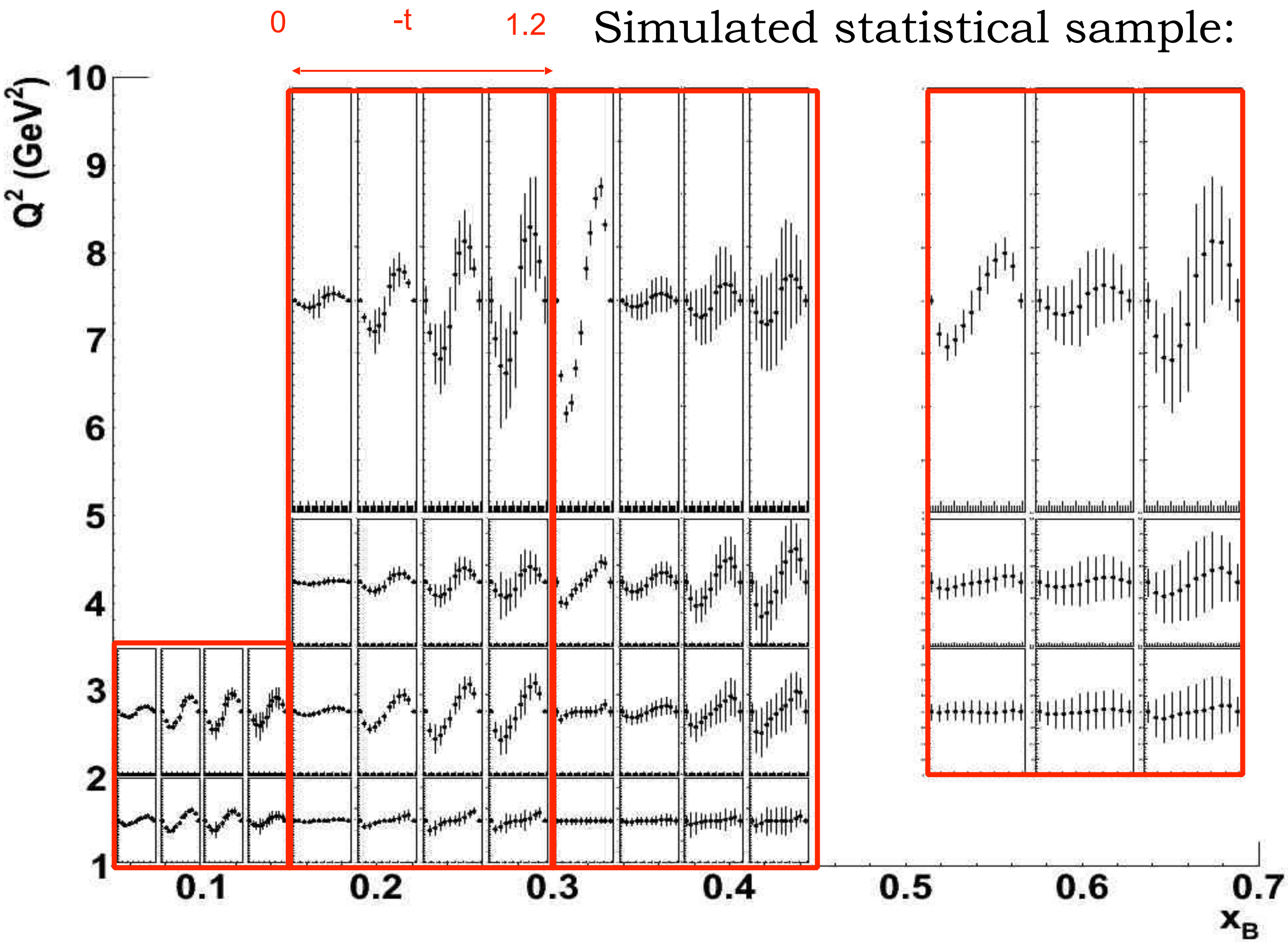

L = 10^{35} cm^{-2}s^{-1}/nucleon

$$e + d \to e' + \gamma + n + (p_s)$$

CLAS12 +

Forward Tagger +

Neutron Detector

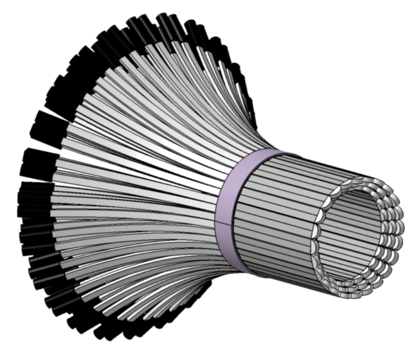

Scheduled: 2019

Proton DVCS with a longitudinally polarised target

CLAS12

Experiment E12-06-119
F. Sabatié et al.

A_{UL} characterised by imaginary parts of CFFs via: $$F_1\tilde{H} + \xi G_M(H + \frac{x_B}{2}E) - \frac{\xi t}{4M^2}F_2\tilde{E} + \ldots$$

$\longrightarrow$ $Im(\widetilde{H}_p)$

Longitudinally polarised NH_3 target:

- Dynamic Nuclear Polarisation (DNP) of target material, cooled to 1K in a *He* evaporation cryostat.
- $P_{proton} > 80\%$
- Statistical error: 2% - 15% on sinφ moments
- Systematic uncertainties: ~ 12%

Tentative schedule: 2020

Target cryostat

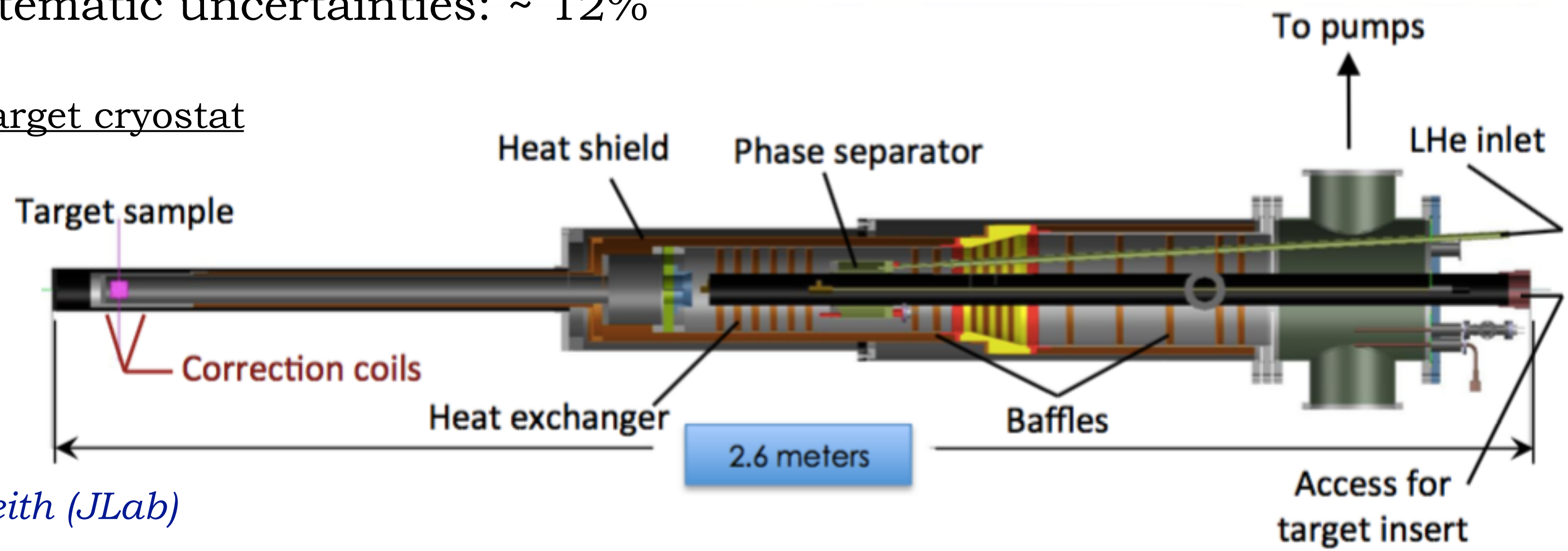

C. Keith (JLab)

CLAS12

Neutron DVCS with a longitudinally polarised target

Experiment E12-06-109A.

S. Niccolai, D. Sokhan et al.

Longitudinally polarised ND_3 target:

- Dynamic Nuclear Polarisation (DNP) of target material in a cryostat shared with the NH_3 target.
- $P_{deuteron}$ up to 50%
- Systematic uncertainties: ~ 12%

A_{UL} characterised by imaginary parts of CFFs via:

$$F_1\tilde{H} + \xi G_M(H + \frac{x_B}{2}E) - \frac{\xi t}{4M^2}F_2\tilde{E} + \ldots$$

→ ***Im*(H$_n$)**

In combination with pDVCS, will allow flavour-separation of the H_q CFFs.

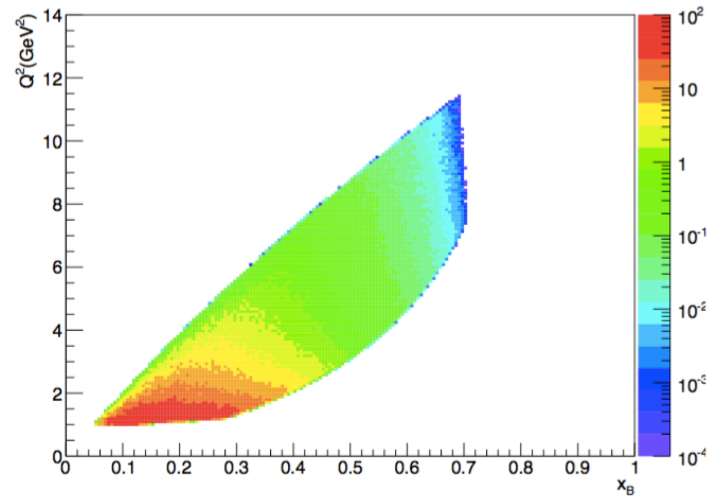

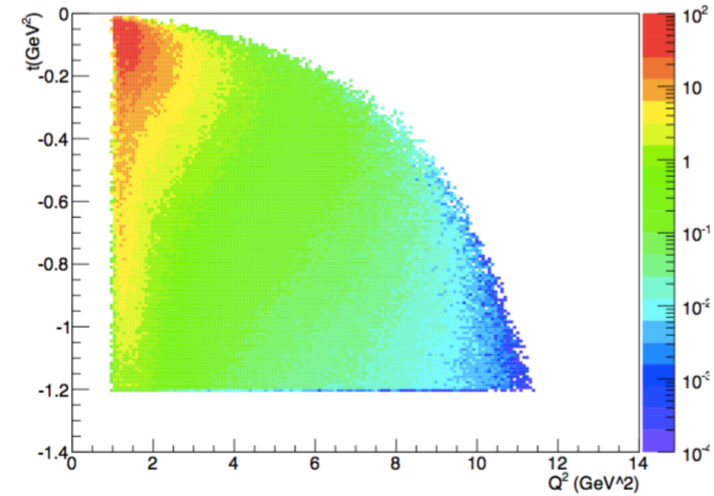

Tentative schedule: 2020

Proton DVCS with transversely polarised target at CLAS12

CLAS12

C12-12-010: with transversely polarised HD target (conditionally approved).

L. Elouardhiri et al.

$\Delta\sigma_{UT} \sim \cos\phi \; \mathrm{Im}\{k(F_2 H - F_1 E) + \ldots..\}d\phi$

Sensitivity to ***Im(E)*** for the proton.

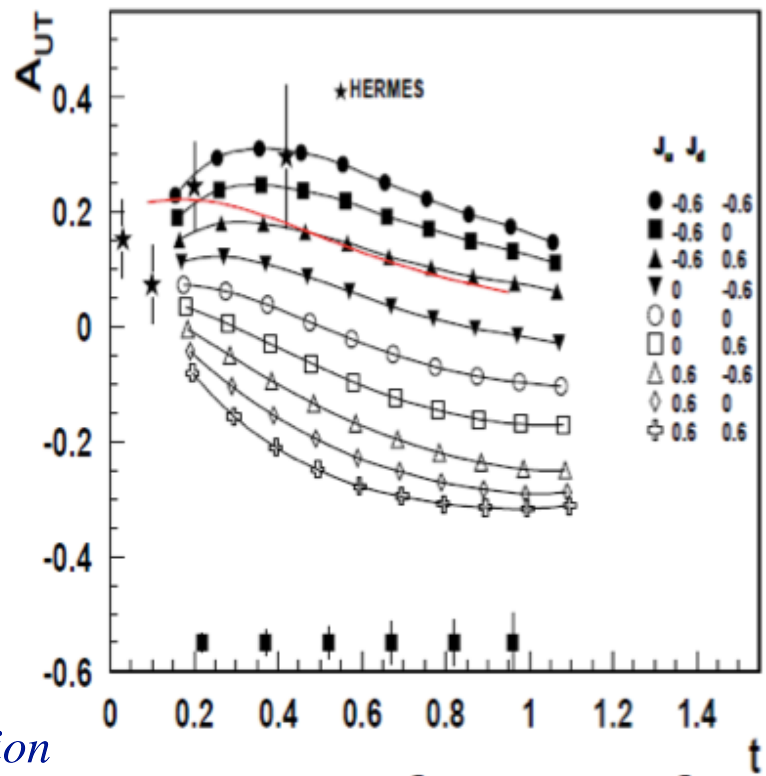

$\langle x \rangle = 0.2, \langle Q^2 \rangle = 2.5\ GeV^2$

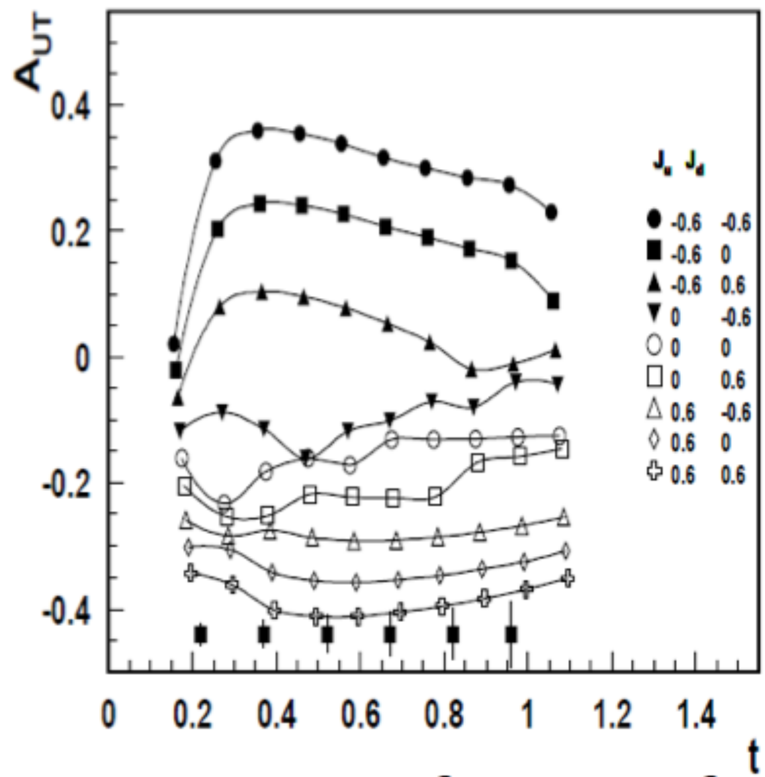

$\langle x \rangle = 0.33, \langle Q^2 \rangle = 2.5\ GeV^2$

VGG extraction (M. Guidal)